Supplementary Methods

Bioorthogonal Cyclization-Mediated *In Situ* Self-Assembly of Small-Molecule Probes for Imaging Caspase Activity *in vivo*

Deju Ye[1†], Adam J. Shuhendler[1†], Lina Cui[1], Ling Tong[2], Sui Seng Tee[1], Grigory Tikhomirov[1], Dean W. Felsher[2] and Jianghong Rao [1*]

[1] *Molecular Imaging Program at Stanford, Departments of Radiology and Chemistry, Stanford University, 1201 Welch Road, Stanford, California 94305-5484, USA,*

[2] *Departments of Medicine and Pathology, Division of Oncology, Stanford University School of Medicine, Stanford, California, USA,*

[†] *These authors contribute equally to this work.*

[*]*e-mail: jrao@stanford.edu*

Table of Contents

		Page
1.	Supplementary Figures S1-27	S3-29
2.	General method	S30
3.	Chemical synthesis and characterization of probes	S31-40
4.	Scheme S1-3. Synthesis of **C-SNAF**, **L-ctrl** and **D-ctrl**	S31-36
5.	Scheme S4. Synthesis of **SIM-1** and control probe **SIM-ctrl**	S37-38
6.	Scheme S5 &6. Synthesis of **C-SNAF-SIM** and **L-ctrl-SIM**	S39
7.	Scheme S7. Synthesis of **L-ctrl-CN**	S40
8.	Scheme S8. Synthesis of **PEG-ctrl**	S40
9.	*In vitro* HPLC assay of enzymatic reactions.	S40-41
10.	Cell culture	S41
11.	Caspase-Glo$^{@}$ 3/7 assay for measuring caspase-3/7 activity in drug-induced apoptotic cells and tumor lysates	S41-42
12.	Analysis of the reaction of **C-SNAF** in cell lysates, cell pellets and tumor lysates	S42-43
13.	Epifluorescence microscopy imaging of DOX-treated HeLa cells.	S43
14.	Flow cytometry studies	S43-44
15.	Active Caspase-3 immunohistochemistry assay	S44-45
16.	Statistical analysis	S45
17.	References	S45
18.	NMR and MALDI-MS spectra	S46-76

Supplementary Figure S1. Characterization of C-SNAF *in vitro*. **a**, Proposed reduction- and caspase-3/7-triggered macrocyclization and self-assembly of **C-SNAF** into nano-aggregates. **b** & **c**, Normalized UV-vis absorption and fluorescent spectra of **C-SNAF (b)** and **C-SNAF-*cycl* (c)** in caspase buffer (pH 7.4). **d**, High-magnification TEM image of **C-SNAF** (50 μM) after incubation with recombinant human caspase-3 (4.9×10^{-3} U/mL) overnight at 37 °C in caspase buffer (pH 7.4). **e**, MALDI-MS spectra of **C-SNAF-*cycl***.

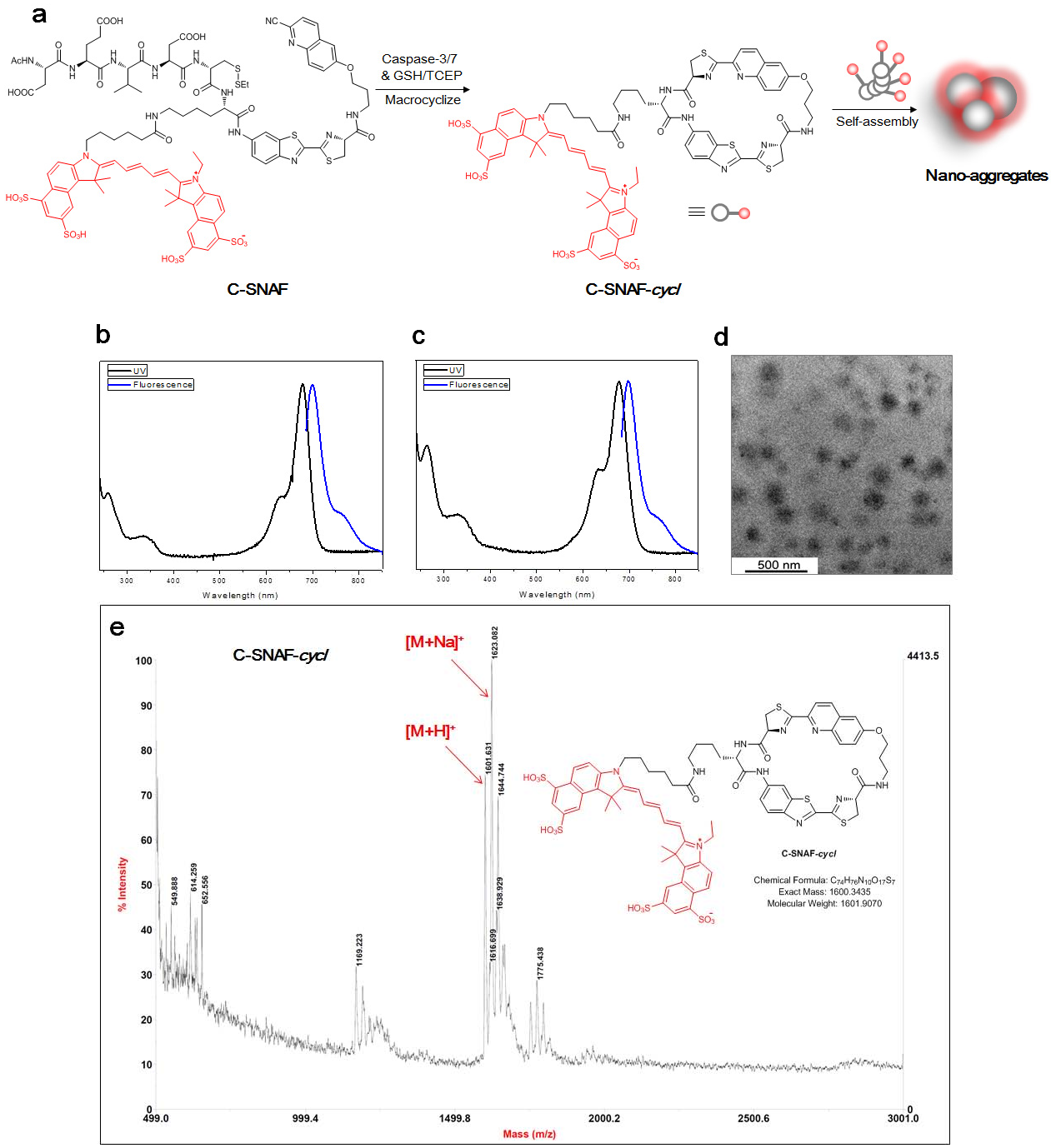

Supplementary Figure S2. Characterization of the enzymatic kinetics and specificity of C-SNAF *in vitro*. **a**, The proposed caspase-3/7 and reduction-triggered molecular transformation of **C-SNAF** to **C-SNAF-*cycl***; When incubating in enzyme reaction buffer (with 10 mM TCEP, pH 7.4), **C-SNAF** was reduced to form intermediate **T1**, which may be reversed to another proposed intermediate **T2**; Both intermediates can be cleaved by caspase-3/7, releasing the *L*-DEVD capping peptide, and spontaneously cyclize to form **C-SNAF-*cycl***. **b**, The longitudinal HPLC traces of **C-SNAF** (25 μM) following incubation with recombinant human caspase-3 (4.9 mU/ml, 0.735 μg/ml), 7 (18.3 U/ml, 0.735 μg/ml) and 9 (0.3 U/ml, 0.735 μg/ml), Legumain (> 250 pmol/min/μg, 0.735 μg/ml) and Cathepsin B (0.27 U/ml, 0.735 μg/ml) at 37 °C in enzyme reaction buffer. **C-SNAF** was first converted to its reduced intermediate **T1** and **T2** when pre-incubating in buffer (with 10 mM TCEP) for 10 min. At that point (t = 0 h), enzyme was added to trigger reaction (proteolysis and cyclization), and the reaction was monitored by HPLC at 0, 1, 1.5, 2, 3, 4 and 6 h. (Peaks * and ** indicate intermediates **T1** and **T2**; peak # indicates the cyclized product **C-SNAF-*cyc***.)

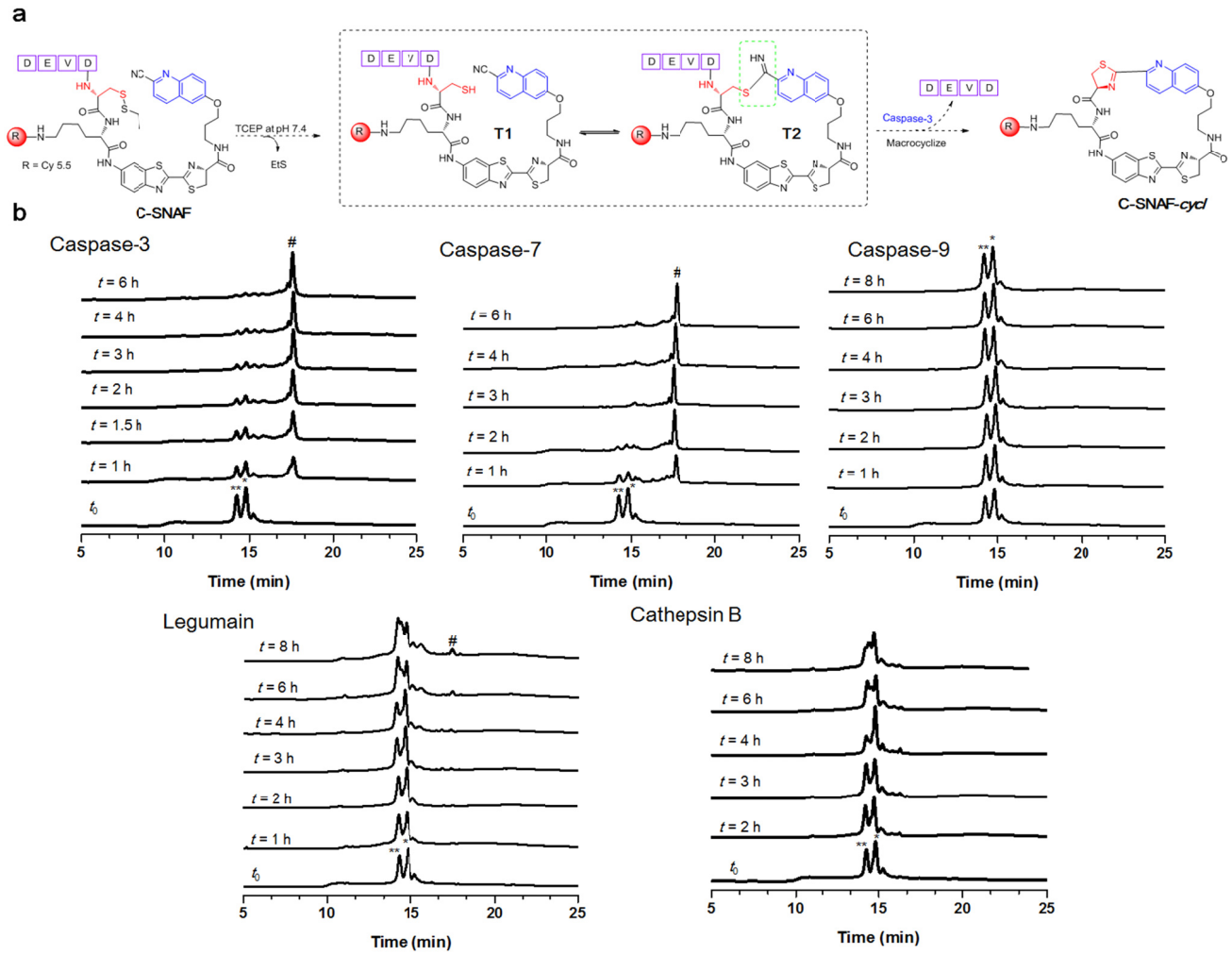

Supplementary Figure S3. Characterization of caspase-3/7-cleavable but non-condensable control probe L-ctrl *in vitro*. **a**, Proposed molecular transformation of **L-ctrl** after incubation with caspase-3. **b**, Normalized UV-vis absorption and fluorescent spectra of **L-ctrl** in caspase buffer (pH 7.4), which show similar UV and fluorescent spectra to **C-SNAF**. **c**, HPLC traces of **L-ctrl** (black, T_R = 15.2 min) and treatment of **L-ctrl** (25 µM) with recombinant human caspase-3 (4.9×10^{-3} U/ml, 1.0 µmolU^{-1}) for 24 h at 37 °C in caspase buffer (pH 7.4) (red, T_R = 16.8 min). MALDI mass of compound **L-ctrl'** corresponding to the HPLC peak (red) in **c** shows a molecular weight (1608 D) that is 500 D less than **L-ctrl**, corresponding to the DEVD peptide cleavage. **d**, TEM image of **L-ctrl** (50 µM) after incubation with recombinant human caspase-3 (4.9×10^{-3} U/mL) overnight at 37 °C in caspase buffer (pH 7.4), showing no nanoparticles on the grid.

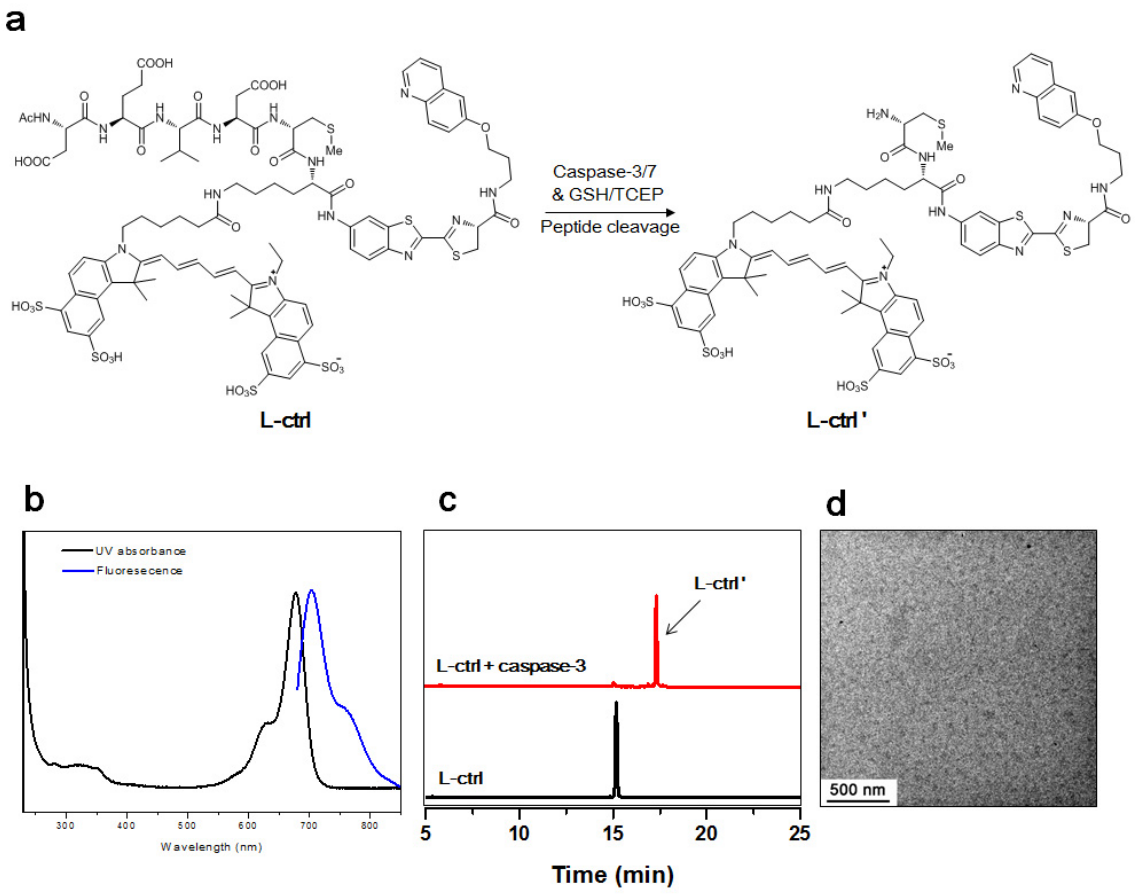

Supplementary Figure S4. Characterization of non-cleavable and non-condensable control D-ctrl *in vitro*. **a**, Proposed molecular transformation of **D-ctrl** after incubation with caspase-3. **b**, Normalized UV-vis absorption and fluorescent spectra of **D-ctrl** in caspase buffer (pH 7.4), which show similar UV and fluorescent spectra to **C-SNAF**. **c**, HPLC traces of **D-ctrl** (black) and incubation of **D-ctrl** (25 μM) with recombinant human caspase-3 (4.9×10^{-3} U/ml, 1.0 μmol/U) for 24 h at 37 °C in caspase buffer (pH 7.4) (red, T_R = 14.7 min). The peak shows the same retention time and an identical molecule weight to **D-ctrl**, which indicates **D-ctrl** resistant to caspase-3. **d**, TEM image of **D-ctrl** (50 μM) after incubation with recombinant human caspase-3 (4.9×10^{-3} U/mL) overnight at 37°C in caspase buffer (pH 7.4), showing no nanoparticles on the grid.

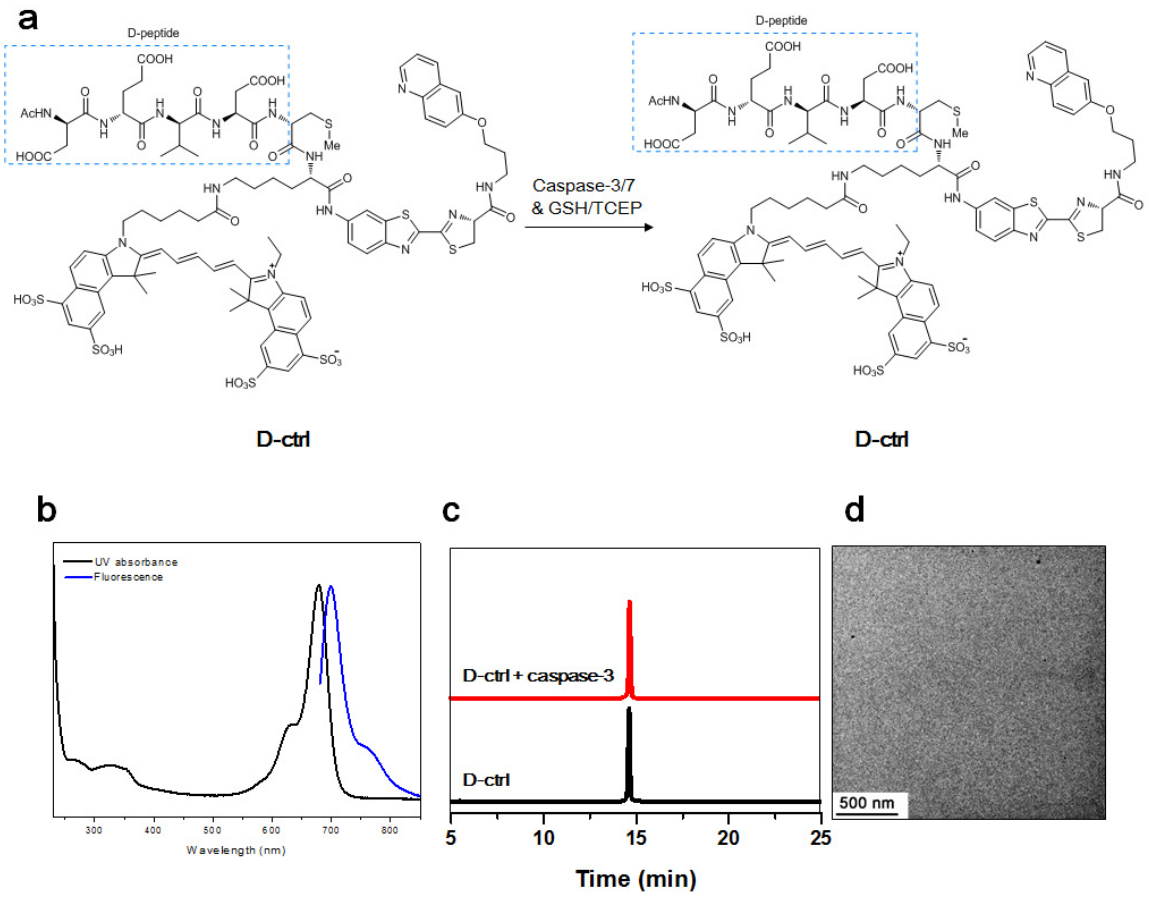

Supplementary Figure S5. STS-induced apoptosis and activation of caspase-3/7 in HeLa cells. **a-c**, Flow cytometry analysis of STS-treated and control HeLa cells stained with FITC-conjugated Annexin V and propidium iodide (PI). Cells were untreated (control), treated with 2 µM of STS for 4 h only, or treated with 2 µM of STS for 4 h followed by another 24 growth in blank culture medium without STS. The quadrants Q are defined as Q1 = viable (Annexin V negative/PI negative), Q2 = early apoptosis (Annexin V positive/PI negative), Q3 = late apoptosis (Annexin V positive/PI positive), and Q4 = necrosis (Annexin V negative/PI positive). **d-f**, Flow cytometry analysis of control and STS-treated HeLa cells stained with fluorescent inhibitor of caspases-3/7 (FLICA (FAM)) and PI. The quadrants R are defined as R1 = FLICA negative/PI negative, R2 = FLICA positive/PI negative, R3 = FLICA positive/PI positive, and R4 = FLICA negative/PI positive. **g**&**h**, Measurements of caspase-3/7 activity in HeLa cells. Cells were treated with 0, 2, 5and 10 µM of STS for 4 h only, or treated with 2 µM of STS for 4 h followed by another 24 h growth in blank culture medium without STS. The caspase-3 activity was then measured using Caspase-Glo® 3/7 Assay, and normalized to the cell number. Each data point and error bar represents the mean and standard deviation of two separate experiments. The results demonstrate efficient induction of HeLa cell apoptosis by 4 h treatment with 2 µM of STS (*quadrants Q2*&*R2*), with an elevated caspase-3/7 activity leading to deterioration of plasma membrane integrity 24 h later (*quadrant Q3*&*R3*).

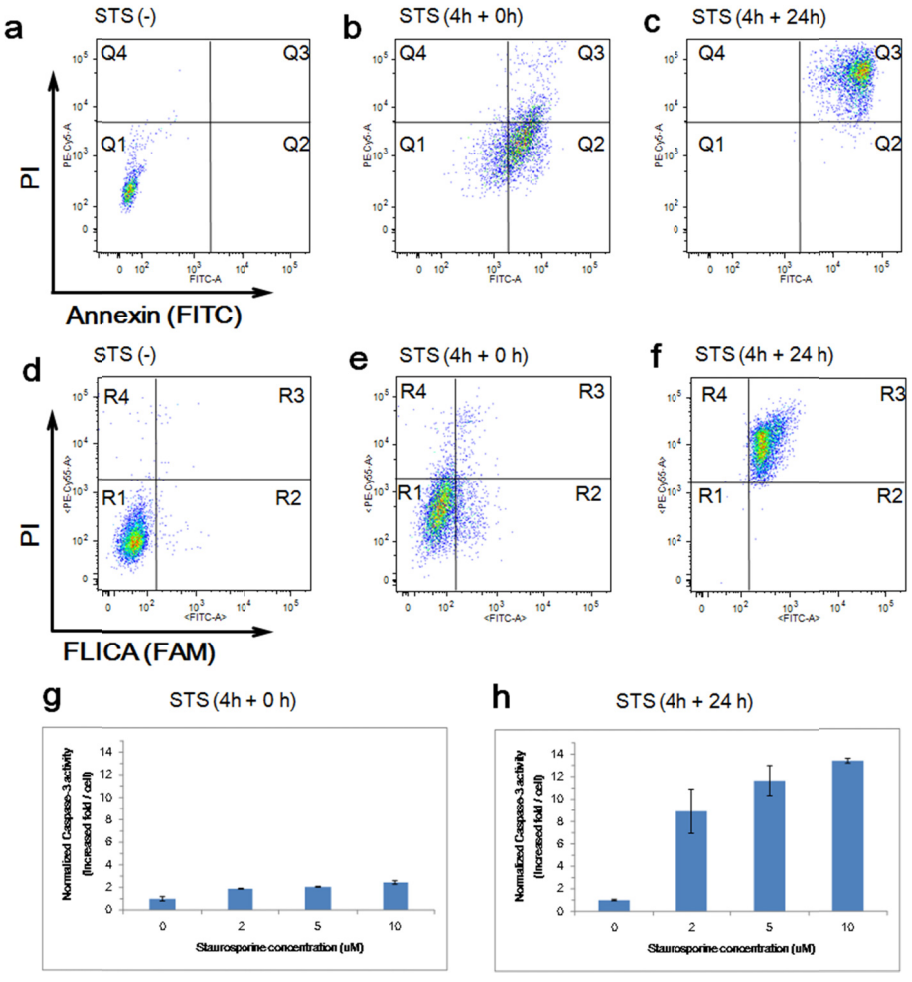

Supplementary Figure S6. Analysis of uptake of C-SNAF, L-ctrl and D-ctrl in viable HeLa cells. a, Representative overlay histograms from flow cytometry analysis of blank viable HeLa cells, and viable HeLa cells incubated with 2 μM of **C-SNAF**, **L-ctrl** or **D-ctrl** for 24 h. Acquisition of 10,000 cells for each sample was collected using Cy5.5 bandpass filter. **b**, Quantitation of the fluorescent intensity of Cy5.5 in cells as derived from flow cytometry analysis in **a** shows that all three probes gave similarly increased intensity compared to blank cells. The mean fluorescence intensity (MFI) for each data point in **b** comes from two separate acquisitions, and error bar represents standard deviation. **c**, Fluorescence microscopy imaging of blank viable cells, and viable HeLa cells incubated with 2 μM **of C-SNAF**, **L-ctrl** or **D-ctrl** for 24 h. Cells were stained with nuclear binding probe Hoechst 33342 (blue), and the images at Cy5.5 channel are compared at the same fluorescence intensity scale. These results suggest that the uptake of all the three probes in viable HeLa cells is at the similarly low level.

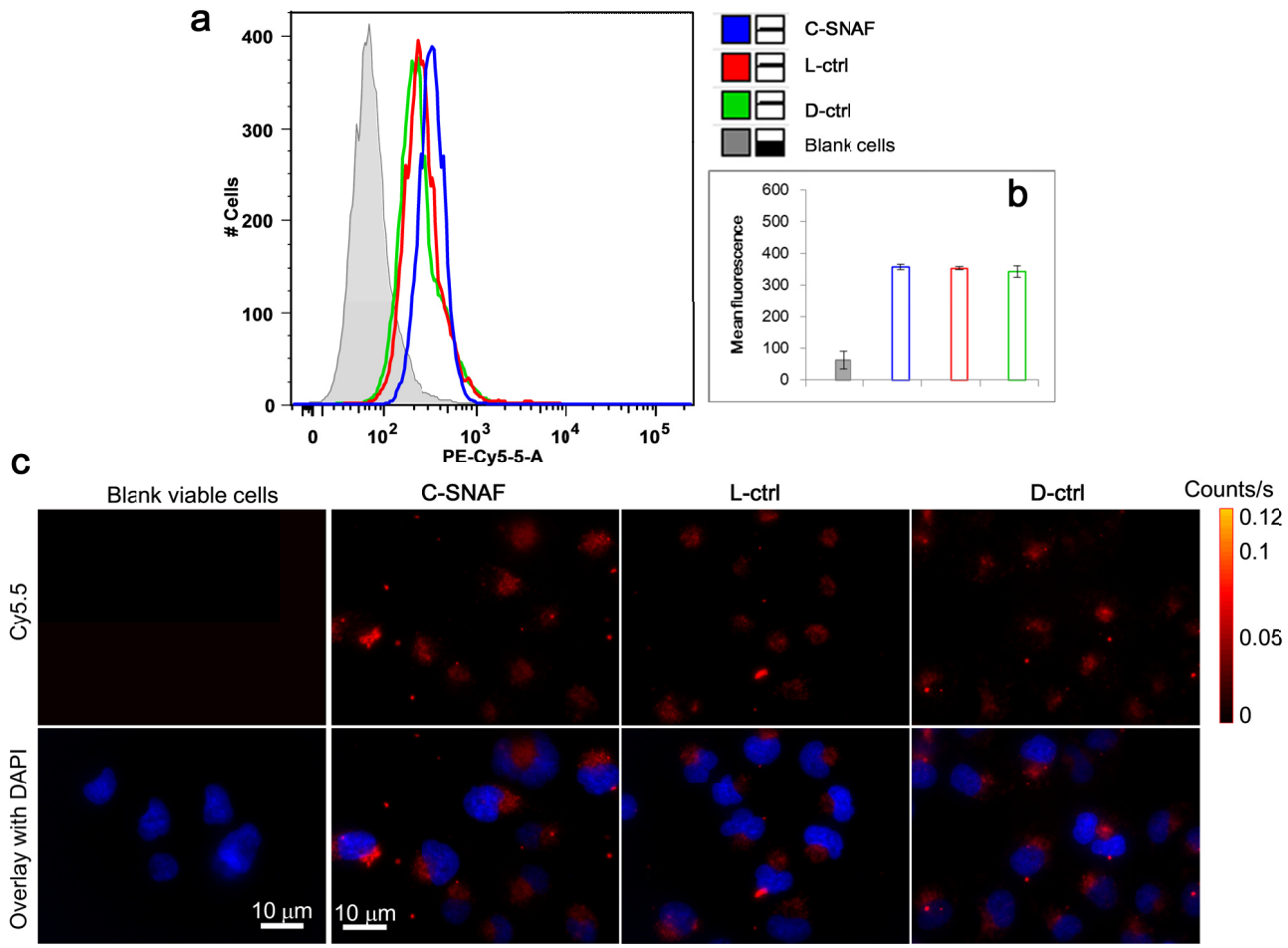

Supplementary Figure S7. Labeling STS-induced apoptotic HeLa cells with C-SNAF. **a**, Representative overlay histograms from flow cytometry results show higher Cy5.5 fluorescence in the apoptotic cells after incubation with **C-SNAF** (2 μM). Acquisition of 10,000 cells for each sample was collected using Cy5.5 bandpass filter. **b**, Quantitation of the fluorescent intensity of Cy5.5 in cells as derived from flow cytometry analysis in **a** shows that apoptotic cells labeled with **C-SNAF** have ~ 13 fold increased intensity compared to viable cells stained with **C-SNAF**. The increased fluorescence was dramatically inhibited by the caspase-3/7 inhibitor Z-VAD-fmk (50 μM). Apoptotic cells incubated with either **L-ctrl** or **D-ctrl** (2 μM) show much lower fluorescence. Each data point and error bar in **b** represents the mean and standard deviation of two separate experiments. **c**, Fluorescence microscopy images of cells are shown at a lower Cy5.5 fluorescence intensity scale compared to that in Fig. 3b, demonstrating significantly higher fluorescence in **C-SNAF**-treated apoptotic cells. Cells were stained with nuclear binding probe Hoechst 33342 (blue).

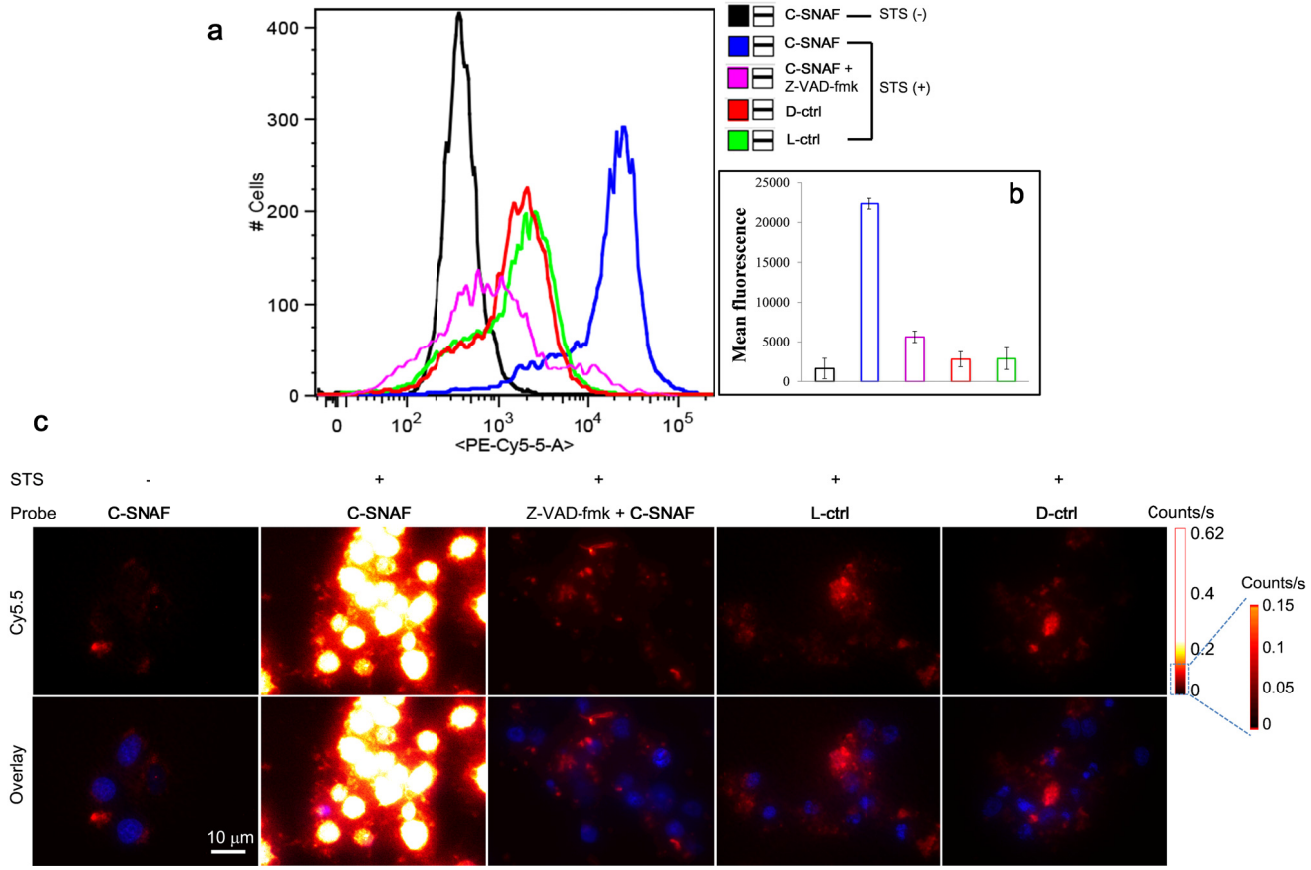

Supplementary Figure S8. Cellular monitoring of STS treatment efficacy on HeLa cells with C-SNAF. a, Fluorescence images of HeLa cells treated with different concentration of STS (0, 0.5, 1 and 2 μM) for 4 h followed by incubating with 2 μM of **C-SNAF** for 24 h. **b**, Fluorescence images of HeLa cells treated with 2 μM of STS for different periods of time (0, 1, 2 and 4 h) followed by incubating with 2 μM of **C-SNAF** for 24 h. **c** & **d**, Percentage of fluorescent cells (cell lit up %) in **a** and **b**; e.g. 158/180 means 158 out of 180 cells are fluorescent. Scale bar, 50 μm, 20×.

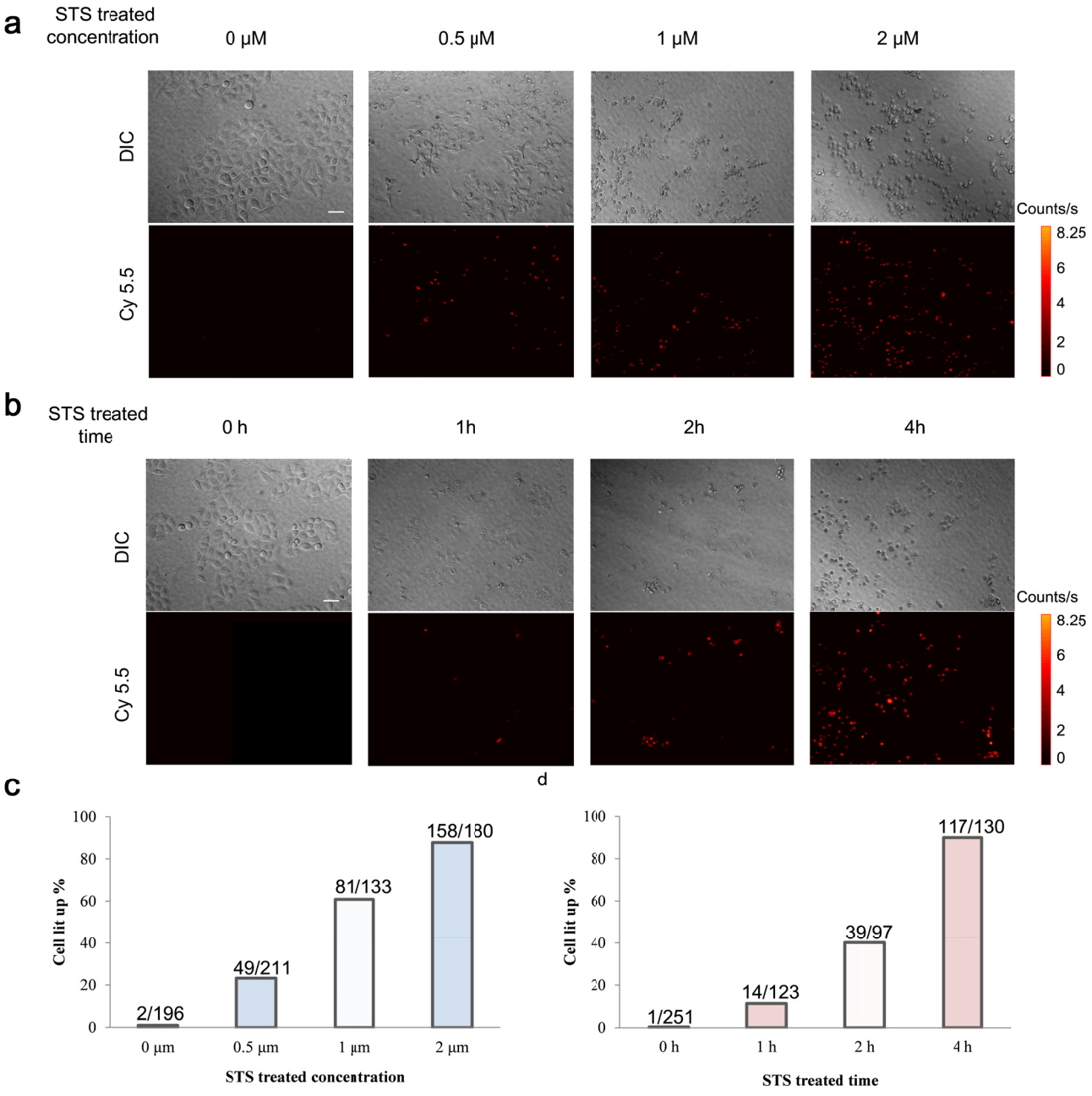

Supplementary Figure S9. Analysis of caspase-3-triggered intramolecular condensation of C-SNAF in viable and STS (2 μM) treated HeLa cells. **a**, HPLC traces of incubation of **C-SNAF** (5 μM) in lysates of viable and apoptotic HeLa cells overnight at 37 °C. HeLa cells (~ 8 millions) were either untreated or treated with 2 μM of STS for 4 h and kept growing in blank culture medium without STS for another 24 h. Cells were then lysed with RIPA buffer, and incubated with **C-SNAF** (5 μM) followed by analyzing the reaction with HPLC (678 nm UV detection). **b**, HPLC traces of viable and apoptotic HeLa cells incubated **C-SNAF** (50 μM) for 24 h. HeLa cells (~ 8 millions) were untreated or treated with 2 μM of STS for 4 h and then incubated with **C-SNAF** (50 μM) for another 24 h after the removal of STS. Cells were then lysed, and analyzed by HPLC assay (675 nm UV detector). Peaks * and ** indicate the disulfide reduction products **T1** and **T2**; peak # indicates the cyclized product **C-SNAF-*cycl***.

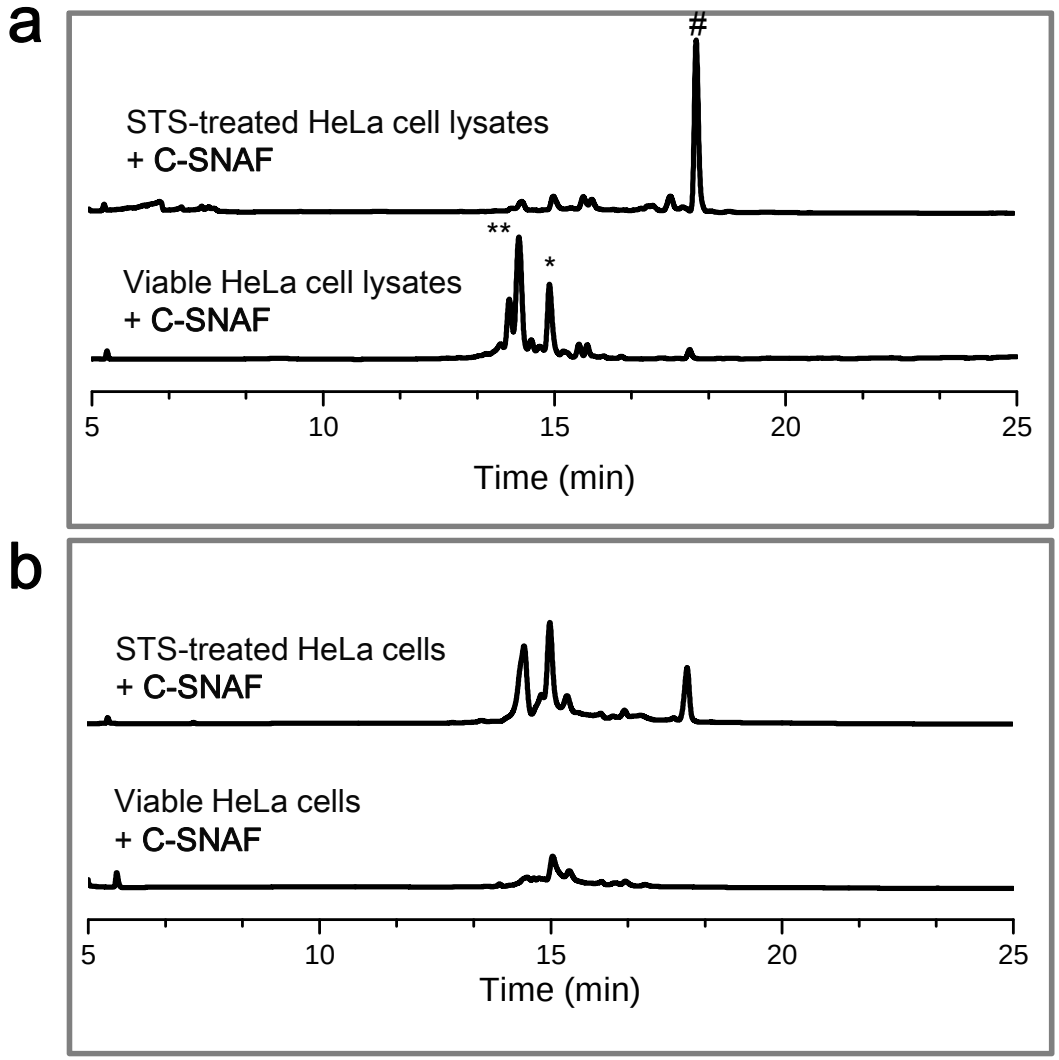

Supplementary Figure S10. DOX-induced apoptosis and activation of caspase-3/7 in HeLa cells. **a**, Flow cytometry analysis of control and DOX-treated HeLa cells stained with Annexin V (FITC) and PI. **b**, Flow cytometry analysis of control and DOX-treated HeLa cells stained with FLICA (FAM) and PI. Q1-4 and R1-4 are defined the same as that in **Supplementary Figure S5**. **c**, The caspase-3 activity obtained in HeLa cells after treatment with 0, 1, 2, and 5 μM of DOX for 24 h. The caspase-3/7 activity was measured using Caspase-Glo® 3/7 Assay, and normalized to cell number. Each data point and error bar represents the mean and standard deviation of two separate experiments. The caspase-3 activity increased with the increasing dose of DOX, with a more than 8-fold increase when cells were treated with 5 μM of DOX. This value is comparable to that found in cells treated with 2 μM of STS. **d**, HPLC traces of incubation of **C-SNAF** (5 μM) in viable and DOX-induced apoptotic HeLa cell lysates overnight at 37 °C. HeLa cells (~ 8 millions) were either untreated or treated with 2 μM DOX for 24 h, then lysed, and incubated with **C-SNAF** (5 μM) followed by HPLC analysis of the reaction **(**675 nm UV detection). Peak # **i**ndicates the cyclized product **C-SNAF-*cycl***.

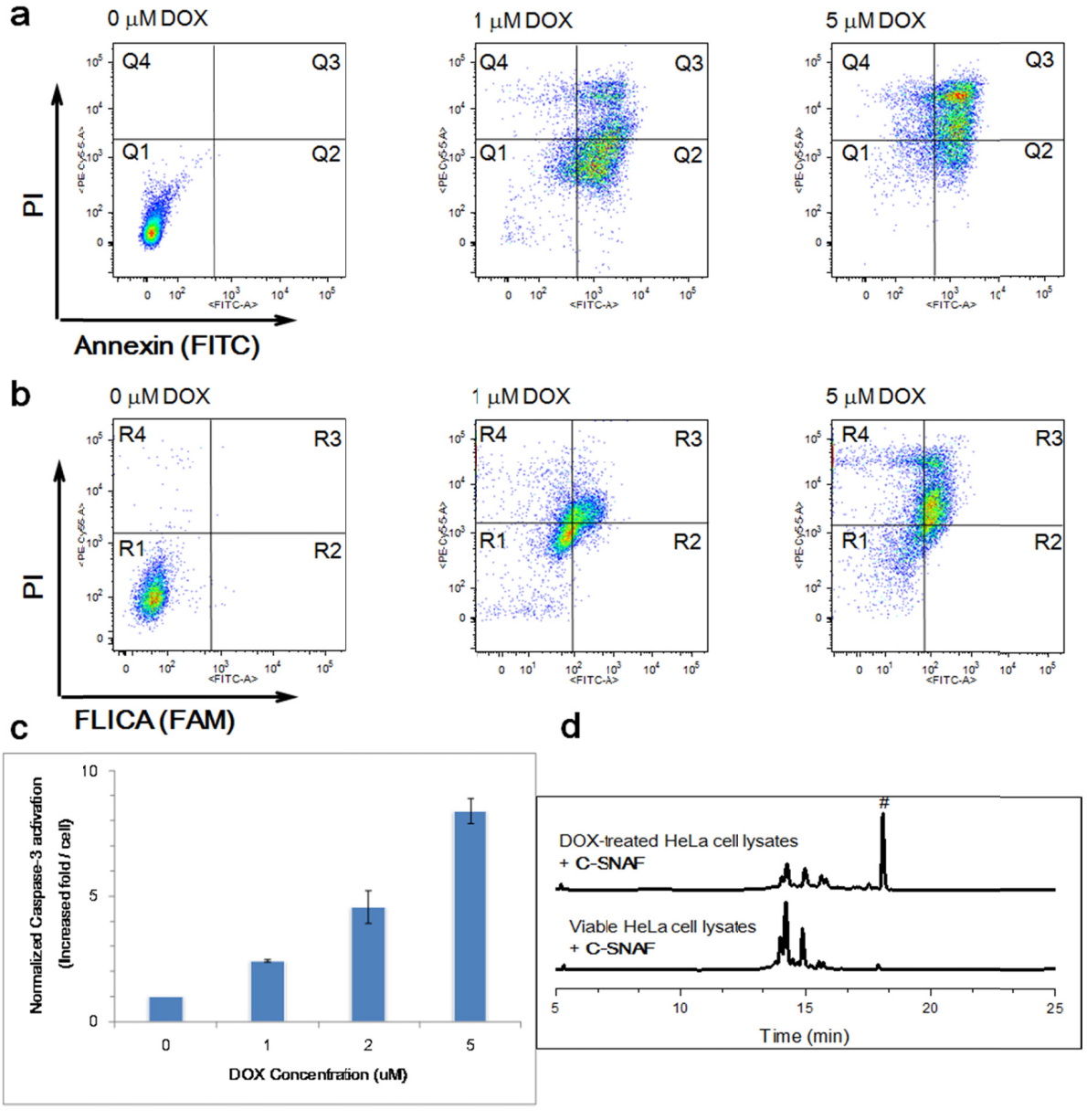

Supplementary Figure S11. Labeling DOX-induced apoptotic HeLa cells with C-SNAF. a, Representative overlay histograms from flow cytometry show high Cy5.5 fluorescence in the apoptotic cells after incubation with 2 μM of **C-SNAF**. Cells were incubated with 5 μM **of** DOX only, or co-incubated with 5 μM of DOX and 2 μM of **C-SNAF**, **L-ctrl**, **D-ctrl**, or **C-SNAF** (2 μM) in the presence of 50 μM of caspase inhibitor Z-VAD-fmk for 24 h. Acquisition of 10,000 cells for each sample was collected using Cy5.5 bandpass filter. **b**, Quantitation of the fluorescence intensity of Cy5.5 in cells derived from the flow cytometry analysis in **a** shows that DOX-induced apoptotic cells incubated with **C-SNAF** (blue) result in a ~ 4-fold increase compared to that without **C-SNAF** incubation (black), or incubation with either **L-ctrl** (green) or **D-ctrl** (red). The labeling of apoptotic cells by **C-SNAF** was blocked by the caspase inhibitor (pink). Each data point and error bar in **b** represents the mean and standard deviation of two separate experiments. **c**, Fluorescence images of DOX-induced apoptotic HeLa cells incubating with **C-SNAF** and its control probes under the same conditions as in **a**. Cells were stained with Hoechst 33342 (blue). (Scale bar: 50 μm, 20×). These results show higher Cy5.5 fluorescence (red) obtained in DOX-induced apoptotic HeLa cells following incubation with **C-SNAF**.

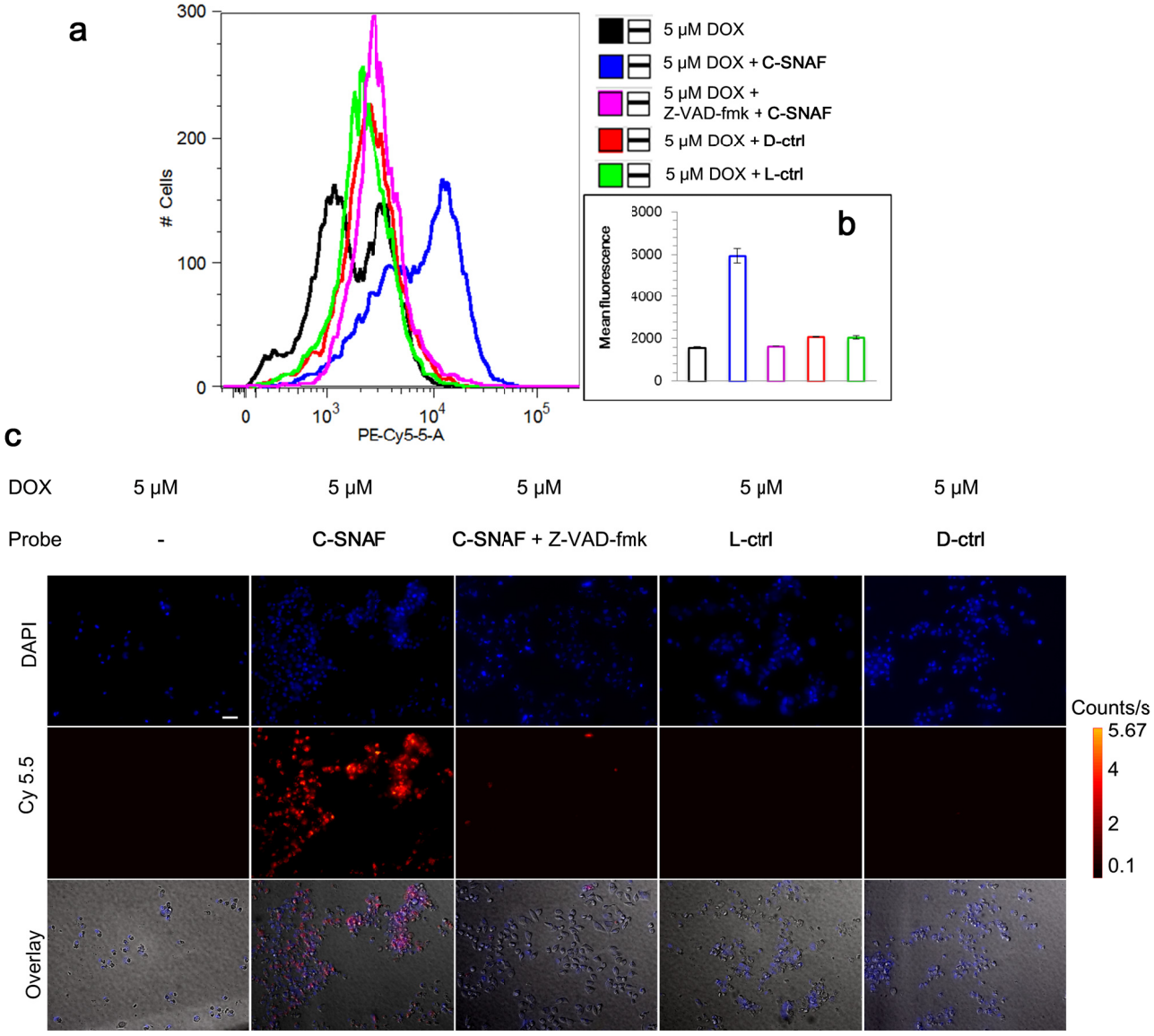

Supplementary Figure S12. Monitoring of HeLa cells response to DOX treatment with C-SNAF. Fluorescence microscopy images of HeLa cells co-incubated with **C-SNAF** (2 μM) and different concentration of DOX (0, 1, 2 and 5 μM) for 24 h, followed by staining with Hoechst 33342. (Scale bar: 50 μm, 20×). The population of cells labeled by **C-SNAF** was dependent on the DOX concentration, resulting in an approximately 10-fold enhancement in cell labeling efficiency (9 to 92%) with a paralleled 5-fold increase in the dose level (1 to 5 μM). The increase in Cy5.5 fluorescence cell population was dependent on the apoptosis level of the cells after DOX treatment, where HeLa cells treated with 5 μM of DOX resulted in a higher level of apoptosis and casapse-3/7 activity compared to that with 1 μM of DOX (**Supplementary Fig. S9**).

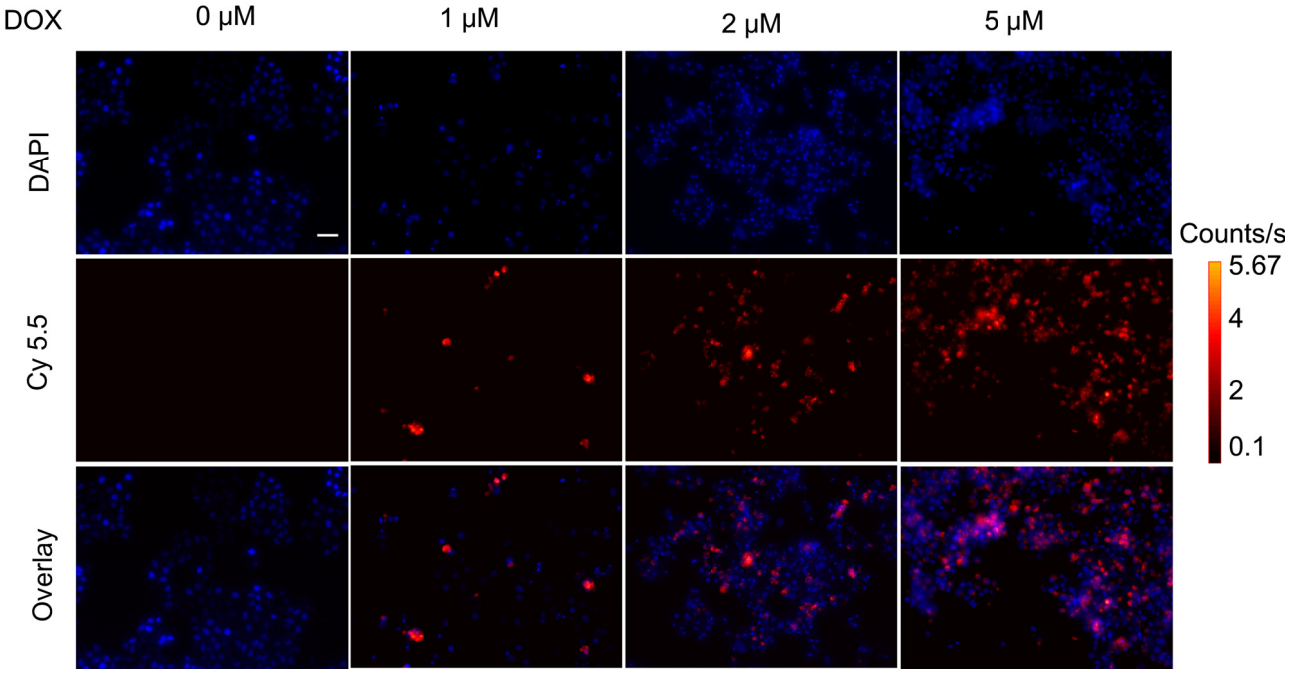

Supplementary Figure S13. Comparison of cellular studies between C-SNAF and L-ctrl-CN. a, The chemical structure of **L-ctrl-CN** and proposed molecular transformation. **L-ctrl-CN** has a similar structure to **L-ctrl**, with a functional cyano group. **b**, HPLC traces of **L-ctrl-CN** (black, T_R = 14.9 min) and treatment of **L-ctrl-CN** (25 μM) with recombinant human caspase-3 (4.9×10^{-3} U/ml) for 24 h at 37 °C in caspase buffer (pH 7.4) (red, T_R = 17.2 min). **c**, TEM image of **L-ctrl-CN** (25 μM) after incubation with recombinant human caspase-3 (4.9×10^{-3} U/mL) overnight at 37 °C in caspase buffer (pH 7.4). **d**, Fluorescence microscopy images of STS-treated HeLa cells following incubation with 2 μM of **C-SNAF**, **L-ctrl-CN** or pre-formed **C-SNAF-*cycl*** for 24 h. Cells were stained with nuclear binding probe Hoechst 33342 (blue), and the images at the Cy5.5 channel are compared at the same fluorescence intensity scale. Scale bar: 50 μm.

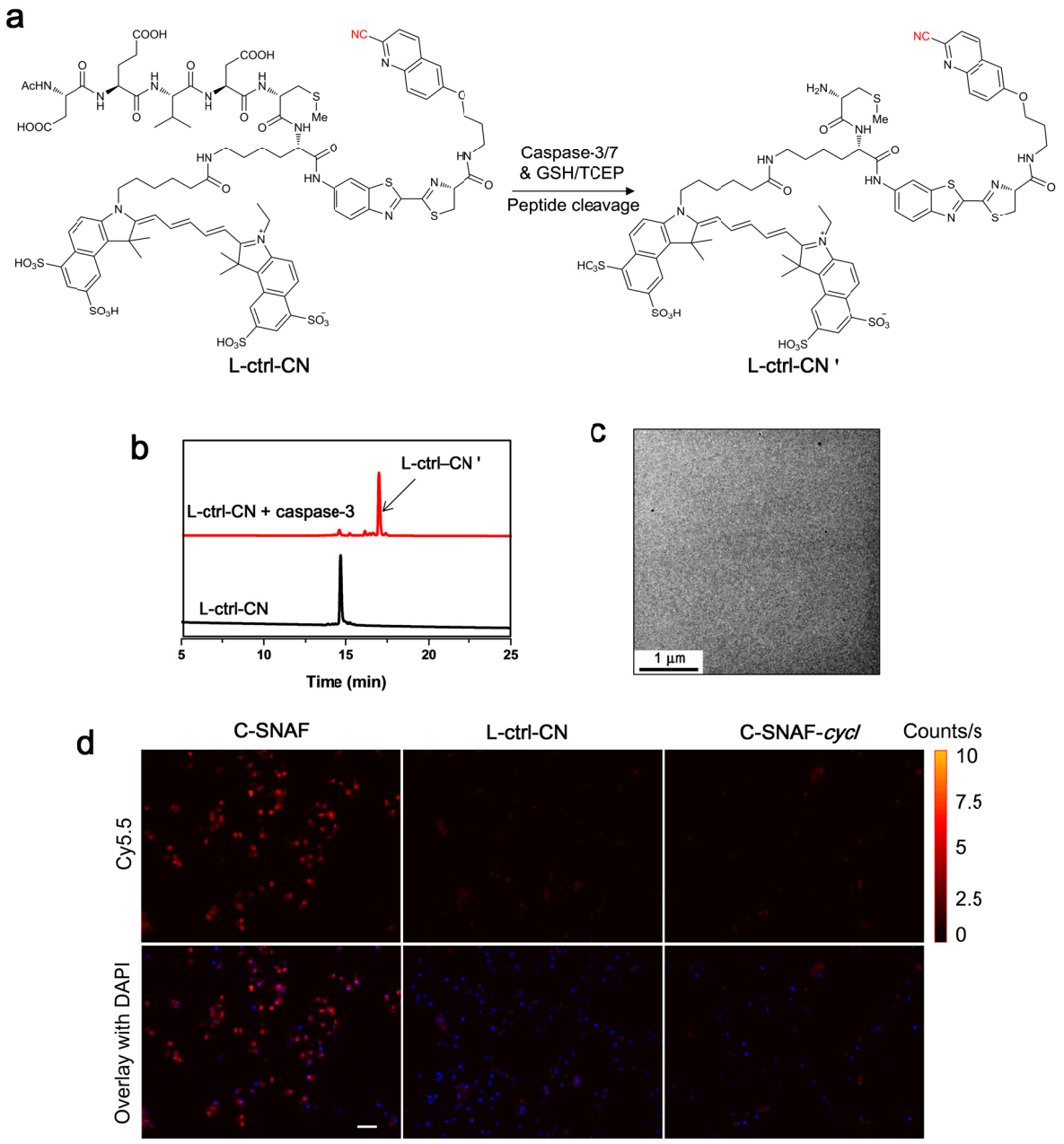

Supplementary Figure S14. Comparison of cellular studies between C-SNAF and PEG-ctrl. a, The chemical structures of control probe **PEG-ctrl** and its precursor **PEG-1**, and proposed conversion of **PEG-ctrl** to **PEG-ctrl-*cycl***. To provide direct evidence that self-assembly is necessary for the mechanism of action of **C-SNAF**, we replaced the rigid and hydrophobic aminoluciferin linker with a flexible and hydrophilic poly(ethylene glycol) (PEG) linker of an equal bond length to form **PEG-ctrl**. This control also contains a reducible thiol and a cleavable DEVD capping peptide, permitting macrocylcization, but is unable to self-assemble into nanostructures due to the lack of strong intramolecular π-π stack after cyclization. **b**, HPLC traces of **PEG-1** (100 μM) following incubation in PBS buffer (with 10 mM TCEP, pH 7.4) at 0, 5, 10, 15, 20 and 30 min. Peaks * and # indicate **PEG-1** and **PEG-*cycl***. **c**, Plot of linear regression analysis of Ln[**PEG-1**] vs. time to determine the pseudo-first-order rate for the intramolecular cyclization of **PEG-1** (k = 1.9 × 10^{-3} s^{-1}, $t_{1/2}$ = 365 s). Ln[**PEG-1**] was obtained based on the HPLC data in **b**. **d**, DLS analysis of **PEG-1** (100 μM) after incubation in PBS buffer (with 10 mM TCEP, pH 7.4) at r.t. for 1 h did not give any detectable nanoparticles. **e**, HPLC traces of **PEG-ctrl** (black, T_R = 14.7 min) and **PEG-ctrl** (red, T_R = 17.3 min) following incubation with caspase-3 at 37 °C for 24 h in the caspase buffer (pH 7.4), indicating efficient conversion of **PEG-ctrl** to **PEG-ctrl-*cycl*** upon activation. **f**, Fluorescence microscopy images of STS-induced apoptotic HeLa cells incubating with 2 μM of **C-SNAF** or **PEG-ctrl** for 24 h, showing significantly higher fluorescence in **C-SNAF** treated apoptotic cells than **PEG-ctrl**. Cells were stained with Hoechst 33342 (blue), and the images at the Cy5.5 channel are compared at the same fluorescence intensity scale. Scale bar: 50 μm.

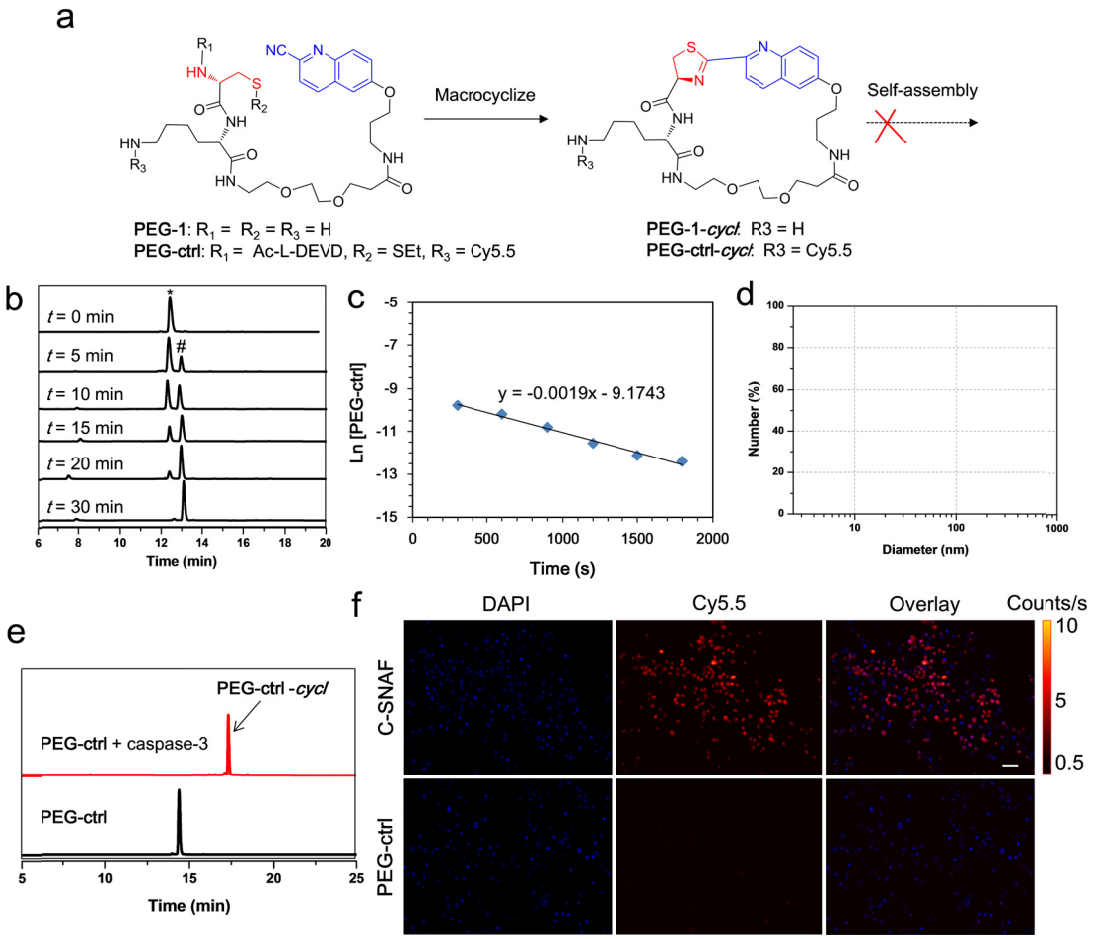

Supplementary Figure S15. Imaging caspase-3/7 activity in STS-induced apoptotic MDA-MB-231 cells. a, The caspase-3/7 activity in MDA-MB-231 cells after treatment with 0, 2, and 5 µM of STS for 4 h followed by another 24 h growth in fresh medium without STS. The caspase-3 activity was measured using Caspase-Glo® 3/7 Assay, and normalized to cell number. **b**, HPLC traces of viable and apoptotic MDA-MB-231 cell lysates incubated with **C-SNAF** overnight at 37 °C. MDA-MB-231 cells (~ 8 millions) were either untreated or treated with STS (2 µM) for 4 h and kept growing in culture medium without STS for another 24 h. Cells were then lysed with RIPA buffer, and incubated with **C-SNAF (**5 µM) followed by analysis of the reaction with an HPLC assay (675 nm UV detection). Peak # indicates the cyclized product **C-SNAF-*cycl***. **c**, Fluorescence images of MDA-MB-231 cells following incubation with 2 µM of **C-SNAF, L-ctrl, D-ctrl** or **C-SNAF** (2 µM) in the presence of 50 µM of Z-VAD-fmk for 24 h. Scale bar: 50 µm, 20×.

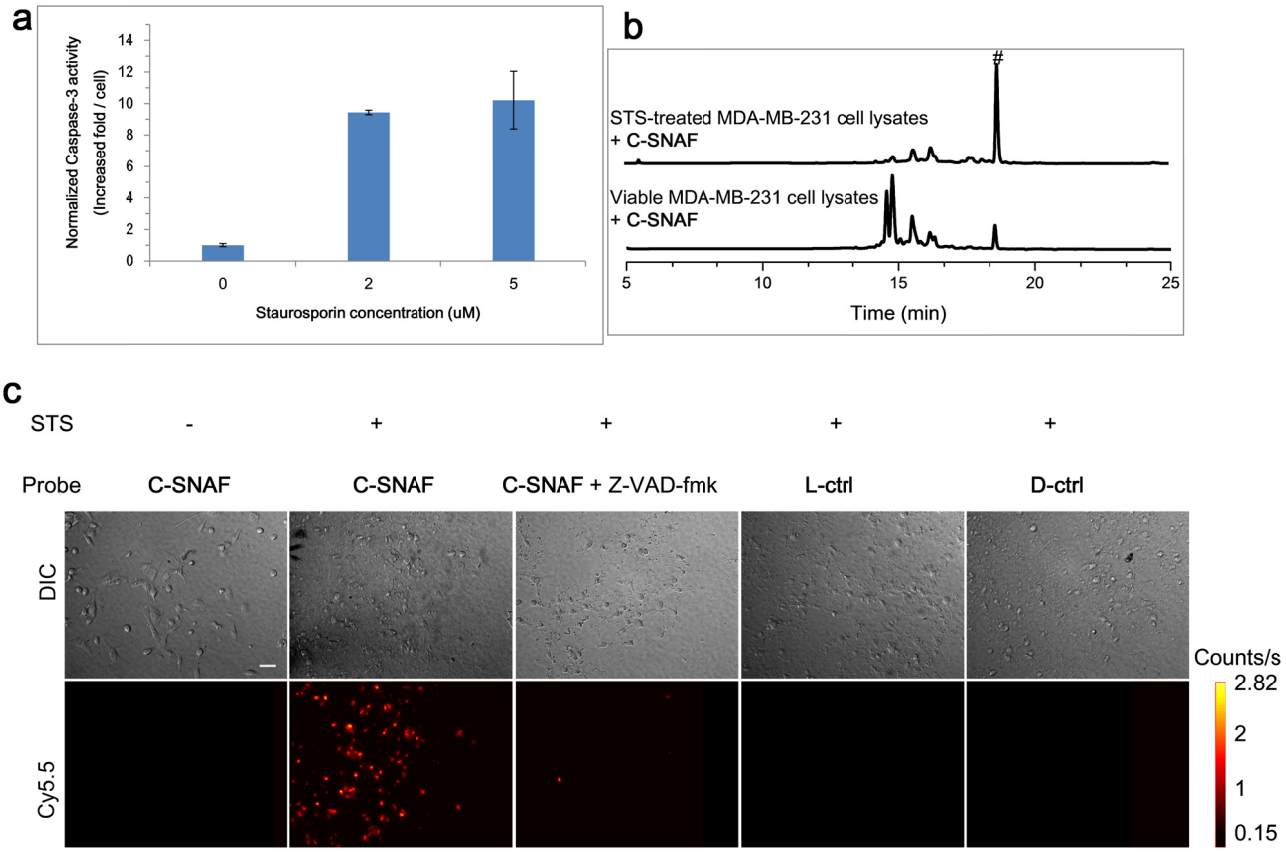

Supplementary Figure S16. Characterization of the molecular transformation of C-SNAF-SIM *in vitro*. **a**, The proposed caspase-3/7- and reduction-triggered macrocyclization of **C-SNAF-SIM** to **C-SNAF-SIM-*cycl***, followed by self-assembling into nano-aggregates. **b**, Time course of conversion (%) of **C-SNAF-SIM** to **C-SNAF-SIM-*cycl*** after incubation with caspase-3 (4.9 mU/ml, 0.735 μg/ml) based on HPLC assay, indicating a fast reaction triggered by reductant and caspase-3. **c**, HPLC traces of **C-SNAF-SIM** (red) in water, and **C-SNAF-SIM** (25 μM) following incubation with caspase-3 (4.9 mU/ml, 0.735 μg/ml) at 37 °C in caspase buffer at 0, 1, 1.5, 2, 3, 4 and 5 h. **C-SNAF-SIM** was first converted to its reduced intermediates (Peaks * and **) when pre-incubating in caspase buffer (with 10 mM TCEP) for 10 min (t = 0 h). Then, caspase-3 was added to trigger the reaction (proteolysis and cyclization), and the reaction was monitored by HPLC as indicated time point (Peaks # and ## indicate the cyclized products **C-SNAF-SIM-*cycl***, which are probable diastereoisomers arising from two different ring-closing orientations [S1]). **d**, DLS analysis of **C-SNAF-SIM** (25 μM) incubating with caspase-3 (0.735 μg/ml) in caspase buffer (pH 7.4) at 37 °C for 6 h, shows the formation of nanoparticles with an average diameter of 151± 53 nm. **e**, TEM image of nano-aggregates after incubation **C-SNAF-SIM** (25 μM) with recombinant human caspase-3 (0.735 μg/ml) at 37 °C in the caspase buffer overnight, showing the shape of nanoparticles with size of 143±27 nm.

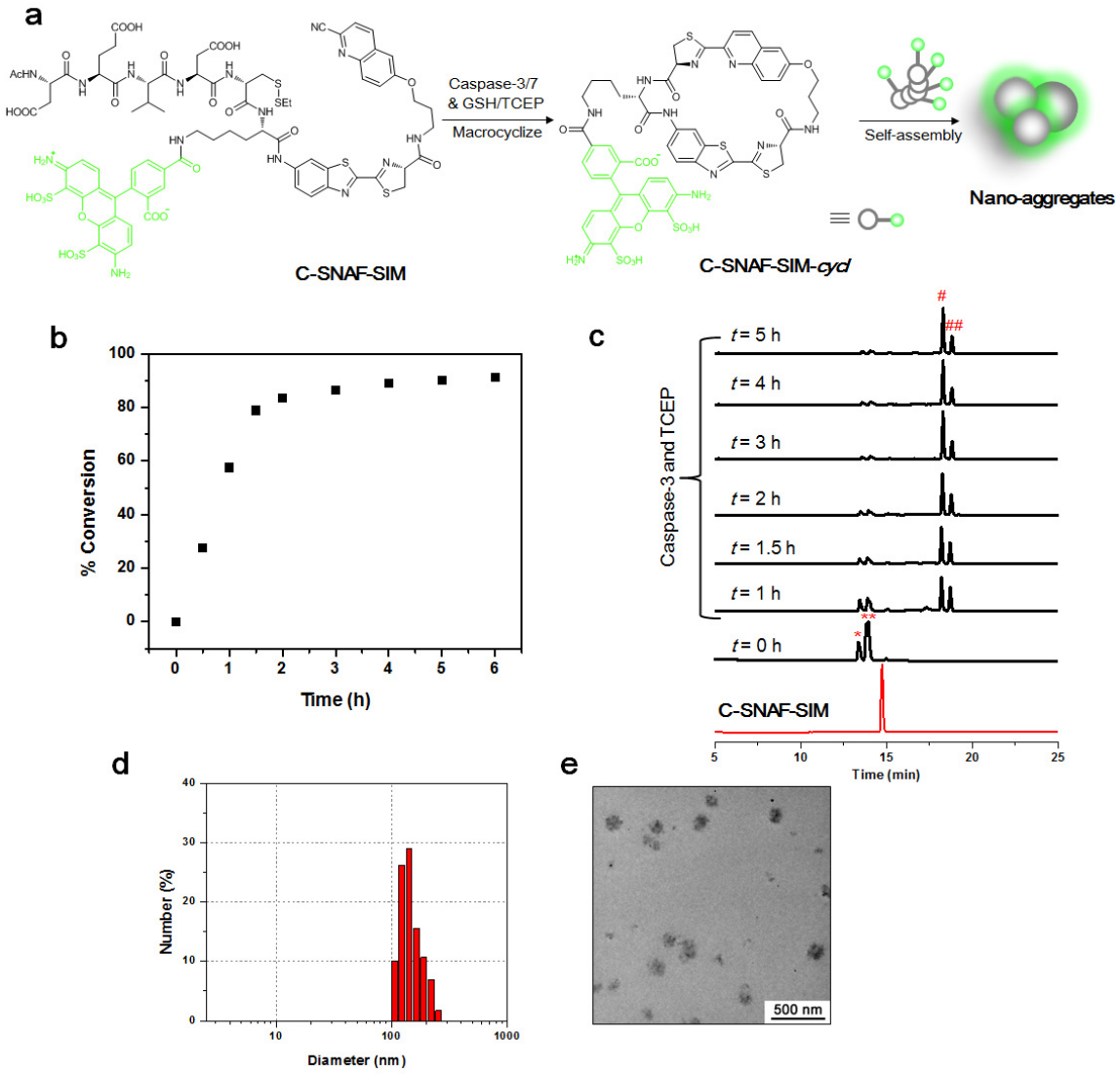

Supplementary Figure S17. Time-dependent nano-aggregation of C-SNAF-SIM following incubation with caspase-3 and TCEP. a & **b**, Plots of time-dependent change in DLS nanoparticle size (**a**) and count rates (**b**) of **C-SNAF-SIM** (25 μM) following incubation with caspase-3 (0.735 μg/ml) in caspase buffer. **c**, DLS analysis of **C-SNAF-SIM** (25 μM) following incubation with caspase-3 in caspase buffer at 0, 0.5, 1, 2, 3, 4, 5 and 6 h. There are obvious particles formed within 1 h with DLS measurement providing hydrodynamic radius ranging from 20 — 300 nm. The mean size of the nano-aggregates at 1 h is about 100 nm, which increased to ~130 nm after 2 h. The nano-aggregates size reached ~150 nm from 3 to 6 h incubation. In addition, the DLS count rates increased gradually from 87 to ~ 300 kcps after 6 h, indicating an increased concentration of particles in solution. These results suggest that the rate of caspase-3-triggered nano-aggregation correlates well with the enzymatic cleavage reaction rate in solution.

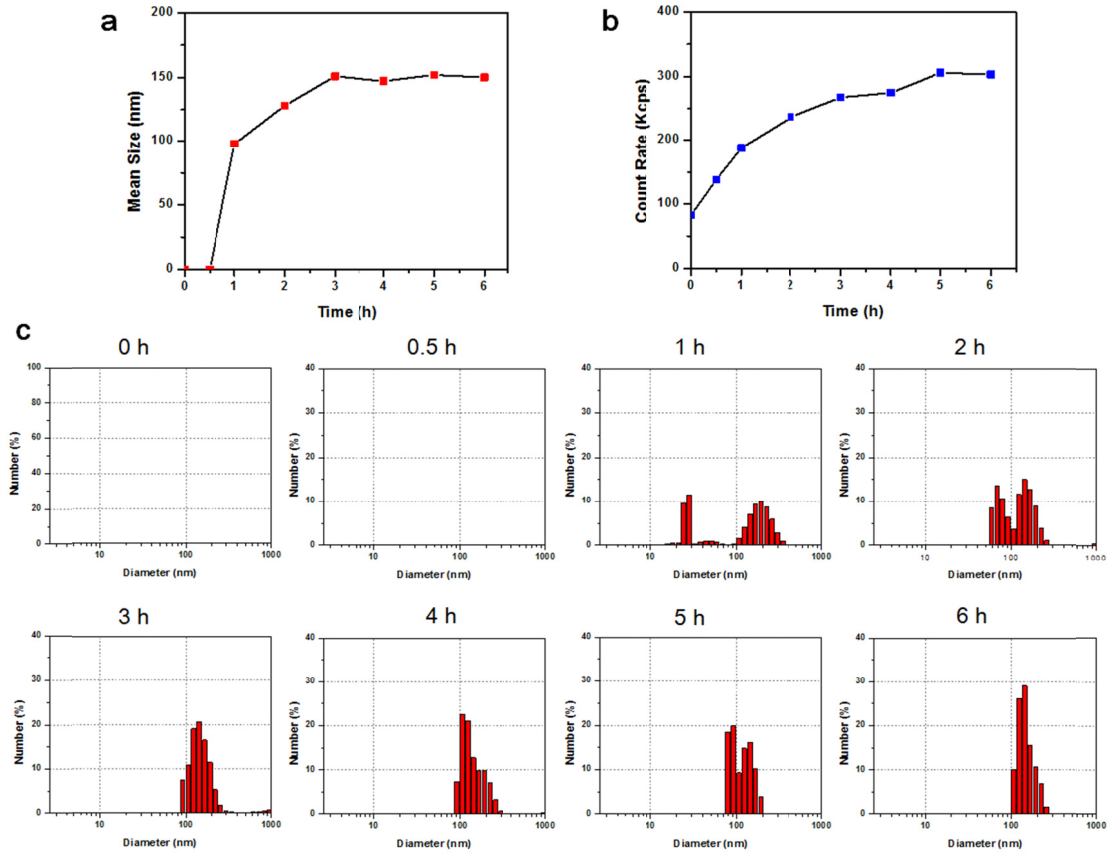

Supplementary Figure S18. Characterization of molecular transformation of L-ctrl-SIM *in vitro*. **a**, The chemical structure of **L-ctrl-SIM** and proposed caspase-3-triggered conversion of **L-ctrl-SIM** to peptide-cleaved product **L-ctrl-SIM'**. **b**, HPLC traces of **L-ctrl-SIM** (black, T_R = 13.8 min) and treatment of **L-ctrl-SIM** (25 μM) with caspase-3 (4.9×10^{-3} U/ml) in caspase buffer (pH 7.4) at 37 °C for 24 h (red, T_R = 16.7 min). **c**, DLS analysis of **L-ctrl-SIM** (25 μM) following incubation with caspase-3 in caspase buffer for 6 h, suggested no nanoparticles formed.

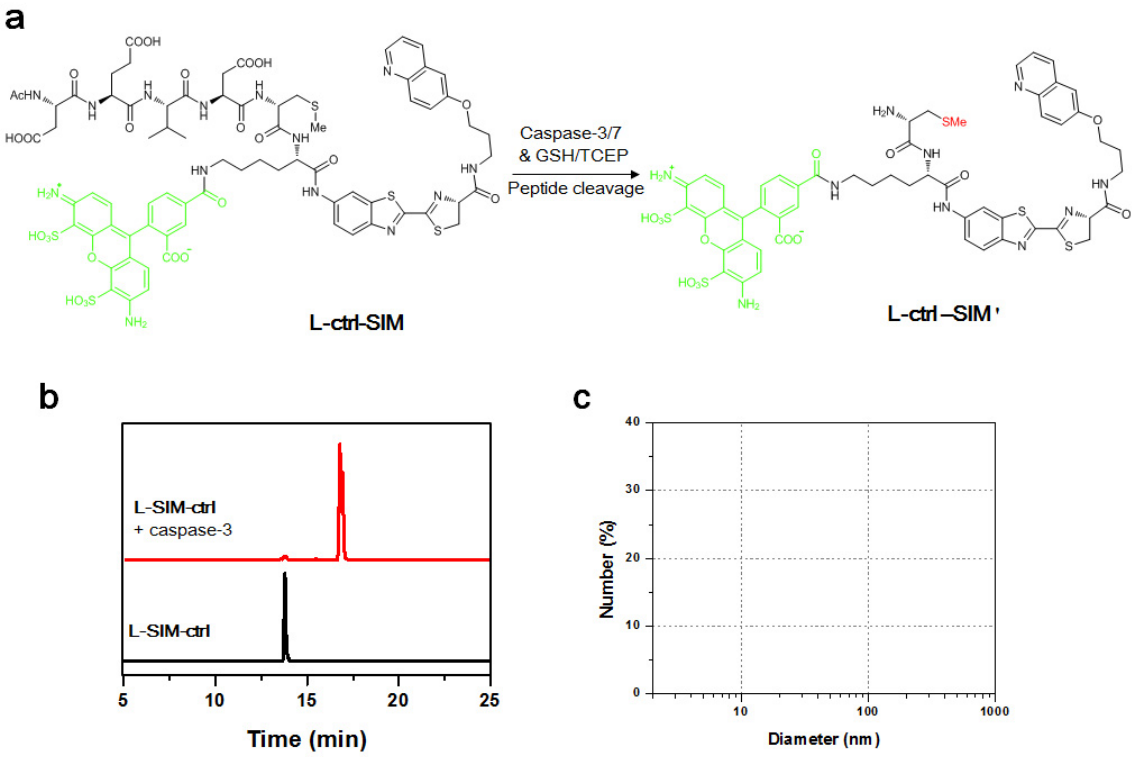

Supplementary Figure S19. 3D-SIM images of HeLa cells. a, Widefield images of viable or STS-treated HeLa cells incubated with **C-SNAF-SIM** or **L-ctrl-SIM** (2 μM). Cells were co-stained with DAPI. Green color indicates the Alexa 488 fluorescence from the probe, and blue color indicates the nucleus. **b-e**, Representative 3D-SIM images of viable cells incubated with **C-SNAF-SIM** (2 μM), showing weak and diffuse fluorescence in cells. Image in **e** is shown at the same intensity scale (1000 →4500) as that in **Fig. 4a** for **C-SNAF-SIM** in apoptotic cells. Images in **b-d** are shown at a lower intensity scale (87→1190). **f-i**, Representative 3D-SIM images of STS-treated cells incubated with **L-ctrl-SIM** (2 μM), showing weak and diffuse fluorescence in the cells. Image in **i** is shown at the same intensity scale (1000→4500) as that in **Fig. 4a** for **C-SNAF-SIM**. Images in **f-h** are shown at a lower intensity scale (200→2500). Neither the incubation of **C-SNAF-SIM** in viable cells nor **L-ctrl-SIM** in apoptotic cells could form fluorescence nano-aggregates compared to **C-SNAF-SIM** in apoptotic cells (**Fig. 4a)**.

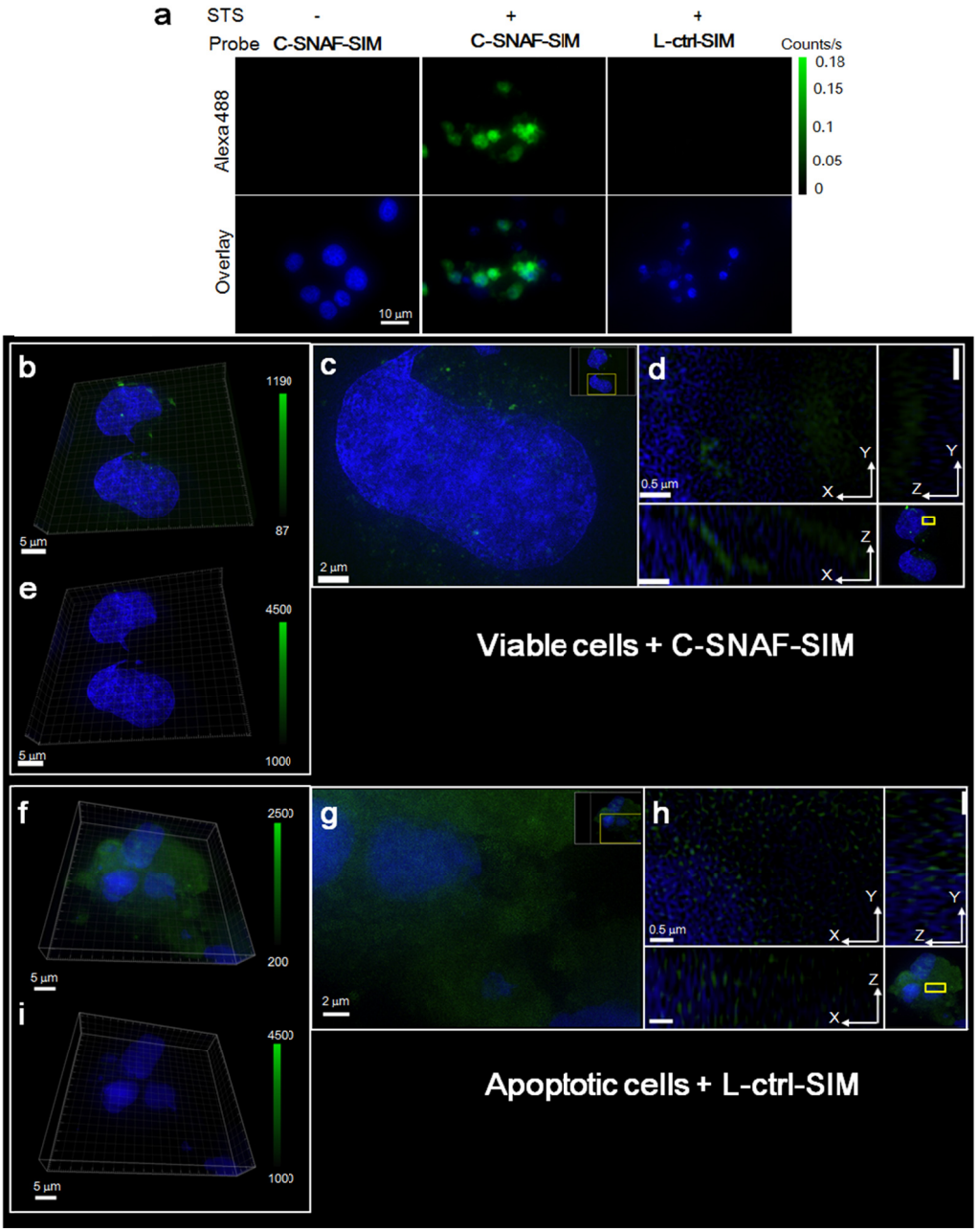

Supplementary Figure S20. Super-resolution imaging of reduction-induced nano-aggregates in apoptotic cells with 3D-SIM. **a**, Chemical structure of Alexa 488 labeled GSH-reducible probe **SIM-1** and control probe **SIM-ctrl**. **b**, Widefield images of STS-treated HeLa cells incubated with 0.5 μM of **SIM-1** or **SIM-ctrl**. **c**-**e**, Representative 3D-SIM images of self-assembled fluorescence nanoparticles in apoptotic cells incubated with **SIM-1**. The arrows in **e** show the views of individual fluorescent nanoparticles in XY, YZ, and XZ panels, respectively. **f-i**, 3D-SIM images of apoptotic cells incubated with **SIM-ctrl**. Image in **i** is shown at the same intensity scale (1800→6970) as that in **c** for **SIM-1**. Image at **f** is shown at a lower intensity scale (41→2660). SIM images showed the incubation of **SIM-1** (0.5 μM) with STS-treated HeLa cells resulted in obvious fluorescence nanoparticles inside cells, with an average size of ~180 nm on x-y plane, which was not observed in apoptotic cells incubated with **SIM-ctrl.**

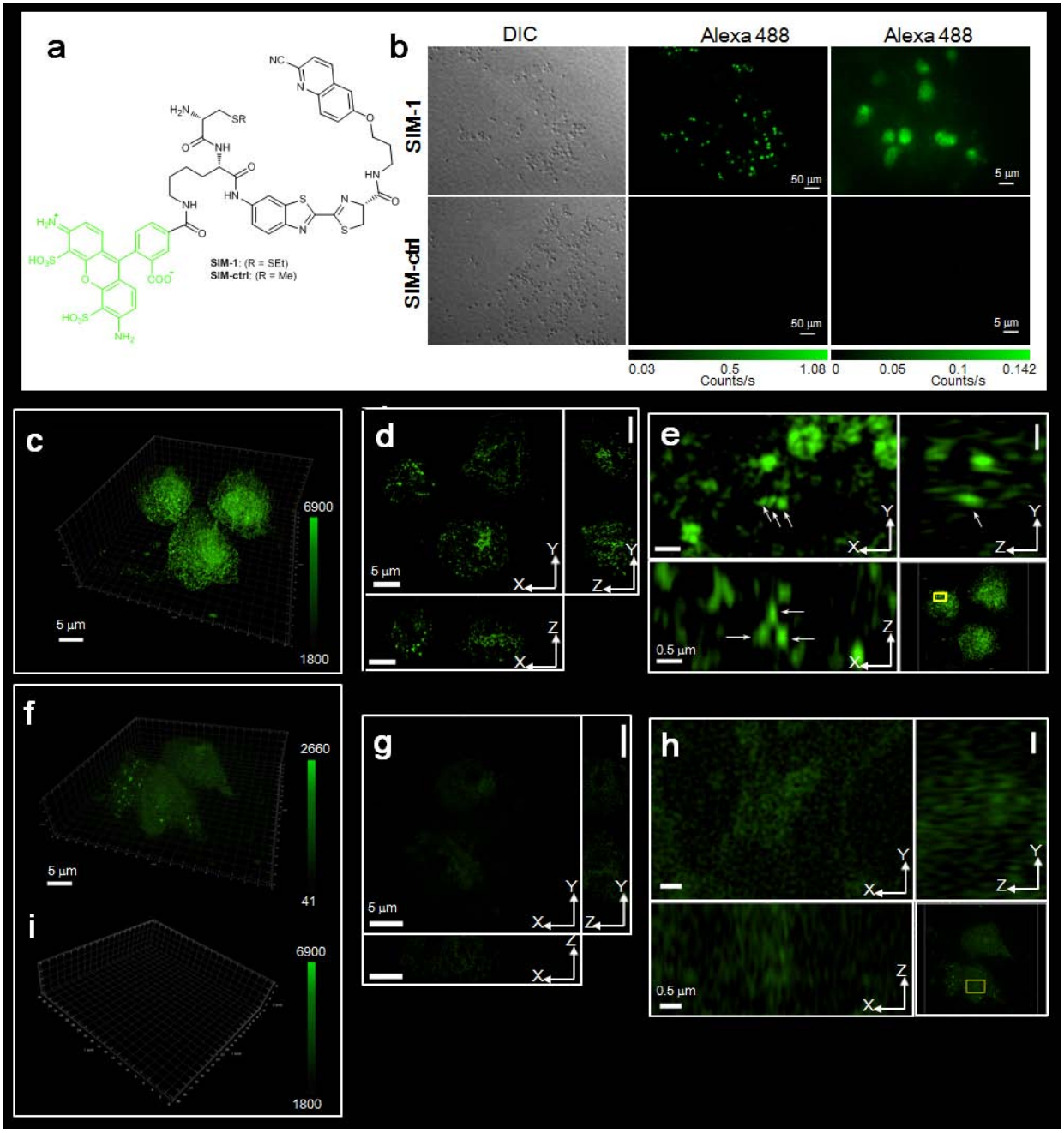

Supplementary Figure S21. 3D-SIM images of DOX-treated tumor tissues following i.v. injection of L-ctrl-SIM (20 nmol). a-d, Representative 3D-SIM images of tissue slice (10 μm thick) from DOX-treated tumor after i.v. injection of **L-ctrl-SIM** (20 nmol), showing weak and diffuse fluorescence. Image in **d** is shown at the same intensity scale (850→2000) as that in **Fig. 4b** for **C-SNAF-SIM**. Images in **a-c** are shown at a lower intensity scale (0→800).

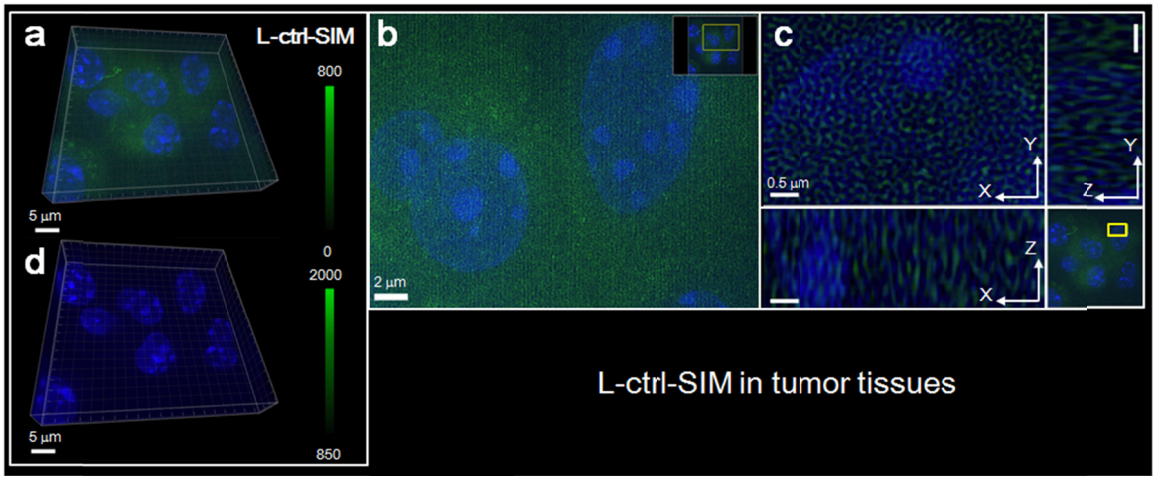

Supplementary Figure S22. Pharmacokinetics of the probes in mice. a, Blood Circulation study of **C-SNAF** (5 nmol) and **L-ctrl** (5 nmol) in healthy nude mice (n = 5). **b,** Biodistribution study of **C-SNAF** in healthy nude mice after i.v. administration of 5 nmol of **C-SNAF** at 2, 6, and 12 h. The amount of **C-SNAF** was measured based on the Cy 5.5 fluorescence intensity in collected blood and organs after i.v. administration.

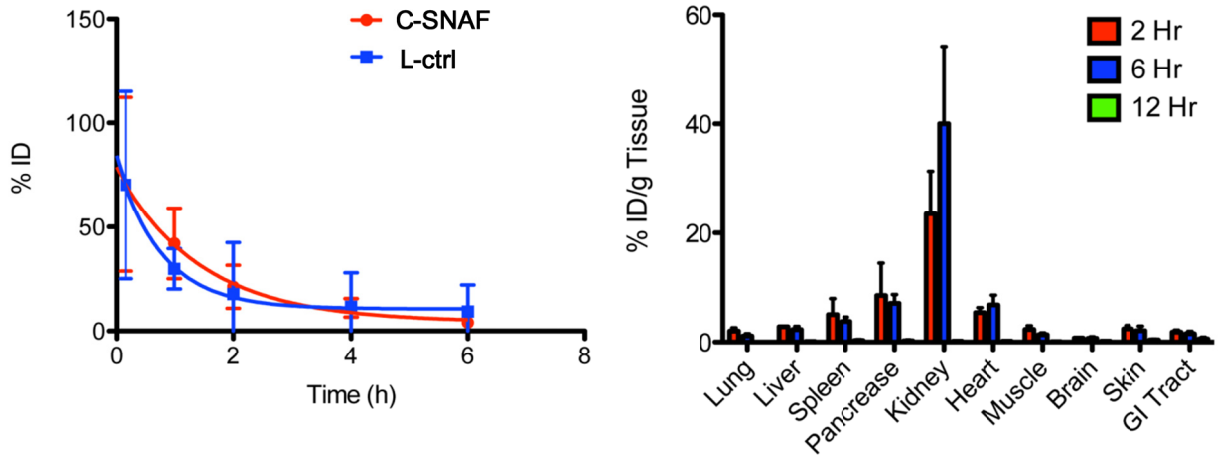

Supplementary Figure S23. The stability studies of probes in mouse serum assayed by HPLC. **a**, The percentage of probes remaining after incubation of respective 25 μM of **C-SNAF**, **D-ctrl, and L-ctrl** in mouse serum at 37 °C for different times. The percentage was obtained by calculating the percentage of peak area of each probe on the corresponding HPLC trace; error bar (S.D.) represents two separate experiments. **b-d**, Representative HPLC traces of 25 μM of **C-SNAF** (**b**), **L-ctrl** (**c**), or **D-ctrl** (**d**) incubated in mouse serum at 37 °C for different times (675 nm UV detector). **e** & **f**, MALDI-MS spectra of compounds corresponding to peaks * and # as observed in **b**. Peak * has a M.W. of 2284.61, indicating a side product corresponding to the coupling of **C-SNAF** to the free cysteine (calculated M.W. 2284.65, $[M+H]^+$); peak # has a M.W. of 2120.06, indicating a probable disulfide reduction intermediate (calculated M.W. 2120.40, $[M+H]^+$).

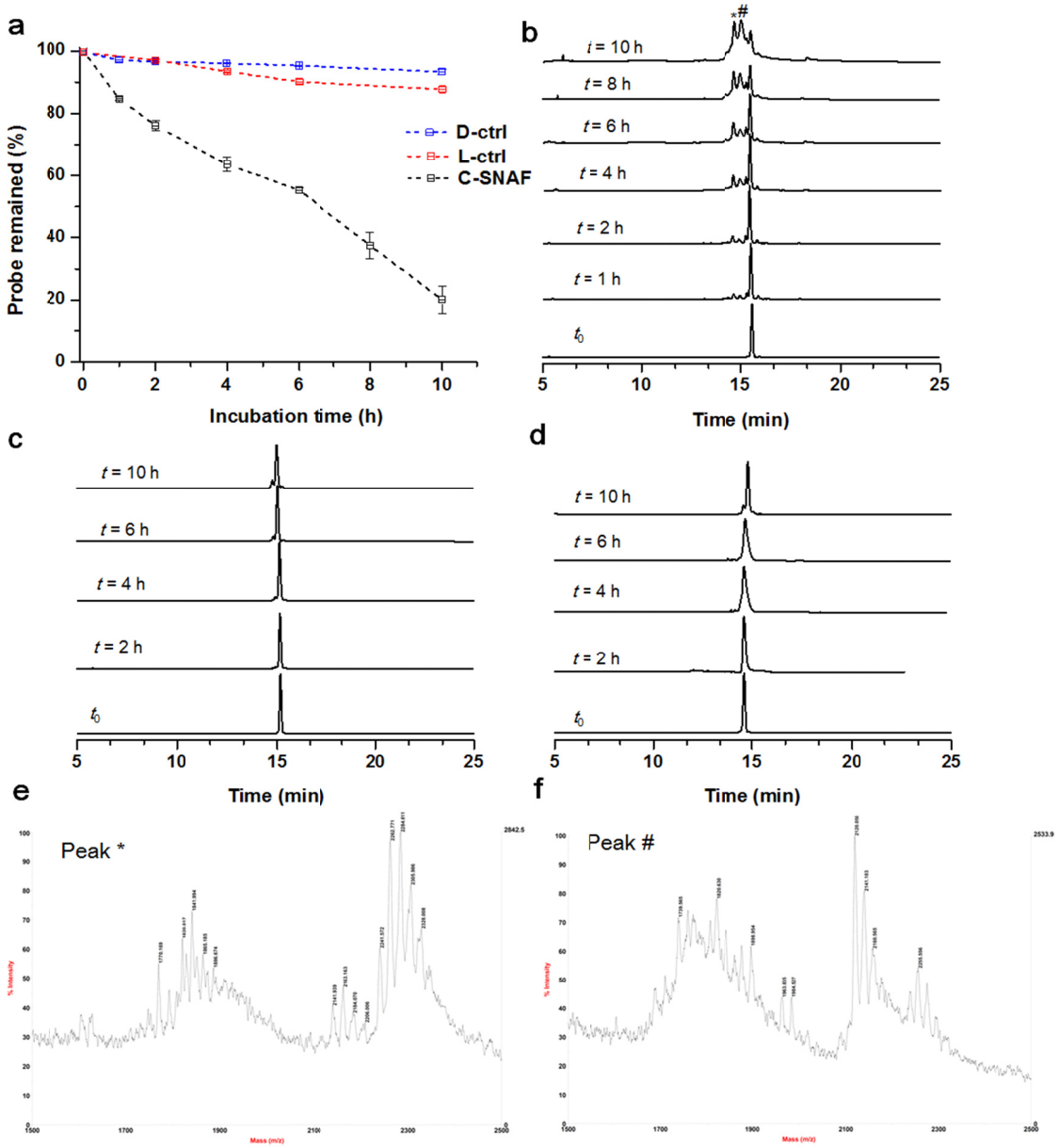

Supplementary Figure S24. Validation of HeLa tumor xenograft mouse model response to chemotherapy. a, Longitudinal monitoring of tumor size change shows a significant decrease in tumor growth rates for 3X DOX- (red, n = 19) relative to saline-treated (blue, n = 15) mice. **b**, Caspase-3/7 activity in tumor lysates shows a ~2-fold increase in 3X DOX- (red) versus saline-treated (blue) mice, which was inhibited by z-VAD-fmk (black). * $p<0.05$ for saline versus 3X DOX treatment, † $p<0.05$ for 3X DOX versus 3X DOX + z-VAD-fmk (n = 4 for all groups). These data confirm that the chosen dose and chemotherapeutic administration schedule is suitable for assessment of **C-SNAF** for monitoring cancer chemotherapeutic response *in vivo*.

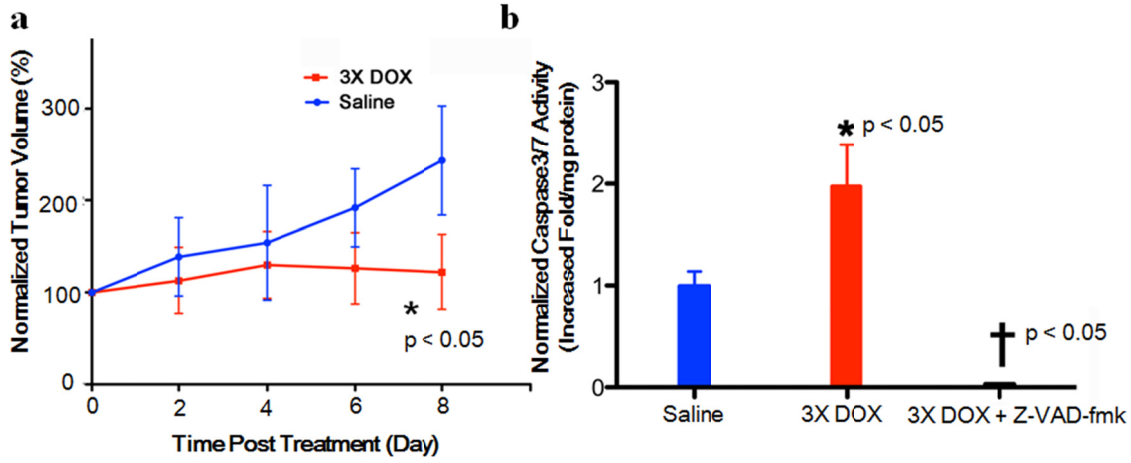

Supplementary Figure S25. The Comparison of tumor fluorescence in saline- and DOX-treated mice with C-SNAF, L-ctrl and D-ctrl. a-c, The average tumor fluorescence intensity (average scaled counts) in the saline- and DOX-treated mice during the time-course studies with i.v. administration of 5 nmol of **C-SNAF**, **L-ctrl** and **D-ctrl**; n = 5 for each. * $p<0.05$ indicates a significant difference in the tumor fluorescence from saline versus DOX treatment. **d** & **e**, Representative longitudinal fluorescence imaging of 3X DOX- (top) and saline-treated (bottom) tumor-bearing mice following i.v. administration of 5 nmol of **L-ctrl** and **D-ctrl**, respectively. Anatomical locations of the tumor and kidneys are indicated. The results showed that only **C-SNAF** is able to produce higher tumor fluorescence with significant difference between DOX- and saline-treated mice.

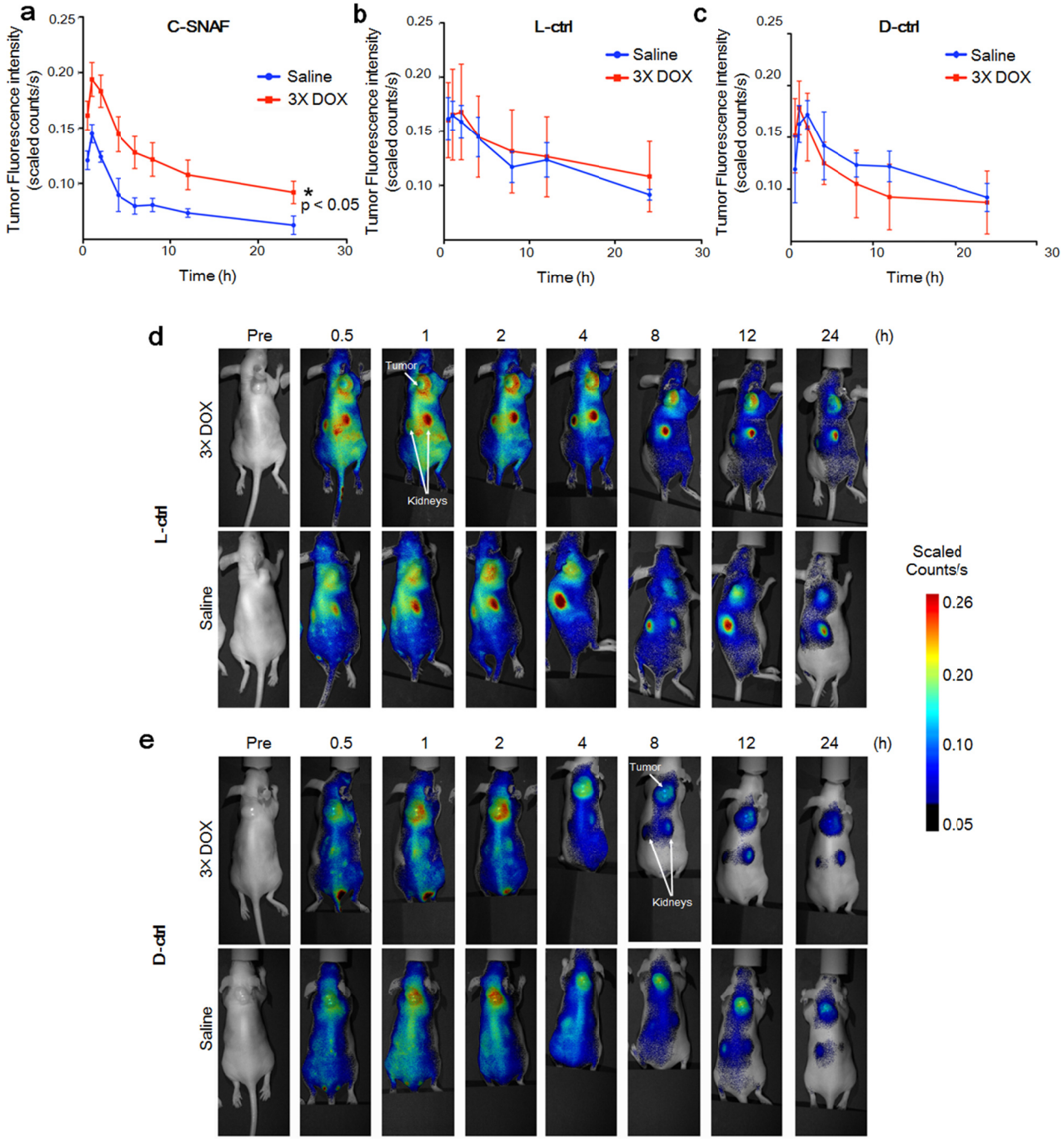

Supplementary Figure S26. Immunohistochemical analyses of L-ctrl and D-ctrl in tumor tissues. a&b, Immunohistochemical analysis of tumors resected from mice treated with saline (top) or 3X DOX (bottom) 4 h following administration of 5 nmol of **L-ctrl** (**a**) or **D-ctrl** (**b**). Tissue sections were stained for nuclei (blue) and active caspase-3 (green). The images showed that both **L-ctrl** and **D-ctrl** result in more fluorescence signal in saline-treated tumor tissues than **C-SNAF,** which is in good agreement with our whole animal imaging data. In contrast, there is less fluorescence signal and less co-localization between active caspase-3 and probe in DOX-treated tumor tissue following i.v. injection of **L-ctrl** or **D-ctrl** compared to **C-SNAF** (**Fig. 6a**).

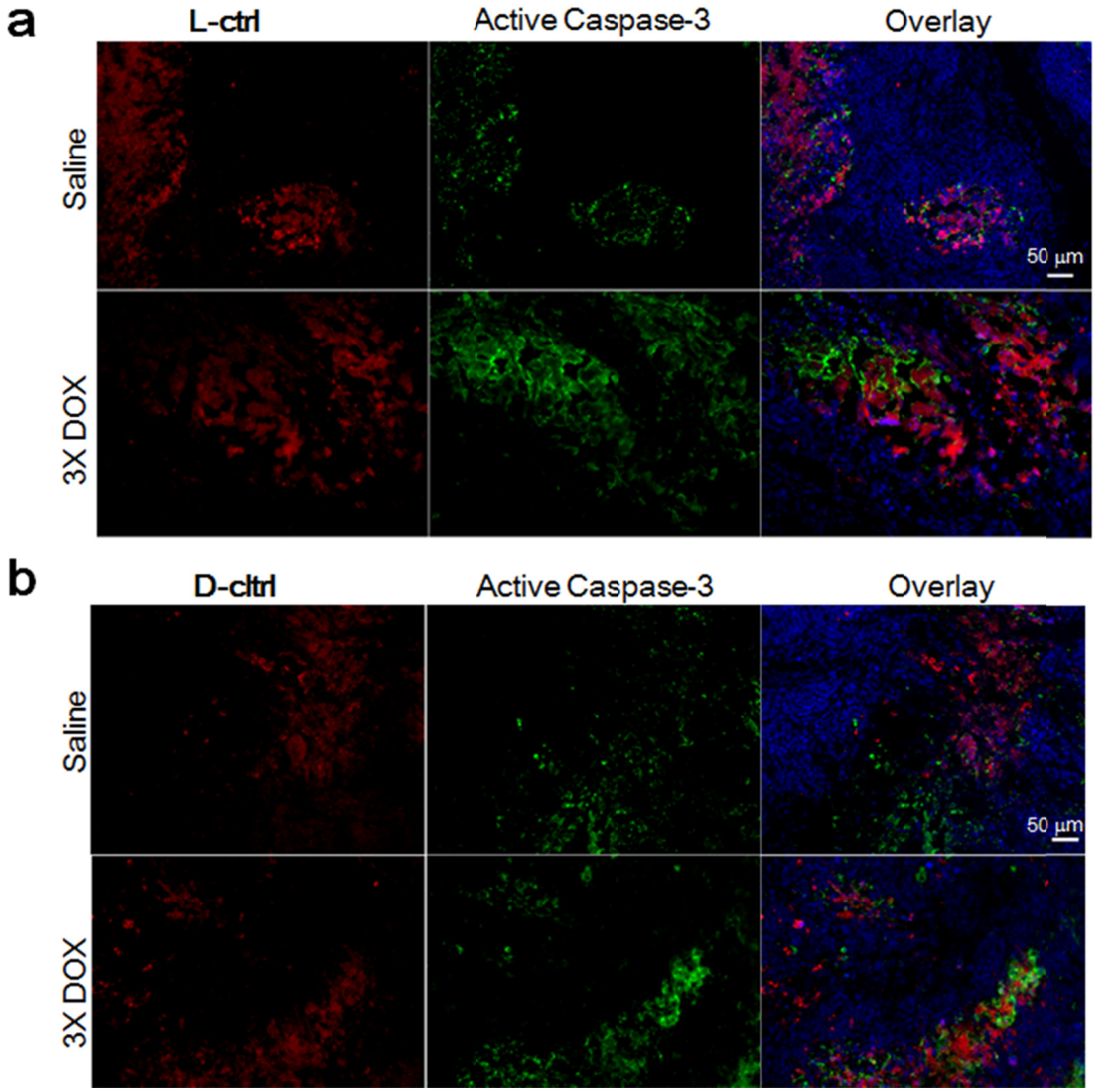

Supplementary Figure S27. Imaging of caspase-3/7 activity in tumor-bearing mice with quenched probe q-C-SNAF. a, Longitudinal fluorescence imaging of DOX- (top) and saline-treated (bottom) tumor-bearing mice with **q-C-SNAF** (5 nmol). **b**, The average tumor fluorescence intensity (average scaled counts) in the saline- and DOX-treated mice during the time-course studies with i.v. administration of 5 nmol of **q-C-SNAF**; n = 4 for each. * $p<0.05$ indicates a significant difference in the tumor fluorescence from saline versus DOX treatment. **c**, Quantification of tumor-to-background ratio in DOX- and saline-treated mice (n = 4) after i.v. injection of **q-C-SNAF**.

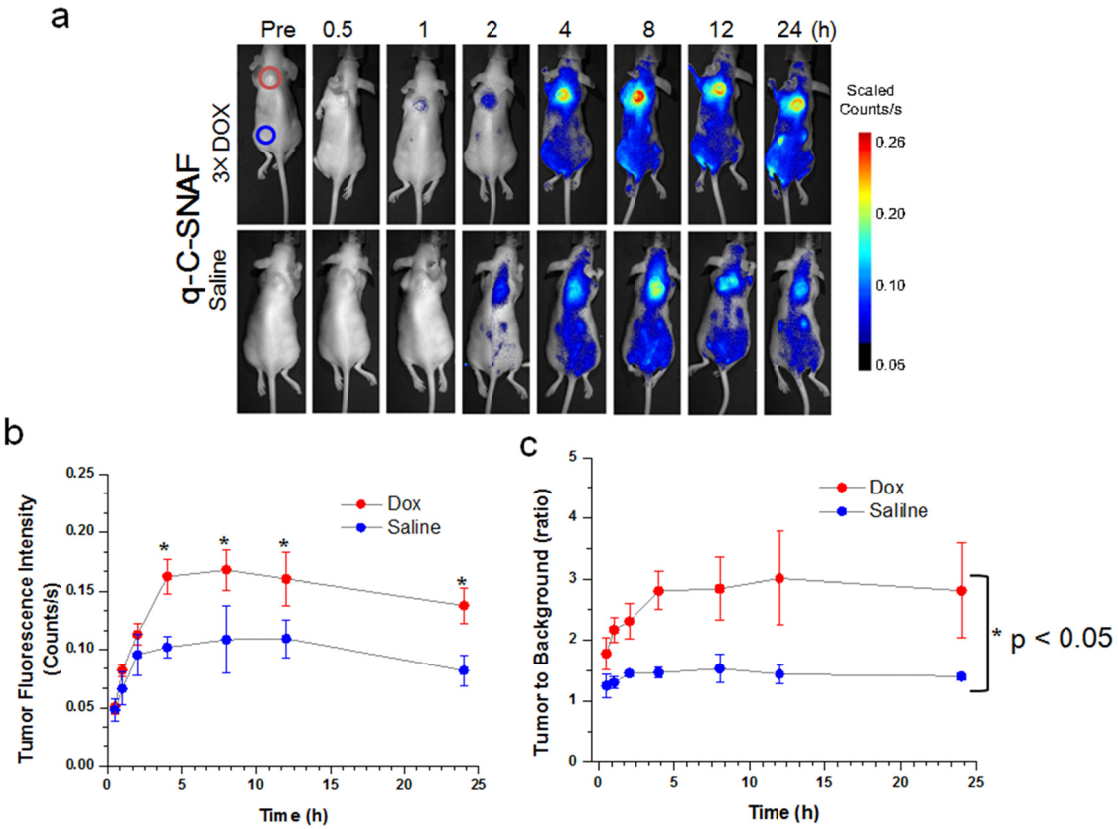

General methods

All chemicals were purchased from commercial sources (such as Aldrich, Anaspect and Chemimpex). Analytical TLC was performed with 0.25 mm silica gel 60F plates with fluorescent indicator (254 nm). Plates were visualized by ultraviolet light. The ^{1}H and ^{13}C NMR spectra were acquired on a Bruker 400 MHz magnetic resonance spectrometer. Data for ^{1}H NMR spectra are reported as follows: chemical shifts are reported as δ in units of parts per million (ppm) relative to chloroform-d (δ 7.26, s); multiplicities are reported as follows: s (singlet), d (doublet), t (triplet), q (quartet), dd (doublet of doublets), m (multiplet), or br (broadened); coupling constants are reported as a *J* value in Hertz (Hz); the number of protons (n) for a given resonance is indicated nH, and based on the spectral integration values. MALDI-MS spectrometric analyses were performed at the Mass Spectrometry Facility of Stanford University. HPLC was performed on a Dionex HPLC System (Dionex Corporation) equipped with a GP50 gradient pump and an in-line diode array UV-Vis detector. A reversed-phase C18 (Phenomenax, 5 μm, 4.6 × 250 mm, 5 μm, 10 × 250 mm or 21.2 × 250 mm) column was used for analysis and semi-preparation. UV absorbance of the probe was recorded on an Agilent 8453 UV spectrophotometer. Fluorescence was recorded on a Fluoromax-3 spectrafluorometer (Jobin Yvon). TEM micrographs were obtained on a JEM 1230 Electron Microscope. DLS was performed on a Malvern ZetaSizer-90 instrument. Flow cytometry analysis of cells was run on the BD FACScan Aria analyzer. Fluorescent microscopy images were acquired on an Olympus inverted fluorescence microscope (IX2-UCB) equipped with a Nuance multispectral imaging camera. Super-resolution images were acquired by 3D-SIM using a DeltaVision OMX imaging system (Applied precision). Live animal fluorescence imaging was performed on a Maestro hyperspectral fluorescent imaging system (PerkinElmer, MA, USA) using a 635±25 nm excitation filter and a 675 nm long-pass emission filter, with images acquired from 670 to 900 nm.

Chemical synthesis and characterization of C-SNAF

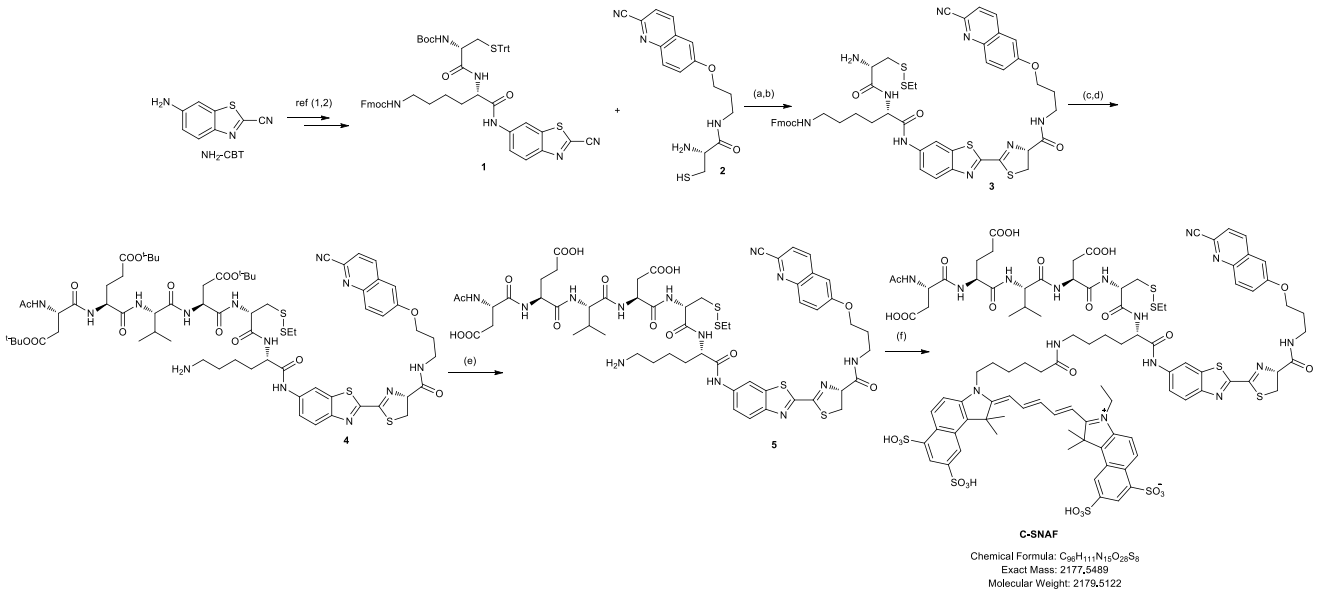

Scheme S1. Synthesis of **C-SNAF**. Reaction conditions: (a) TCEP, DIPEA, DCM/MeOH, Ar, r.t. 1 h; (b) (i) 20% TFA/DCM; (ii) PySSEt, MeOH, 71%; (c) Ac-Asp(O^{t}Bu)-Glu(O^{t}Bu)-Val-Asp(O^{t}Bu)-COOH, HBTU, DIPEA, THF; (d) piperidine, DMF, 43% in two steps; (e) TFA/TIPSH/DCM (95%/2.5%/2.5%), 83%; (f) Cy 5.5-NHS, DMF, DIPEA, 53%.

Synthesis of compound **1**: Starting from NH_2-CBT, compound **1** was obtained as a white solid according to methods reported previously [ref s1 and s2]. ^{1}H NMR (400 MHz, $CDCl_3$) δ 9.71 (s, 1H), 8.48 (s, 1H), 7.87 (d, J = 9.0 Hz, 1H), 7.64 (d, J = 7.5 Hz, 2H), 7.54 (m, 2H), 7.47 (d, J = 7.2 Hz, 2H), 7.35 – 7.23 (m, 8H), 7.22 – 7.05 (m, 11H), 4.44 (m, 1H), 4.25 (d, J = 6.9 Hz, 2H), 4.11 – 4.01 (m, 1H), 3.84 (m, 3H), 3.01 (m, 2H), 2.52 (m, 2H), 1.87 (s, br, 1H), 1.65 (m, 1H), 1.42 (m, 2H), 1.32 (s, 9H); ^{13}C NMR (101 MHz, $CDCl_3$) δ 171.87, 171.07, 157.30, 155.97, 148.56, 144.40, 144.01, 141.37, 139.00, 136.66, 135.18, 129.59, 128.20, 127.83, 127.18, 127.10, 125.13, 125.02, 121.40, 120.08, 113.20, 111.71, 80.70, 67.25, 66.71, 54.21, 54.12, 49.77, 49.56, 49.34, 49.13, 48.92, 48.70, 48.49, 40.33, 33.74, 31.39, 29.40, 28.70, 28.31, 22.68. MS: calcd. for $C_{56}H_{55}N_6O_6S_2$ [$(M+H)^+$]: 971.4; found MALDI-MS: m/z 971.

Synthesis of compound **3**: To a solution of **1** (0.3 mmol), tris(2-carboxyethyl) phosphine hydrochloride (TCEP, 0.3 mmol), and DIPEA (1.8 mmol) in 20 ml CH_2Cl_2/MeOH (1/1) under N_2 at room temperature was added a solution of **2** (0.33 mmol) in MeOH dropwise, and the mixture was kept

stirring at r.t. for 30 min. After the reaction was completed, the solvent was removed under vacuum, and the residue was dissolved in ethyl acetate (EA, 30 ml). The solution was washed with water (2 × 20 ml), brine, and dried with Na_2SO_4. After removal of EA, the residue was directly dissolved in 20% TFA/CH_2Cl_2 solution, and the mixture was kept stirring at r.t. for another 1 h to completely deprotect the Boc and Trt groups. The solvent was removed, and cold Et_2O (35 ml) was added to precipitate the intermediate. After centrifugation (2500 rmp), the precipitate was dissolved in MeOH, to which was added PySSEt (0.4 mmol), and the reaction was continued for another 20 min. After the reaction, MeOH was removed, and the residue was precipitated with cold Et_2O (35 ml), followed by purification by silica gel chromatography with eluent of CH_2Cl_2/MeOH (40/1 to 20/1) to afford compound **3** as light yellow foam. ^{1}H NMR (400 MHz, DMSO-d_6) δ 10.63 (s, 1H), 9.10 (d, J = 7.5 Hz, 1H), 8.54 (s, 1H), 8.41 (m, 4H), 8.31 (t, J = 5.6 Hz, 1H), 8.06 (d, J = 8.9 Hz, 1H), 7.97 (d, J = 9.3 Hz, 1H), 7.90 (d, J = 8.5 Hz, 1H), 7.84 (d, J = 7.5 Hz, 2H), 7.68 (d, J = 9.1 Hz, 1H), 7.63 (d, J = 7.4 Hz, 2H), 7.53 (dd, J = 9.3, 2.6 Hz, 1H), 7.44 (d, J = 2.6 Hz, 1H), 7.37 (t, J = 7.4 Hz, 2H), 7.28 (m, 3H), 5.32 (t, J = 9.3 Hz, 1H), 4.51 (dd, J = 13.6, 7.4 Hz, 1H), 4.24 (d, J = 6.9 Hz, 2H), 4.21 – 4.10 (m, 5H), 3.74 – 3.61 (m, 2H), 3.10 – 3.24 (m, 2H), 2.97 (m, 3H), 2.75 (q, J = 8 Hz, 2H), 2.08 – 1.96 (m, 2H), 1.70 (m, 3H), 1.41 (m, 3H), 1.25 (t, J = 8 Hz, 3H). MS: calcd. for $C_{50}H_{52}N_9O_6S_4$ [$(M+H)^+$]: 1002.3; found ESI-MS: m/z 1002.7.

Synthesis of **4**: A solution of **3** (0.1 mmol), Ac-Asp(O^{t}Bu)-Glu(O^{t}Bu)-Val-Asp(O^{t}Bu)-COOH (1.05 equiv.), HBTU (1.1 equiv.), and DIPEA (2.0 equiv.) in dry THF (20 ml) was stirred at r.t. for 2~3 h. After the reaction was completed, THF was removed. The residue was purified with a short silica gel column with an eluent of CH_2Cl_2/MeOH (15/1), which was followed by deprotection of the Fmoc-group with 5% piperidine in DMF at r.t. for 10 min. The reaction was quenched with 1 N HCl, and purified by HPLC to result in compound **4** after lyophilization. A combined yield of 43% was obtained for the two steps. ^{1}H NMR (400 MHz, DMSO-d_6) δ 10.42 (s, 1H), 8.60 (dd, J = 7.9, 1.8 Hz, 1H), 8.43 (d, J = 8.5 Hz, 2H), 8.31 (m, 2H), 8.19 (m, 2H), 8.06 (d, J = 8.9 Hz, 1H), 8.01 – 7.86 (m, 3H), 7.80 – 7.60 (m, 5H), 7.53 (dd, J = 9.3, 2.7 Hz, 1H), 7.45 (d, J = 2.1 Hz, 1H), 5.31 (t, J = 9.2 Hz, 1H), 4.62 – 4.47 (m, 3H), 4.42 (s, br, 1H), 4.32 (s, br, 1H), 4.19 (t, J = 6.1 Hz, 2H), 4.14 – 4.02 (m, 1H), 3.84 – 3.61 (m, 10H), 3.06 (m, 1H), 2.99 – 2.90 (m, 1H), 2.81 – 2.73 (m, 2H), 2.69 (m, 2H), 2.59 (dd, J = 15.9, 5.3 Hz, 1H), 2.44 – 2.35 (m, 1H), 2.13 (m, 2H), 2.02 (m, 2H), 1.92 – 1.79 (m, 5H), 1.67

(s, br, 2H), 1.54 (m, 2H), 1.46 – 1.26 (m, 29H), 1.21 (t, *J* = 8.0 Hz, 3H), 0.84 – 0.68 (m, 6H). ^{13}C NMR (101 MHz, DMSO-*d*6) δ 172.44, 171.66, 171.44, 171.29, 171.03, 170.20, 170.06, 169.96, 169.80, 164.89, 159.84, 159.38, 159.14, 158.81 (TFA), 149.33, 144.30, 138.74, 137.20, 136.96, 131.38, 131.00, 130.58, 125.38, 124.87, 124.79, 120.37, 118.60, 112.15, 106.86, 80.92, 80.77, 80.20, 79.96, 66.78, 63.74, 58.27, 54.06, 53.06, 52.46, 50.38, 50.13, 41.27, 39.35, 37.99, 36.71, 35.27, 32.26, 31.90, 31.28, 29.12, 28.31, 27.86, 27.30, 23.15, 23.02, 19.76, 18.72, 14.93. MS: calcd. for $C_{67}H_{94}N_{13}O_{15}S_4$ [$(M+H)^+$]: 1448.6; found MALDI-MS: m/z 1449.1.

Synthesis of **5**: Compound **4** was deprotected using a solution of TFA/CH_2Cl_2/TIPSH (95/2.5/2.5) at r.t. for 3 h. After the solvent was removed, cold Et_2O was added, and the precipitate was dried under vacuum to give compound **5** in 83% yield without further purification. ^{1}H NMR (400 MHz, DMSO-d_6) δ 10.37 (s, 1H), 8.59 (d, *J* = 9.7 Hz, 1H), 8.43 (d, *J* = 8.0 Hz, 2H), 8.36 – 8.13 (m, 4H), 8.12 – 7.86 (m, 5H), 7.66 (m, 5H), 7.53 (d, *J* = 9.2 Hz, 1H), 7.46 (s, 1H), 5.30 (t, *J* = 9.0 Hz, 1H), 4.66 – 4.27 (m, 5H), 4.18 (s, br, 2H), 4.13 – 4.04 (m, 1H), 3.36 (m, 3H), 3.15 – 3.02 (m, 1H), 2.96 (m, 1H), 2.85 – 2.64 (m, 5H), 2.56 (m, 2H), 2.44 (m, 1H), 2.16 (m, 2H), 2.09 – 1.63 (m, 11H), 1.54 (s, br, 2H), 1.37 (m, 2H), 1.21 (t, *J* = 6.9 Hz, 3H), 0.77 (m, 6H); ^{13}C NMR (101 MHz, DMSO) δ 174.81, 172.40, 172.36, 171.82, 171.70, 171.42, 170.31, 169.81, 164.92, 159.87, 159.39, 149.32, 144.30, 138.72, 137.22, 136.99, 131.39, 131.01, 130.58, 125.40, 124.89, 124.81, 120.39, 118.62, 112.18, 106.87, 79.94, 66.76, 58.39, 54.10, 53.19, 52.65, 50.48, 50.29, 39.38, 36.70, 36.64, 36.48, 35.30, 32.28, 31.75, 31.11, 30.73, 29.11, 27.51, 27.30, 23.17, 23.05, 19.76, 18.71, 14.96. MS: calcd. for $C_{55}H_{70}N_{13}O_{15}S_4$ [$(M+H)^+$]: 1280.4; found MALDI-MS: m/z 1280.8.

Synthesis of **C-SNAF**: To a solution of **5** (4 mg) in dry DMF (0.3 ml) was added Cy5.5-mono NHS ester (1.5 mg) and DIPEA (5 μl), and the mixture was kept stirring at r.t. for a further 1 h. After the reaction was completed, the mixture was purified by HPLC to afford **C-SNAF** in 53% yield. > 99% purity was achieved after purification. MS: calcd. for $C_{96}H_{112}N_{15}O_{28}S_8$ [$(M+H)^+$]: 2178.6; found MALDI-MS: m/z 2178.7.

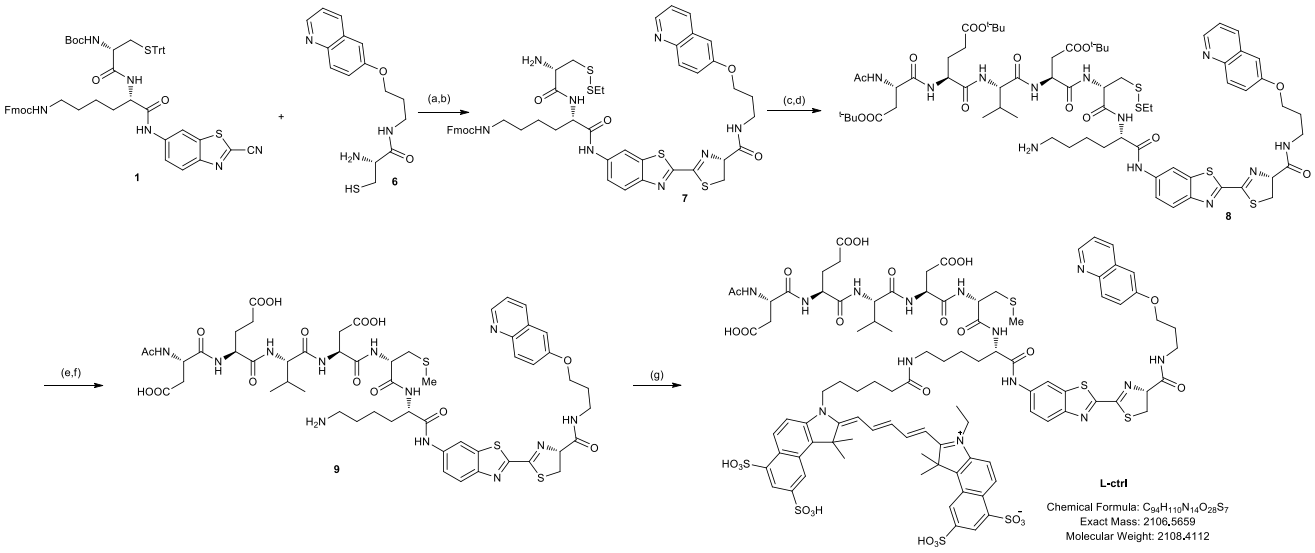

Scheme S2. Synthesis of **L-ctrl**. Reaction conditions: (a) TCEP, DIPEA, DCM/MeOH, Ar, r.t. 1 h; (b) (i) 20% TFA/DCM; (ii) PySSEt, MeOH; (c) Ac-Asp(O^{t}Bu)-Glu(O^{t}Bu)-Val-Asp(O^{t}Bu)-COOH, HBTU, DIPEA, THF; (d) piperidine, DMF, 43% in two steps; (e) TFA/TIPSH/DCM (95%/2.5%/2.5%), 81%; (f) TCEP, $NaHCO_3$, MeI, 91%; (g) Cy 5.5-NHS, DMF, DIPEA, 51%.

Synthesis of **7**: A solution of **1** (0.3 mmol), **6** (0.33 mmol), tris(2-carboxyethyl) phosphine hydrochloride (TCEP, 0.3 mmol), and DIPEA (1.8 mmol) in 20 ml CH_2Cl_2/MeOH (1/1) was stirred at room temperature for 30 min. After the reaction was completed, the solvent was removed under vacuum, and the residue was dissolved in ethyl acetate (EA, 30 ml). The solution was washed with water (2 × 20 ml), brine, and dried with Na_2SO_4. After removal of EA, the residue was directly dissolved in 20% TFA/CH_2Cl_2, and the mixture was kept stirring at r.t. for another 1 h to completely deprotect the Boc and Trt groups. The solvent was removed, and cold Et_2O (35 ml) was added to precipitate the intermediate. After centrifugation (2500 rmp), the precipitate was dissolved in MeOH, to which was added PySSEt (0.4 mmol), and the reaction was continued for another 20 min. After the reaction, MeOH was removed, and the residue was precipitated with cold Et_2O (35 ml), followed by purification by silica gel chromatography with eluent of CH_2Cl_2/MeOH (30/1 to 15/1) to afford compound **7** as light yellow foam. ^{1}H NMR (400 MHz, DMSO-d_6) δ 10.64 (s, 1H), 9.13 (d, J = 7.3 Hz, 1H), 8.94 (d, J = 4.3 Hz, 1H), 8.63 (d, J = 8.3 Hz, 1H), 8.54 (s, 1H), 8.44 (s, br, 2H), 8.34 (t, J = 5.5 Hz, 1H), 8.06 (dd, J = 9.0, 2.3 Hz, 2H), 7.83 (d, J = 7.5 Hz, 2H), 7.75 (m, 1H), 7.62 (m, 4H), 7.53 (d, J = 2.5 Hz, 1H), 7.36 (t, J = 7.4 Hz, 2H), 7.28 (m 3H), 5.33 (t, J = 9.2 Hz, 1H), 4.51 (m, 1H), 4.31 – 4.07 (m, 6H), 3.79 – 3.60 (m, 2H), 3.18 (m, 2H), 2.98 (m, 2H), 2.74 (m, 2H), 2.13 – 1.95 (m, 2H),

1.75 (m, 2H), 1.54 – 1.24 (m, 6H), 1.24 (t, J = 7.2 Hz, 3H); ^{13}C NMR (101 MHz, DMSO) δ 171.30, 169.80, 167.60, 164.92, 159.88, 159.52, 159.19 (TFA), 158.29, 156.76, 149.38, 145.20, 144.55, 141.37, 141.03, 138.71, 138.46, 136.95, 130.47, 128.23, 127.67, 126.34, 125.92, 125.76, 124.91, 122.69, 120.76, 120.41, 112.24, 107.49, 79.96, 66.73, 65.87, 54.63, 51.86, 47.41, 39.54, 36.72, 35.30, 32.34, 31.93, 29.74, 29.14, 23.34, 14.76. MS: calcd. for $C_{49}H_{53}N_8O_6S_4$ [$(M+H)^+$]: 977.3; found ESI-MS: m/z 978.1.

Synthesis of **8**: A solution of **7** (0.1 mmol), Ac-Asp(O^{t}Bu)-Glu(O^{t}Bu)-Val-Asp(O^{t}Bu)-COOH (1.05 equiv.), HBTU (1.1 equiv.), and DIPEA (2.0 equiv.) in dry THF (20 ml) was kept stirring at r.t. for 2~3 h. After the reaction was completed, THF was removed. The residue was purified with a short silica gel column with CH_2Cl_2/MeOH (15/1) as eluent, which was followed by deprotection of the Fmoc-group with 5% piperidine in DMF at r.t. for 10 min. The reaction was quenched with 1 N HCl, and purified by HPLC to provide compound **4** after lyophilization (51% yield in two steps). ^{1}H NMR (400 MHz, DMSO-d_6) δ 10.43 (s, 1H), 8.90 (d, J = 4.7 Hz, 1H), 8.64 – 8.52 (m, 2H), 8.46 (m, 1H), 8.31 (m, 2H), 8.21 (m, 2H), 8.10 – 7.91 (m, 3H), 7.89 – 7.62 (m, 6H), 7.56 (dd, J = 9.2, 2.5 Hz, 1H), 7.51 (d, J = 2.3 Hz, 1H), 5.31 (t, J = 9.2 Hz, 1H), 4.54 (m, 3H), 4.42 (s, br, 1H), 4.34 (m, 1H), 4.17 (t, J = 6.1 Hz, 2H), 4.13 – 4.06 (m, 1H), 3.78 – 3.58 (m, 2H), 3.47 (t, J = 5.3 Hz, 1H), 3.15 – 3.03 (m, 1H), 2.95 (m, 1H), 2.84 – 2.64 (m, 5H), 2.60 (dd, J = 15.8, 5.1 Hz, 1H), 2.48 – 2.35 (m, 2H), 2.24 – 2.08 (m, 2H), 2.02 (m, 2H), 1.95 – 1.76 (m, 6H), 1.70 (s, br, 2H), 1.55 (m, 2H), 1.50 – 1.26 (m, 30H), 1.25 – 1.17 (m, 3H), 0.75 (m, 6H); ^{13}C NMR (101 MHz, DMSO) δ 172.44, 171.67, 171.46, 171.30, 171.04, 170.23, 170.08, 169.96, 169.81, 164.89, 159.82, 159.77, 159.44, 159.10, 158.76 (TFA), 158.11, 149.32, 145.79, 140.09, 139.48, 138.76, 136.96, 130.35, 127.15, 125.41, 124.86, 122.63, 120.38, 118.59, 115.66, 112.16, 107.45, 80.98, 80.91, 80.80, 80.76, 80.18, 79.96, 72.95, 66.69, 60.93, 58.31, 54.10, 53.09, 52.49, 50.41, 50.25, 50.17, 41.29, 39.33, 37.99, 37.88, 36.73, 35.28, 32.27, 31.91, 31.80, 31.27, 29.17, 28.33, 28.30, 27.85, 27.29, 23.13, 23.04, 19.76, 18.72, 14.91. MS: calcd. for $C_{66}H_{95}N_{12}O_{15}S_4$ [$(M+H)^+$]: 1423.6; found MALDI-MS: m/z 1424.2.

Synthesis of **9**: Compound **8** was deprotected using a solution of TFA/CH_2Cl_2/TIPSH (95/2.5/2.5) at r.t. for 3 h. After the solvent was removed, cold Et_2O was added. The precipitate was dissolved in MeOH, to which was added TCEP (1.1 equiv.), and the solution was stirred at r.t. for 10 min. $NaHCO_3$ was used to adjust the pH of the solution to 7, then the free thiol group was methylated with

MeI (5 equiv.) at r.t. for 2 h. The mixture was purified by HPLC to afford compound 9 (72% yield in two steps). ^{1}H NMR (400 MHz, DMSO-d_6) ^{1}H NMR (400 MHz, DMSO) δ 10.41 (s, 1H), 8.89 (d, J = 4.7 Hz, 1H), 8.63 – 8.52 (m, 2H), 8.48 (d, J = 7.5 Hz, 1H), 8.32 (m, 2H), 8.21 (d, J = 7.5 Hz, 1H), 8.07 (d, J = 8.9 Hz, 1H), 7.99 (m, 2H), 7.80 – 7.61 (m, 5H), 7.60 – 7.47 (m, 2H), 5.31 (t, J = 9.1 Hz, 1H), 4.63 – 4.47 (m, 5H), 4.42 (m, 1H), 4.28 (m, 1H), 4.17 (t, J = 5.9 Hz, 2H), 4.12 – 4.06 (m, 1H), 3.68 (m, 2H), 2.82 – 2.72 (m, 3H), 2.72 – 2.50 (m, 3H), 2.46 – 2.40 (m, 1H), 2.18 (m, 2H), 2.11 – 1.96 (m, 4H), 1.90 (m, 2H), 1.84 – 1.61 (m, 5H), 1.53 (m, 2H), 1.38 (m, 2H), 0.76 (m, 6H).

Synthesis of **L-ctrl**: To a solution of **9** (4 mg) in dry DMF (0.3 ml) was added Cy5.5-mono NHS ester (1.5 mg) and DIPEA (5 μl), and the mixture was stirred at r.t. for a further 1 h. After the reaction was completed, the mixture was purified by HPLC to afford **L-ctrl** in 51% yield. > 99% HPLC purity. MS: calcd. For $C_{94}H_{110}N_{14}O_{28}S_7$ [$(M+H)^+$]: 2107.6; found MALDI-MS: 2108.5.

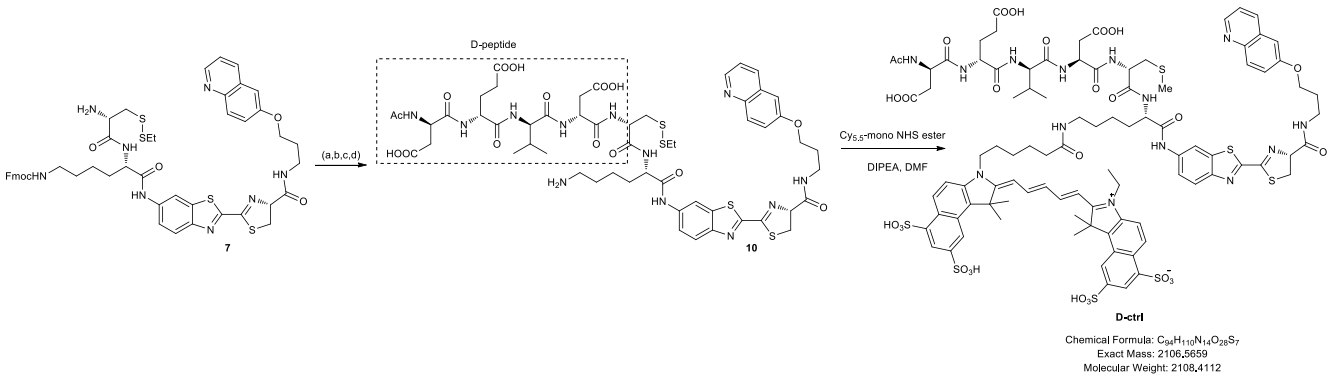

Scheme S3. Synthesis of **D-ctrl**. Reaction conditions: (a) Ac-$_D$-Asp(O^{t}Bu)-$_D$-Glu(O^{t}Bu)-$_D$-Val-$_D$-Asp(O^{t}Bu)-COOH, HBTU, DIPEA, THF; (B) piperidine, DMF, 42% in two steps; (e) TFA/TIPSH/DCM (95%/2.5%/2.5%), 81%; (f) TCEP, $NaHCO_3$, MeI, 87%; (g) Cy 5.5-NHS, DMF, DIPEA, 47%.

Synthesis of **10**: Starting from compound **7**, **10** was synthesized according to the methods as described for compound **9** with replacement of Ac-Asp(O^{t}Bu)-Glu(O^{t}Bu)-Val-Asp(O^{t}Bu)-COOH by Ac-$_D$-Asp(O^{t}Bu)-$_D$-Glu(O^{t}Bu)-$_D$-Val-$_D$-Asp(O^{t}Bu)-COOH. ^{1}H NMR (400 MHz, DMSO-d_6) δ 10.23 (s, 1H), 8.86 (d, J = 4.3 Hz, 1H), 8.64 – 8.53 (m, 2H), 8.48 (m, 1H), 8.36 (d, J = 6.3 Hz, 1H), 8.29 (s, br, 1H), 8.22 (d, J = 7.7 Hz, 1H), 8.13 – 7.91 (m, 4H), 7.66 (m, 5H), 7.58 – 7.43 (m, 2H), 5.31 (t, J = 9.2 Hz, 1H), 4.59 – 4.48 (m, 2H), 4.46 – 4.36 (m, 2H), 4.26 (m, 1H), 4.19 – 4.11 (m, 4H), 3.68 (m,

2H), 3.28 (m, 1H), 2.82 – 2.55 (m, 6H), 2.47 – 2.40 (m, 1H), 2.20 (m, 2H), 2.07 (s, 3H), 2.03 – 1.89 (m, 3H), 1.81 (s, 3H), 1.75 – 1.63 (m, 2H), 1.53 (d, J = 6.5 Hz, 2H), 1.36 (s, 2H), 0.79 (m, 6H). MS: calcd. for $C_{53}H_{69}N_{12}O_{15}S_3$ [$(M+H)^+$]: 1209.4; found MALDI-MS: m/z 1209.8.

Synthesis of **D-ctrl**: To a solution of **10** (3 mg) in dry DMF (0.3 ml) was added Cy5.5-mono NHS ester (1.1 mg) and DIPEA (5 µl), and the mixture was stirred at r.t. for a further 1 h. After the reaction was completed, the mixture was purified by HPLC to afford **D-ctrl** in 47% yield. > 99% HPLC purity after purification. MS: calcd. For $C_{94}H_{110}N_{14}O_{28}S_7$ [M^+]: 2106.6; found MALDI-MS: 2106.2.

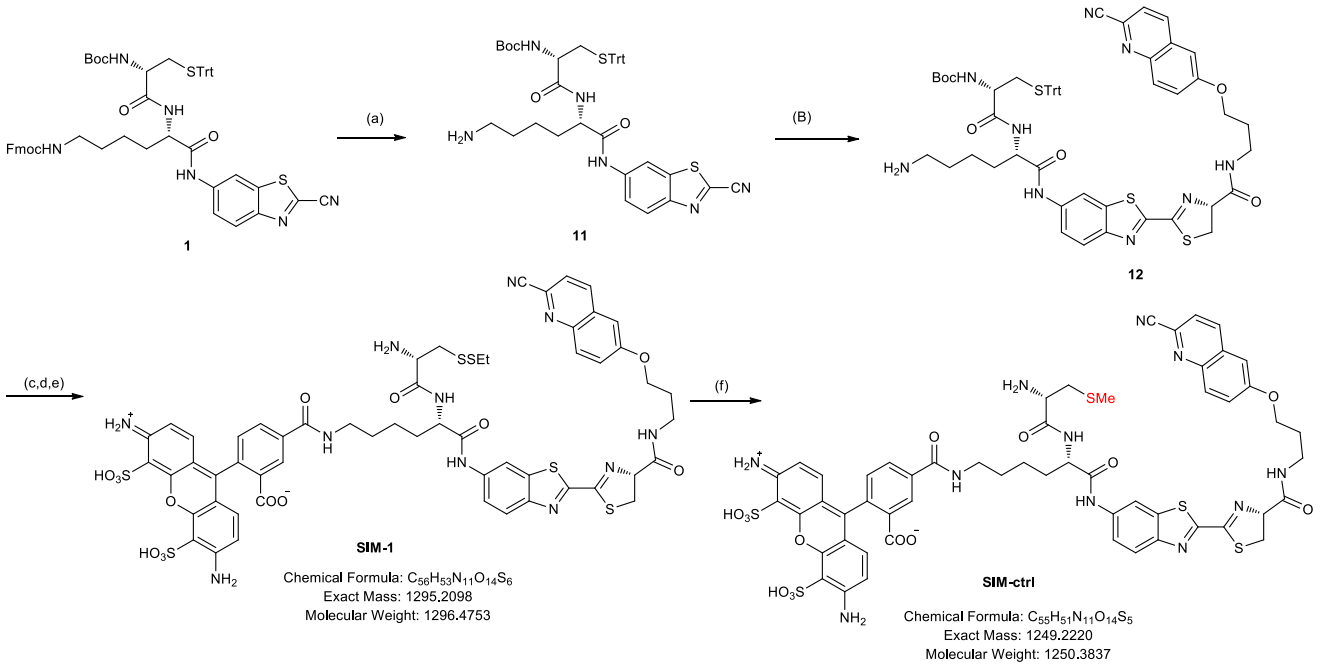

Scheme S4. Synthesis of high-resolution imaging probe **SIM-1** and control probe **SIM-ctrl**. Reaction conditions: (a) piperidine, DMF, 63%; (b) TCEP, DIPEA, DCM/MeOH, Ar, r.t. 1 h; (c) Alexa Fluor® 488 5-TFP, DIPEA, DMF; (d) TFA/TIPSH/DCM (25%/72.5%/2.5%); (e) PySSEt, MeOH; (f) TCEP, $NaHCO_3$, MeI.

Synthesis of compound **11**: Compound **1** was dissolved in 5% piperidein/DMF to completely remove Fmoc group. The reaction was then quenched with 1N HCl, and purified by HPLC to afford compound **11** as a white powder after lyophilization. ^{1}H NMR (400 MHz, CD_3OD) δ 8.60 (s, 1H), 7.99 (d, J = 9.0 Hz, 1H), 7.77 (d, J = 8.9 Hz, 1H), 7.34 (m, 6H), 7.26 (m, 6H), 7.20 (m, 3H), 4.55 (dd, J = 9.6, 4.3 Hz, 1H), 3.96 (t, J = 6.8 Hz, 1H), 2.88 – 2.76 (m, 2H), 2.54 (m, 2H), 2.05 (s, br, 1H), 1.83 – 1.24 (m, 14H); ^{13}C NMR (101 MHz, DMSO-d_6) δ 171.57, 171.18, 159.52, 159.18, 155.79, 148.43,

144.93, 139.83, 137.28, 135.77, 129.65, 128.71, 127.44, 125.40, 121.63, 118.63, 115.70, 114.19, 112.21, 79.26, 66.61, 54.16, 54.02, 34.44, 31.74, 28.73, 27.29, 23.00. MS: calcd. for $C_{41}H_{45}N_6O_4S_2$ [$(M+H)^+$]: 749.3; found LC-MS: m/z 749.7.

Synthesis of compound **12**: A solution of **2** (0.12 mmol) in MeOH was added dropwise to a solution of **11** (0.1 mmol), TCEP (0.1 mmol), and DIPEA (0.6mmol) in 15 ml CH_2Cl_2/MeOH (1/1) under N_2 at room temperature , and the mixture was stirred at r.t. for a further 30 min. After the reaction was completed, the solvent was removed under vacuum, and the residue was purified by HPLC to afford compound **12** as a light yellow powder after lyophilization. ^{1}H NMR (400 MHz, DMSO-d_6) δ 10.20 (s, 1H), 8.53 (s, 1H), 8.42 (d, J = 8.6 Hz, 1H), 8.31 (m, 2H), 8.06 (d, J = 9.0 Hz, 1H), 7.98 (d, J = 9.2 Hz, 1H), 7.91 (d, J = 8.5 Hz, 1H), 7.78 (s, br, 3H), 7.66 (d, J = 8.8 Hz, 1H), 7.53 (dd, J = 9.3, 2.7 Hz, 1H), 7.45 (d, J = 2.7 Hz, 1H), 7.35 – 7.24 (m, 15H), 7.13 (d, J = 7.3 Hz, 1H), 5.31 (t, J = 9.2 Hz, 1H), 4.38 (m, 1H), 4.18 (t, J = 6.1 Hz, 4H), 4.01 (m, 1H), 3.76 – 3.62 (m, 2H), 2.69 (m, 2H), 2.32 (d, J = 6.8 Hz, 2H), 2.09 – 1.94 (m, 2H), 1.80 (s, 1H), 1.67 – 1.49 (m, 3H), 1.29 (m, 11H); ^{13}C NMR (101 MHz, DMSO-d_6) δ 171.29, 171.18, 169.75, 164.88, 159.91, 159.38, 155.84, 144.91, 144.30, 137.19, 136.89, 131.38, 131.00, 130.58, 129.74, 129.62, 128.94, 128.75, 127.47, 125.40, 124.87, 124.81, 118.62, 112.30, 106.86, 79.95, 79.30, 66.76, 66.61, 54.19, 53.90, 39.28, 36.70, 35.27, 34.27, 31.71, 29.09, 28.74, 27.33, 23.00. MS: calcd. for $C_{57}H_{60}N_9O_6S_3$ [$(M+H)^+$]: 1062.4; found ESI-MS: m/z 1062.5.

Synthesis of compound **SIM-1**: To a solution of **12** (3 mg) in dry DMF was added Alexa Fluor® 488 5-TFP ester (1 mg) and DIPEA (2 μL), and the mixture was stirred at r.t. for a further 2h. After the reaction, cold Et_2O was added to precipitate the product, which was directly dissolved in a solution of TFA/TIPSH/DCM (25%/72.5%/2.5%) and reacted for 1 h. The solvent was removed, and the residue was precipitated with cold Et_2O, following by reaction with PySSEt in MeOH to afford **SIM-1** after purification by HPLC. 52% yield from Alexa Fluor® 488 5-TFP ester. MS: calcd. for $C_{56}H_{53}N_{11}O_{14}S_6$ [M^+]: 1295.2; found MALDI-MS: m/z 1295.7.

Synthesis of compound **SIM-ctrl**: **SIM-1** from last step was dissolved in a solution of CH_3CN/H_2O (1/1), to which was added TCEP and MeI. The pH value of the reaction solution was adjusted to 6 with $NaHCO_3$, and the reaction was stirred at r.t. for another 2 h, followed by purification with HPLC to produce **SIM-ctrl** (83% yield). MS: calcd. for $C_{55}H_{51}KN_{11}O_{14}S_5$ [$(M+K)^+$]: 1288.2; found MALDI-MS: m/z 1289.2.

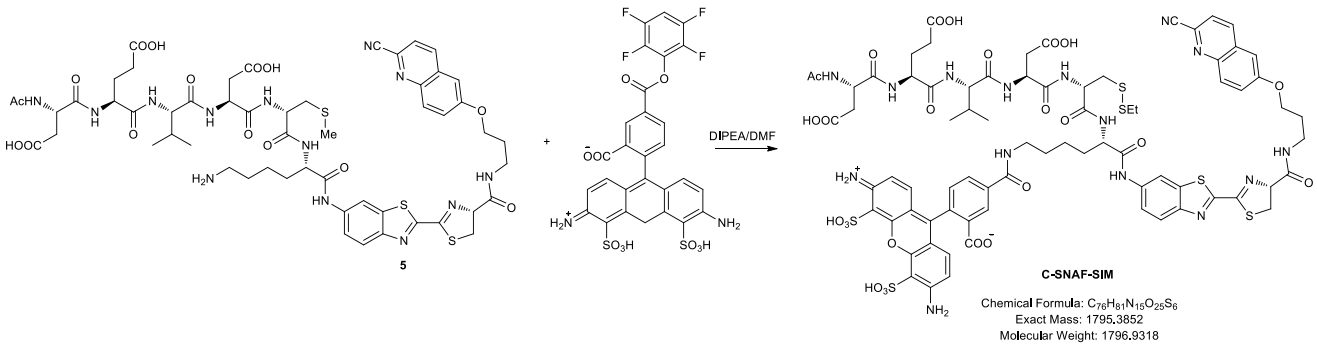

Scheme S5. Synthesis of probe **C-SNAF-SIM**.

To a solution of **5** (3 mg) in dry DMF was added Alexa Fluor® 488 5-TFP ester (1 mg) and DIPEA (2 μL), and the mixture was stirred at r.t. for 2 h. After the reaction was complete, the mixture was purified by HPLC to afford **C-SNAF-SIM** in 42% yield based on Alexa Fluor® 488 5-TFP ester. MS: calcd. For $C_{76}H_{81}N_{15}NaO_{25}S_6$ $[M+Na]^+$:1818.4; found MALDI-MS: 1817.9.

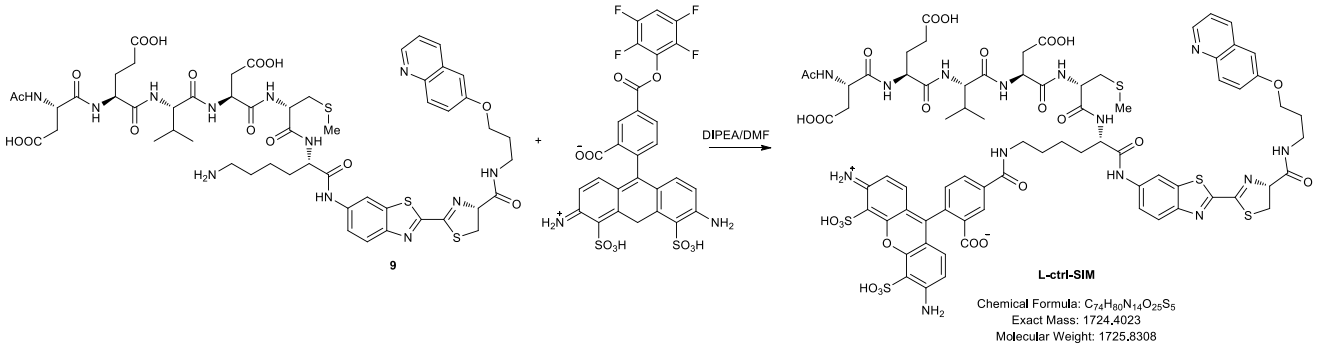

Scheme 6. Synthesis of **L-ctrl-SIM.**

To a solution of **9** (3 mg) in dry DMF was added Alexa Fluor® 488 5-TFP ester (1 mg) and DIPEA (2 μL), and the mixture was kept stirring at r.t. for 2 h. After the reaction was complete, the mixture was purified by HPLC to afford **C-SNAF-SIM** in 45% yield based on Alexa Fluor® 488 5-TFP ester. MS: calcd. For $C_{74}H_{81}N_{14}O_{25}S_5^+$ $[M+H]^+$:1725.4; found MALDI-MS: 1725.6.

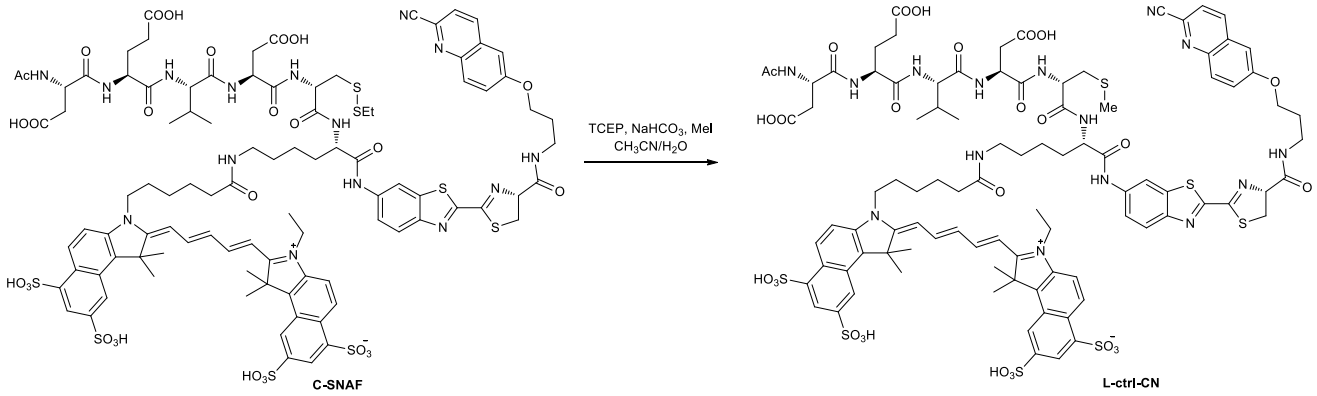

Scheme S7. Synthesis of probe **L-ctrl-CN**.

C-SNAF was dissolved in a solution of CH_3CN/H_2O (1/1), to which was added TCEP and MeI. The pH value of the reaction solution was carefully adjusted to 6 with $NaHCO_3$, and the reaction was stirred at r.t. for another 2 h, followed by purification with HPLC to produce **L-ctrl-CN** (53% yield). MS: calcd. for $C_{95}H_{110}N_{15}O_{28}S_7^+$ $[(M+H)^+]$: 2134.4; found MALDI-MS: m/z 2136.0.

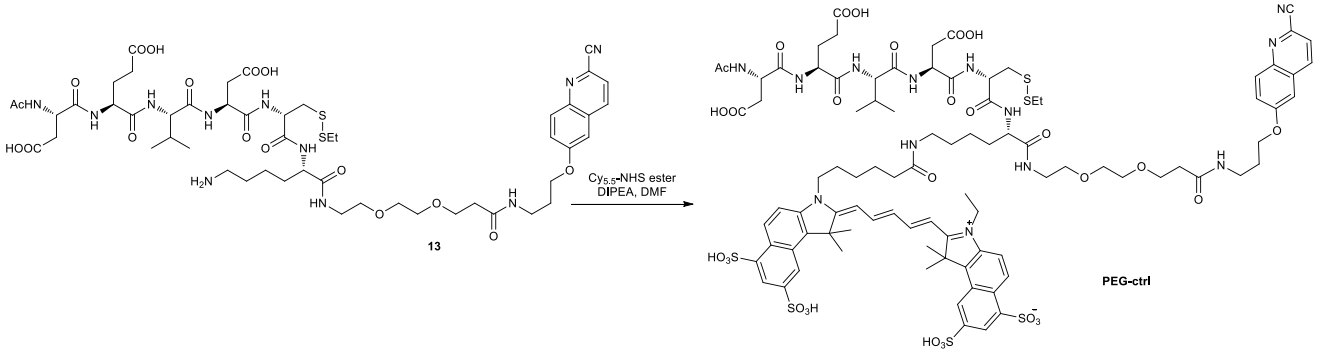

Scheme S8. Synthesis of probe **PEG-ctrl**.

To a solution of **13** (3 mg) in dry DMF (0.3 ml) was added Cy5.5-mono NHS ester (1.0 mg) and DIPEA (2 μl), and the mixture was stirred at r.t. for a further 1 h. After the reaction was complete, the mixture was purified by HPLC to afford **PEG-ctrl** in 41% yield. > 99% HPLC purity after purification. MS: calcd. For $C_{92}H_{118}N_{13}O_{30}S_6^+$ $[(M+H)^+]$: 2078.4; found MALDI-MS: 2079.8.

***In vitro* HPLC assay of enzymatic reactions.**

Caspase (human, recombinant from *E. coli*) assays were performed for caspase-3 (4.9×10^{-3} U; 7.35×10^{-4} mg, Sigma), -7 (18.3 U; 7.35×10^{-4} mg, Calbiochem), and -9 (0.3 U; 7.35×10^{-4} mg, Calbiochem). All caspase assays were conducted in caspase buffer with 50 mM HEPES, 100 mM NaCl, 1 mM EDTA, 10 mM TCEP, 10% glycerol, and 0.1% CHAPS at pH 7.4. Cathepsin B (human

liver; 0.27 U; 7.35×10^{-4} mg, Calbiochem) and Legumain (human, recombinant from mouse myeloma cell line; > 250 pmol/min/μg; 7.35×10^{-4} mg, R&D Systems) were conducted in reaction buffer with 50 mM sodium acetate, 50 mM NaCl, 0.5 mM EDTA and 10 mM TCEP at pH 5.5. **C-SNAF** was diluted in the respective enzyme reaction buffer (25 μM, 1 mL) and incubated at r.t. for 10 min for efficient disulfide reduction. The respective enzyme was then added to initiate the enzymatic reaction. Reactions were performed at 37 °C, and monitored by HPLC at 0, 1, 1.5, 2, 3, 4 and 6 h. The percentage conversion of the reaction was calculated based on the percentage of peak area of **C-SNAF-*cycl*** in the HPLC trace at 675 nm UV detection, which indicated the efficacy of enzymatic cleavage of **C-SNAF**.

Cell culture.

HeLa human cervical adenocarcinoma epithelial cells and MDA-MB-231 human breast adenocarcinoma epithelial cells from the ATCC were cultured in Dulbecco's modified eagle medium (GIBCO) supplemented with 10% fetal bovine serum (FBS, GIBCO), 100 U/mL penicillin and 100 μg/mL streptomycin (GIBCO). For Caspase-Glo@ 3/7 assays, HeLa and MDA-MB-231 cells were plated onto 96-well plates (Costar) and allowed to reach ~ 70% confluency. For epifluorescence microscopy experiments, cells were plated onto #1.5 borosilicate 8-well chambered coverslips (Nunc) and grown to ~ 70% confluency. For flow cytometry experiments, HeLa cells were plated onto 12-well clear plates and grown to ~70% confluency. For super-resolution microscopy experiments, HeLa cells were plated on micro cover glass (20 × 20 mm) and grown to ~ 70% confluency.

Caspase-Glo@ 3/7 assays to measure the caspase-3/7 activity in drug-induced apoptotic cells.

~ 5000 HeLa or MDA-MB-231 cells in 100 μL of DMEM medium were seeded onto 96-well plates. After reaching ~ 70% confluency, medium was removed and 100 μL of fresh medium containing different concentration of STS (0, 2, 5, and 10 μM) or DOX (0, 1, 2, and 5 μM) was added to the wells and incubated for 4 h (STS) or 24 h (DOX). For STS-treated cells, medium with STS was replaced with 100 μL of fresh medium without STS after 4 h, and further incubated for 0 or another 24 h. The cell number was counted using trypan blue, and the caspase-3/7 activity in each well was measured using the Caspase-Glo@ 3/7 assay (Promega) according to the standard protocol. Briefly, 100 μL of Caspase-Glo@ 3/7 reagent was added to each well. The plate was then covered and gently mixed, and incubated in the dark at r.t. for 1 h. Then, 120 μL of solution from each well was added to an

eppendorf tube, and the luminescence was immediately measured by a luminometer (Turner Biosystems) as directed by the luminometer manufacturer. Data were then background-corrected, normalized by cell number, and the caspase-3/7 activity in drug-treated cells were expressed as normalized increased fold/cell compared to the negative control cells.

Caspase-Glo@ 3/7 assays to measure the caspase-3/7 activity in saline- and 3X DOX-treated tumor lysates.

HeLa tumor xenografted mice were treated with saline or 3X DOX (8 mg/Kg) according to the protocol for the chemotherapy mouse model. After treatment, the mice were sacrificed, and the tumors were resected and lysed with RIPA buffer (1g tissue / 1 ml buffer). The solution was homogenized for 1 min on ice, three times. The lysed solution was kept on ice for another 30 min, and centrifuged at 14,000×g for 30 min at 4 °C. The supernatant was collected, and the protein concentration was measured by Bradford assay with BSA as standard. The caspase-3/7 activity in the lysed solution was measured by Caspase-Glo@ 3/7 assay, and normalized to the protein concentration.

Analysis of the reaction of C-SNAF in viable and apoptotic cell lysates.

Adherent HeLa (or MDA-MB-231) cells (~ 8 million) were either untreated or treated with 2 μM STS for 4 h or 2 μM DOX for 24 h. After replacing STS-containing medium with blank medium, the cells were kept growing for another 24 h. The medium was then carefully removed and the cells were washed with cold PBS (1×). The cells were trypsinzed to form cell pellets, and RIPA (RadioImmuno Precipitation Assay, sigma) buffer was added to cells at a volume of 100 μL of buffer per 4 million cells, followed by incubation on ice for 0.5 h. The cell lysate was gathered, centrifuged at 14,000×g at 4 °C for 15 min. The supernatant was collected and the caspase-3/7 activity was determined by Caspase-Glo@ 3/7 assay. The cell lysate was diluted with caspase reaction buffer (2×, 1 to 1 diluted), and incubated with **C-SNAF** (5 μM) at 37 °C overnight and then injected into an HPLC system (Dionex) for analysis.

Analysis of the reaction of C-SNAF in viable and apoptotic HeLa cells.

HeLa cells (~ 8 million) were either untreated or treated with STS (2 μM) for 4 h. The medium with STS was removed, and fresh medium containing **C-SNAF** (50 μM) was added. Cells were kept growing for another 24 h. The culture medium was carefully removed and the cells were washed with

cold PBS (1×). The cells were trypsinzed to form cell pellets. 0.1% SDS aqueous solution (pH 7.4) was added to lyse the cells, and the solution was homogenized for three cycles of 1 min. Following centrifugation at 14,000×g at 4 °C for 15 min, the supernatant of the cell lysate was collected and injected into an HPLC system for analysis.

Analysis of the reaction of C-SNAF in saline- and 3X DOX-treated HeLa tumor lysates

HeLa tumor xenografted mice were treated with saline or 3X DOX (8 mg/Kg) according to the protocol for the chemotherapy mouse model. After treatment, the mice were sacrificed and the tumors were resected and lysed with RIPA buffer (1g tissue / 1 ml buffer). The solution was homogenized for 1 min on ice, repeated three times per sample. The lysed solution was kept on ice for another 30 min, and centrifuged at 14,000×g for at 4 °C 30 min. The supernatant was collected, and diluted with caspase reaction buffer (2×: 100 mM HEPES, 200 mM NaCl, 2 mM EDTA, 20 mM TCEP, 20% glycerol, and 0.2% CHAPS at pH 7.4; 1 to 1 diluted). **C-SNAF** (5 μM) was added to the tumor lysates, and incubated at 37 °C overnight, followed by HPLC analysis.

Epifluorescence microscopy imaging of DOX-treated HeLa cells.

HeLa cells in #1.5 borosilicate 8-well chambered coverslips (Nunc) were either incubated with **C-SNAF** (2 μM) alone or co-incubated with DOX (1, 2, and 5 μM), caspase inhibitor (Z-VAD-fmk, 50 μM), or **D-ctrl** or **L-ctrl** control probes at 2 μM for 24 h. Then the medium was removed, the cells were carefully washed with PBS (1×) three times, and stained with nuclear binding probe Hoechst 33342 (2 μM) at 37 °C for 30 min. After several rinses with PBS (1×), the medium was replaced and fluorescence images were acquired with DAPI and Cy5.5 filters.

Flow Cytometry analysis of anti-cancer drug-induced apoptotic HeLa cells.

Approximately 100,000 HeLa cells in 1 mL DMEM medium were seeded onto 12-well plates. The following day, the medium was replaced with 500 μL of fresh medium containing STS (0, and 2 μM). After 4 h incubation, the medium containing STS was removed and fresh medium without STS was added. The cells were kept growing for 0 or another 24 h to induce different levels of apoptosis. After gentle washing with PBS (1X), the cells were detached from the plates with trypsin (100 uL per well), and the cell pellets were collected after centrifugation at 2000 rpm at 4 °C for 2 min. After washing with PBS (1X), the pellets were resuspended in 300 μL PBS (1X) and stained with the Alexa Fluor@

488 Annexin V/Dead Cell Apoptosis Kit (Invitrogen: V13241) for flow cytometry. For the FLICA staining experiment, the cell pellets were resuspended in 1X wash buffer and stained with the *Vybrant*@ FAM Caspase-3 and -7 Assay Kit (Invitrogen: V35118). All assays were performed according to the manufacturer instructions, and the cell population was analyzed by FACScan analyzer using FITC (Annexin V and FLICA) and PI channels. The count number for each flow cytometry analysis was ~5000 to 10000, and the data was processed using FlowJo software.

For the DOX-induced apoptotic experiments, HeLa cells in 12-well plates were treated with DOX (0, 1, and 5 μM) for 24 h, stained with Alexa@ Fluor Annexin V and PI or FLICA (FAM) and PI according to the aforementioned procedure, and applied for flow cytometry analysis.

Flow Cytometry analysis of apoptotic HeLa cells labelled with C-SNAF.

Approximately $1x10^5$ HeLa cells in 1 mL DMEM medium were seeded onto 12-well plates. The following day, the medium was replaced with 500 μL of fresh medium containing STS (0, 2 μM). After 4 h incubation, the STS-containing medium was replaced with 500 μL of fresh medium containing 2 μM **C-SNAF**, **L-ctrl** or **D-ctrl**. For the inhibitor blocking experiment, the STS-treated cells were first incubated with the caspase inhibitor Z-VAD-fmk (50 μM, R&D Systems) for 30 min, and then 2 μM **C-SNAF** was added. After 24 h, cells were trypsinized and the formed cell pellets were stained with the *Vybrant*@ FAM Caspase-3 and -7 Assay Kit. Cells were washed with PBS (1X) three times, resuspened in 300 μL PBS and applied for flow cytometry analysis using the FITC and Cy5.5 channels. The cell number for each flow cytometry analysis was ~5000 to 10000, and the data was processed using FlowJo software.

For DOX-induced apoptotic cells, HeLa cells in 12-well plates were co-incubated with DOX (5 μM) and 2 μM **C-SNAF**, **L-ctrl** and **D-ctrl**, or 2 μM **C-SNAF** together with 50 μM of Z-VAD-fmk for 24 h. After washing with PBS (1X) three times, the cells pellets were resuspened in 300 μL of PBS, and applied for flow cytometry analysis using the Cy5.5 channels. The cell number for each flow cytometry analysis was 10000, and the data was processed using FlowJo software.

Active Caspase-3 immunohistochemistry assay.

Following fluorescence imaging studies at 4 h, tumor tissues were excised, fixed in formalin, frozen in Optimal Cutting Temperature medium (OCT) and sectioned into 10-μm slices. For active caspase-3

staining, the sections were further fixed with cold acetone, blocked with avidin/biotin blocking kit and DAKO blocking, and immunostained with primary cleaved caspase-3 antibody (Asp175, 1:100, Cell signaling 9661) overnight at 4 °C, followed by incubation for 30 min with biotinylated anti-rabbit IgG (1:300, Vector Labs) and 30 min with Cy3-conjugated streptavidin (1:300, Jackson ImmunoResearch). Then the sections were mounted in Vectashield mounting media containing DAPI (Vector Labs). The images were captured using an Olympus inverted fluorescence microscope (IX2-UCB) equipped with a Nuance multispectral imaging camera and standard DAPI, FITC, and Cy5.5 excitation filter sets. The images were processed using the standard CRi Nuance software, analyzed using *Image J* software package (NIH).

Statistical Analysis

Results are expressed as the mean±standard deviation unless otherwise stated. Statistical comparisons between two groups were determined by t-test, and between 3 or more groups by one-way ANOVA followed by a post-hoc Tukey's HSD test. Time course analysis between groups was performed by general linear model repeated-measures analysis. Correlation analyses were performed by one-tailed Spearman r (non-parametric). For all tests, $p<0.05$ was considered statistically significant. All statistical calculations were performed using GraphPad Prism v. 5 (GraphPad Software Inc., CA, USA), except for general linear model analyses, which were performed using SPSS (IBM).

References

[S1] Ye, D., Liang, G., Ma, M.L. & Rao, J. Controlling intracellular macrocyclization for the imaging of protease activity. *Angew. Chem. Int. Ed.* **50**, 2275-2279 (2011).

[S2] Liang, G., Ren, H. & Rao, J. A biocompatible condensation reaction for controlled assembly of nanostructures in living cells. *Nat. chem.* **2**, 54-60 (2010).

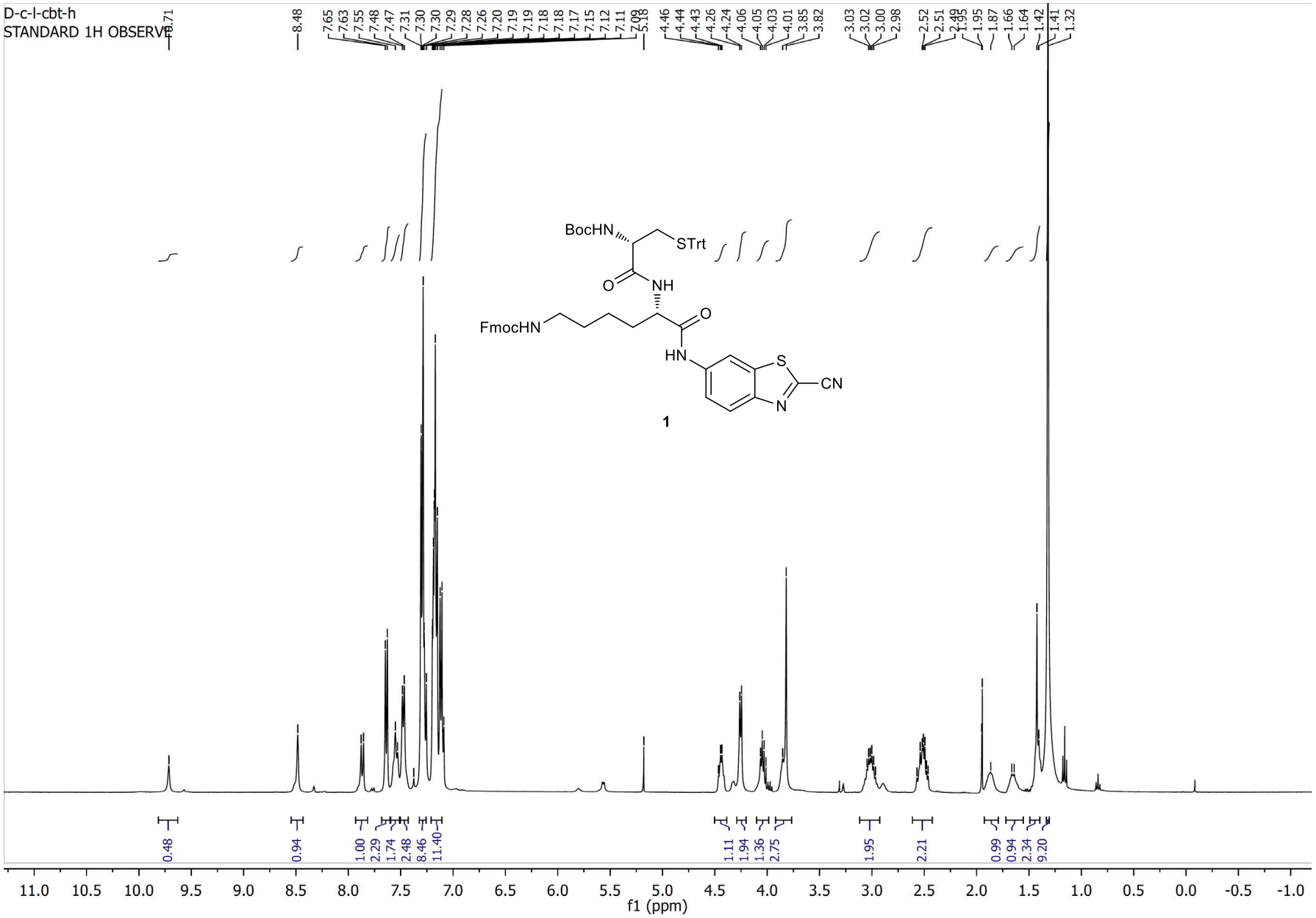
D-c-l-cbt-h
STANDARD 1H OBSERVE
8.71
8.48
7.65
7.63
7.55
7.48
7.47
7.31
7.30
7.30
7.29
7.28
7.26
7.20
7.19
7.19
7.18
7.18
7.17
7.15
7.12
7.11
7.09
5.18
4.46
4.44
4.43
4.26
4.24
4.06
4.05
4.03
4.01
3.85
3.82
3.03
3.02
3.00
2.98
2.52
2.51
2.49
1.95
1.87
1.66
1.64
1.42
1.41
1.32
BocHN
STrt
O
NH
FmocHN
O
HN
S
CN
N
1
0.48
0.94
1.00
2.29
1.74
2.48
8.46
11.40
1.11
1.94
1.36
2.75
1.95
2.21
0.99
0.94
2.34
9.20
11.0
10.5
10.0
9.5
9.0
8.5
8.0
7.5
7.0
6.5
6.0
5.5
5.0
4.5
4.0
3.5
3.0
2.5
2.0
1.5
1.0
0.5
0.0
-0.5
-1.0
f1 (ppm)

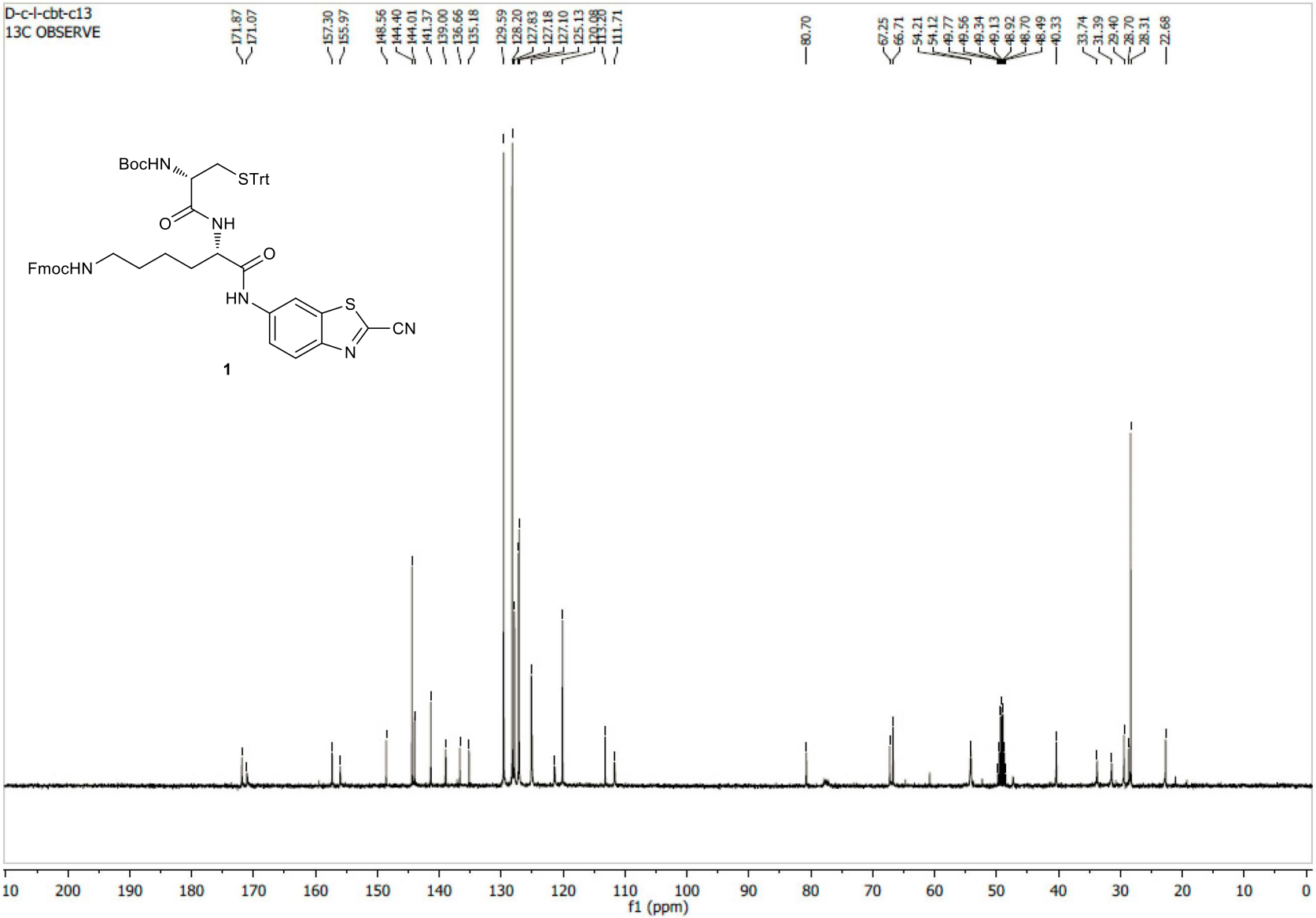
D-c-l-cbt-c13
13C OBSERVE
171.87
171.07
157.30
155.97
148.56
144.40
144.01
141.37
139.00
136.66
135.18
129.59
128.20
127.83
127.18
127.10
125.13
120.08
113.28
111.71
80.70
67.25
65.71
54.21
54.12
49.77
49.56
49.34
49.13
48.92
48.70
48.49
40.33
33.74
31.39
29.40
28.70
28.31
22.68
BocHN
STrt
O
NH
FmocHN
O
HN
S
CN
N
1
10
200
190
180
170
160
150
140
130
120
110
100
90
80
70
60
50
40
30
20
10
0
f1 (ppm)

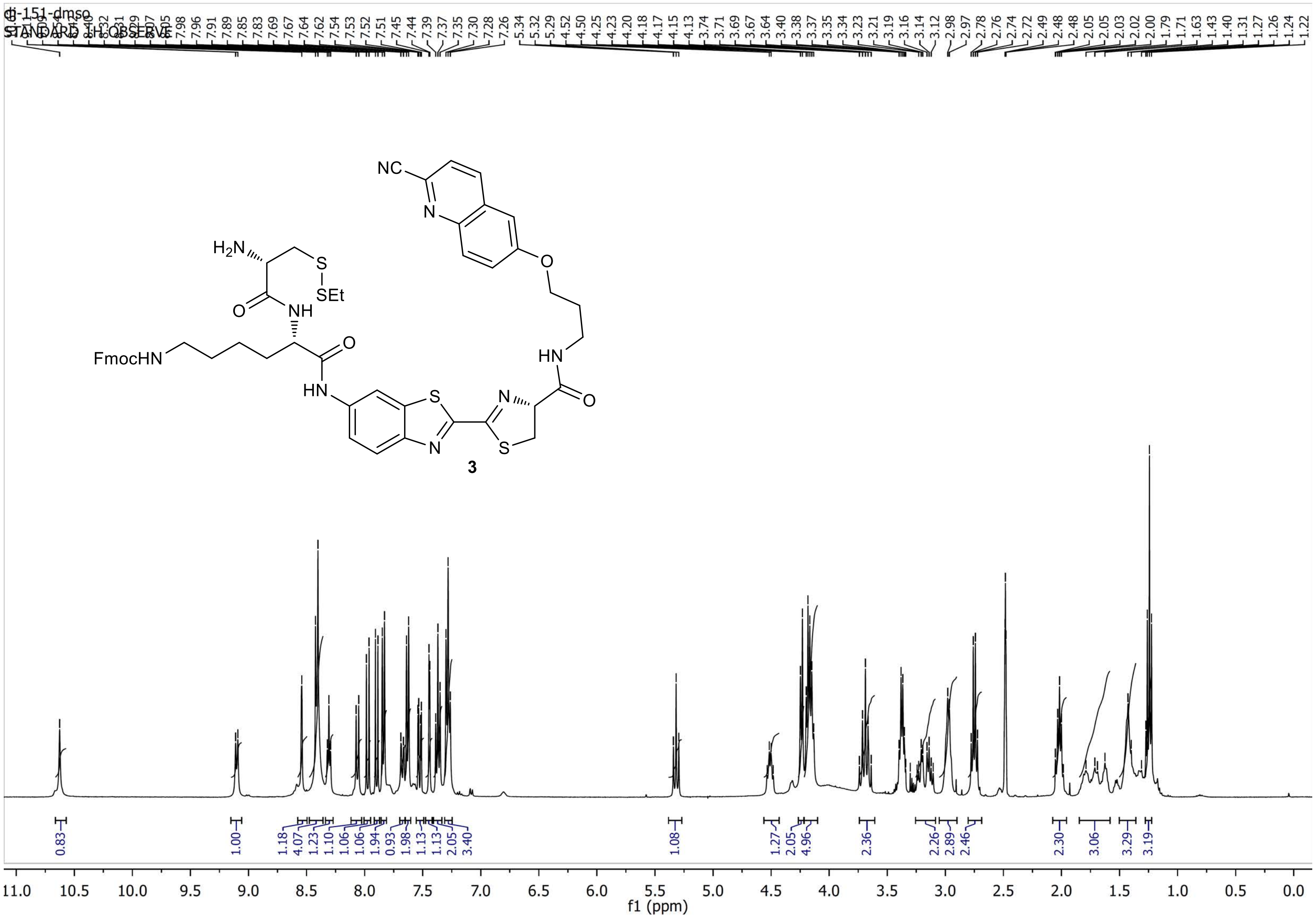

ql-151-dmso
STANDARD 1H OBSERVE
NC
N
O
H2N
S
SEt
O
NH
FmocHN
O
HN
S
N
N
S
HN
O
3
f1 (ppm)

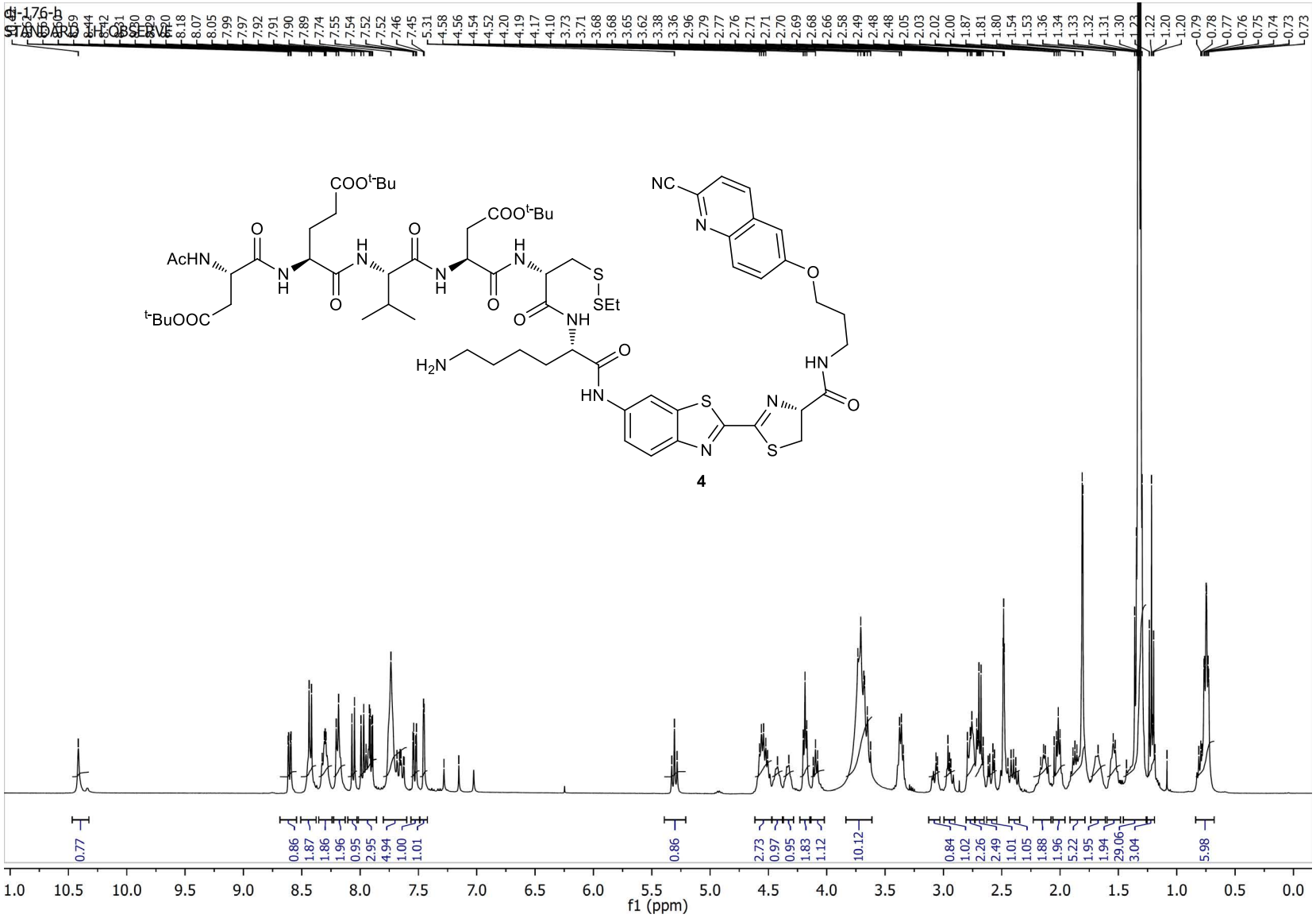
dj-176-h
STANDARD 1H OBSERVE
AcHN
COO^{t}Bu
^{t}BuOOC
SEt
NC
H_2N
HN
NH
4
f1 (ppm)

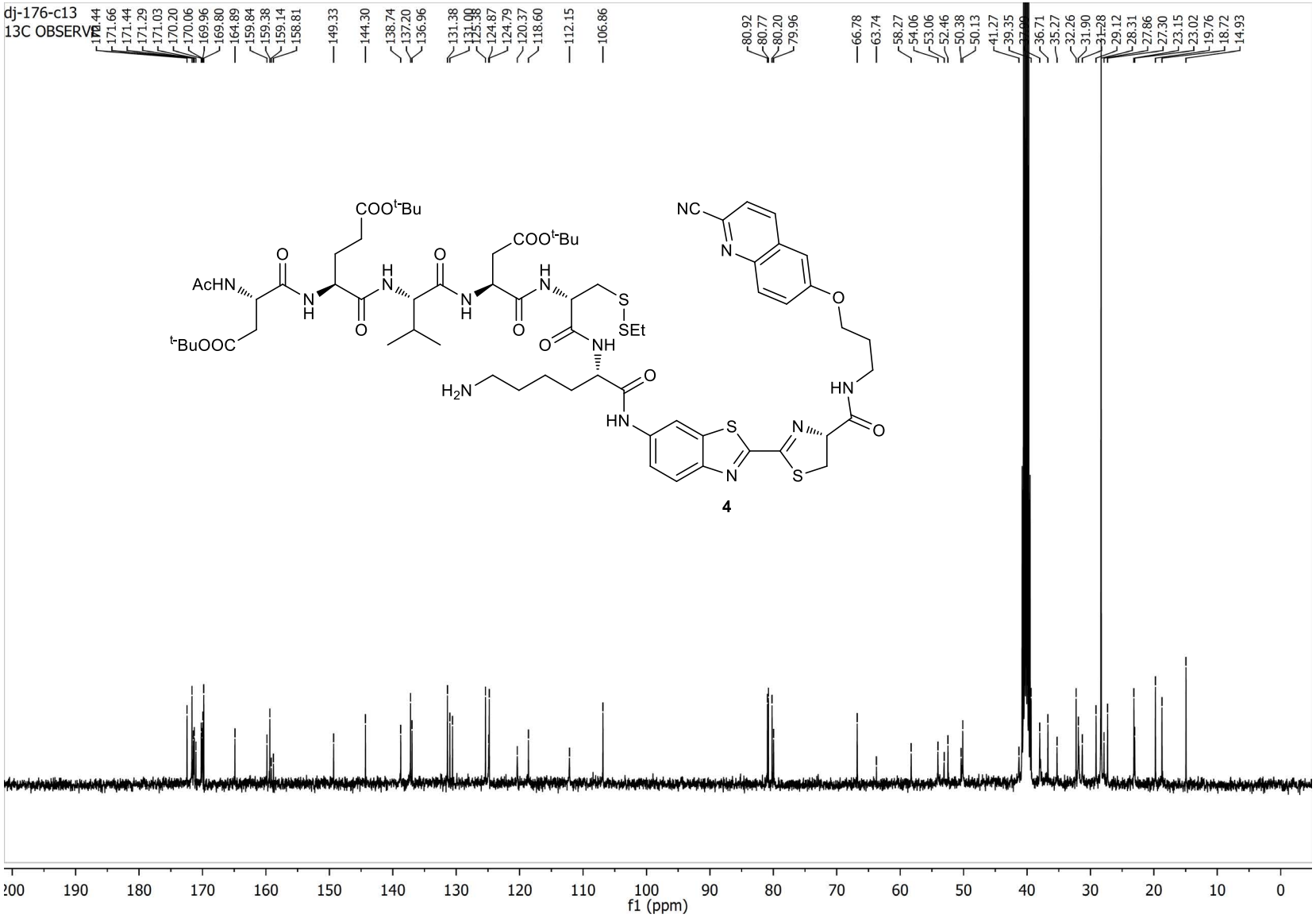
dj-176-c13
13C OBSERVE
171.44
171.66
171.44
171.29
171.03
170.20
170.06
169.96
169.80
164.89
159.84
159.38
159.14
158.81
149.33
144.30
138.74
137.20
136.96
131.38
131.00
125.38
124.87
124.79
120.37
118.60
112.15
106.86
80.92
80.77
80.20
79.96
66.78
63.74
58.27
54.06
53.06
52.46
50.38
50.13
41.27
39.35
37.00
36.71
35.27
32.26
31.90
31.28
29.12
28.31
27.86
27.30
23.15
23.02
19.76
18.72
14.93
COO^t-Bu
COO^t-Bu
AcHN
^{t}-BuOOC
SEt
NC
H_2N
HN
HN
4
200
190
180
170
160
150
140
130
120
110
100
90
80
70
60
50
40
30
20
10
0
f1 (ppm)

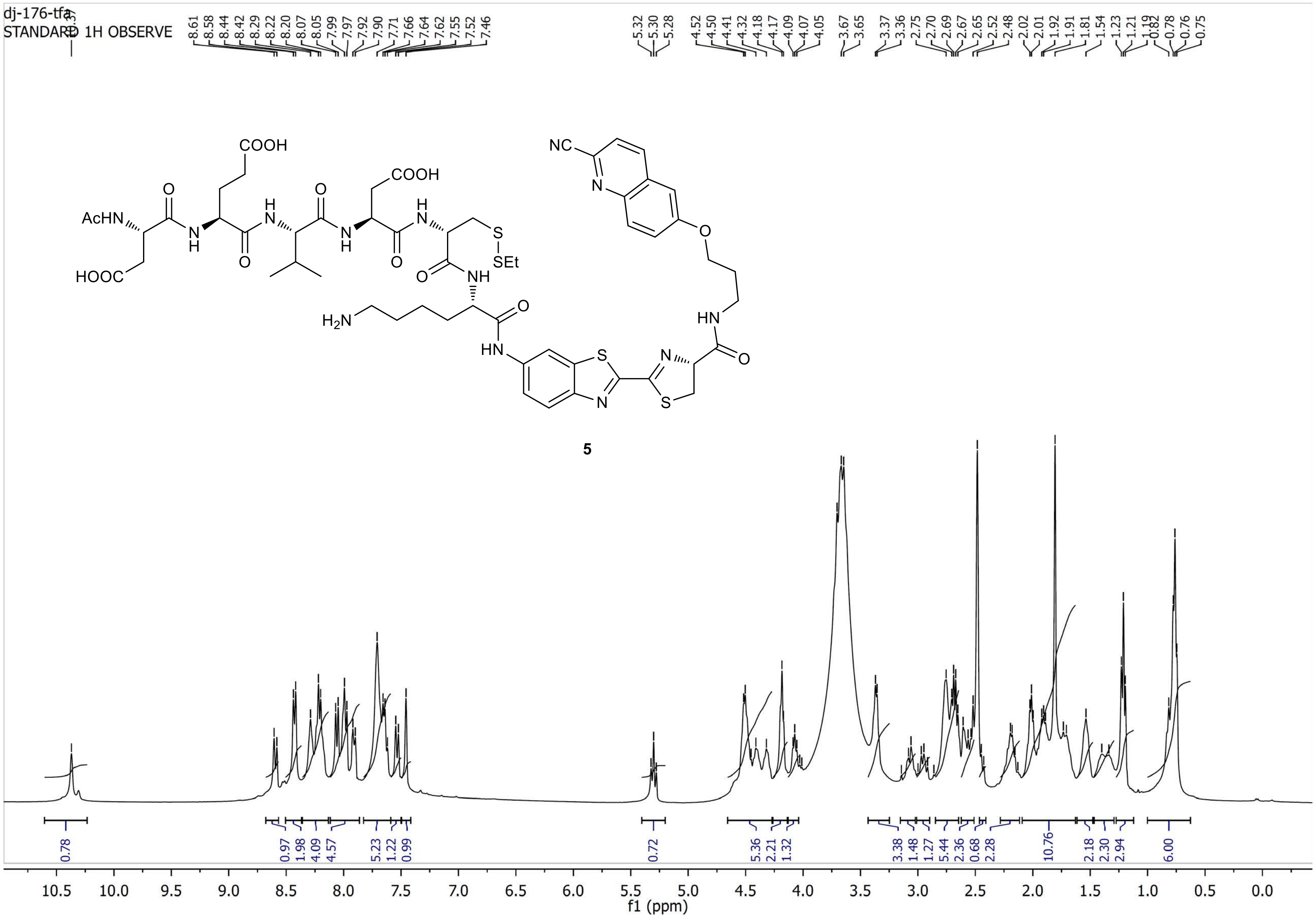
dj-176-tfa
STANDARD 1H OBSERVE
f1 (ppm)
AcHN
HOOC
COOH
COOH
SEt
H2N
NC

5

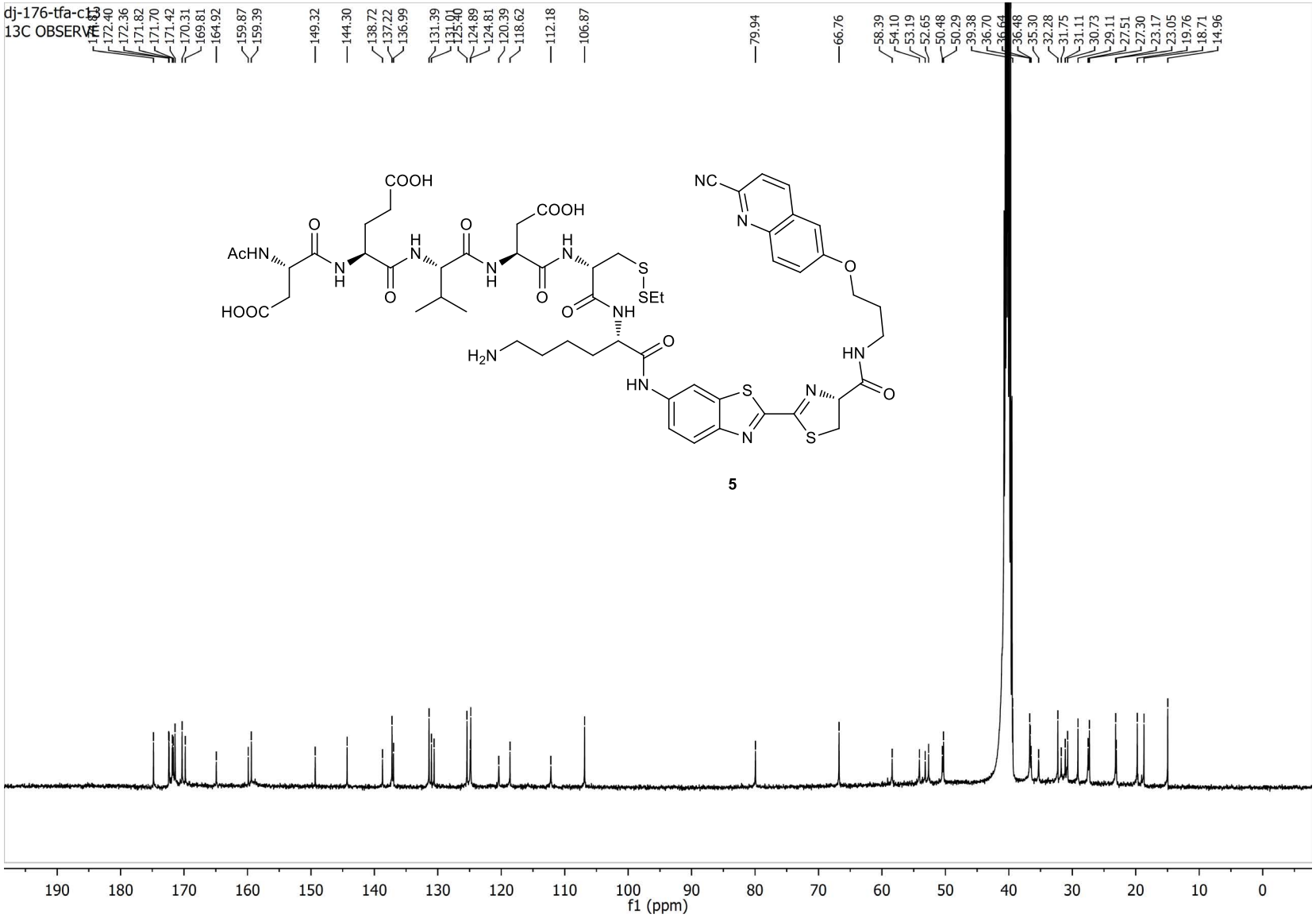
dj-176-tfa-c13
13C OBSERVE
174.83
172.40
172.36
171.82
171.70
171.42
170.31
169.81
164.92
159.87
159.39
149.32
144.30
138.72
137.22
136.99
131.39
131.01
125.40
124.89
124.81
120.39
118.62
112.18
106.87
79.94
66.76
58.39
54.10
53.19
52.65
50.48
50.29
39.38
36.70
36.64
36.48
35.30
32.28
31.75
31.11
30.73
29.11
27.51
27.30
23.17
23.05
19.76
18.71
14.96
COOH
COOH
AcHN
HOOC
SEt
NC
HN
HN
H_2N
5
190
180
170
160
150
140
130
120
110
100
90
80
70
60
50
40
30
20
10
0
f1 (ppm)

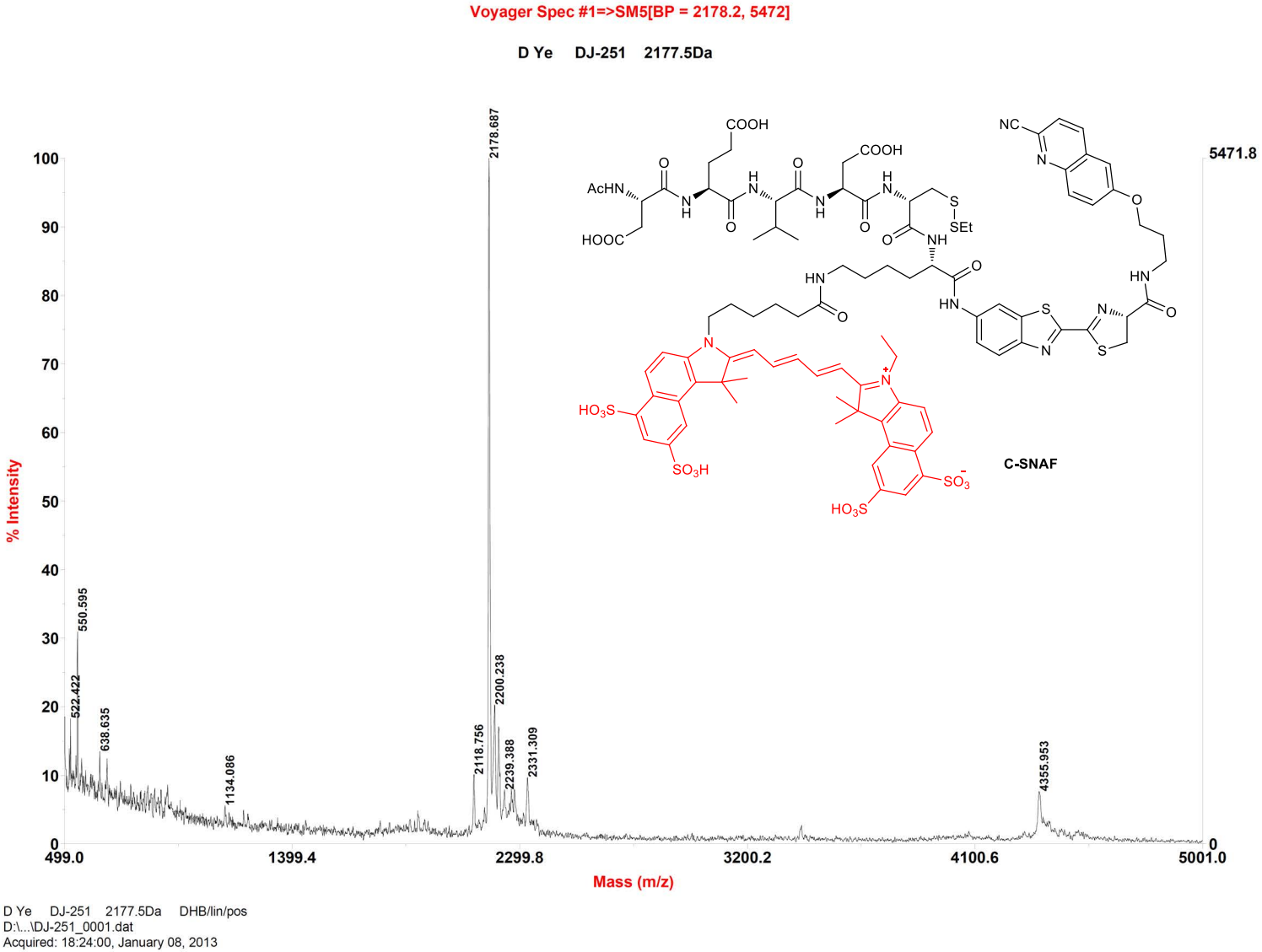
Voyager Spec #1=>SM5[BP = 2178.2, 5472]
D Ye DJ-251 2177.5Da
% Intensity
Mass (m/z)
2178.687
550.595
522.422
638.635
1134.086
2118.756
2200.238
2239.388
2331.309
4355.953
5471.8
C-SNAF
D Ye DJ-251 2177.5Da DHB/lin/pos
D:\...\DJ-251_0001.dat
Acquired: 18:24:00, January 08, 2013

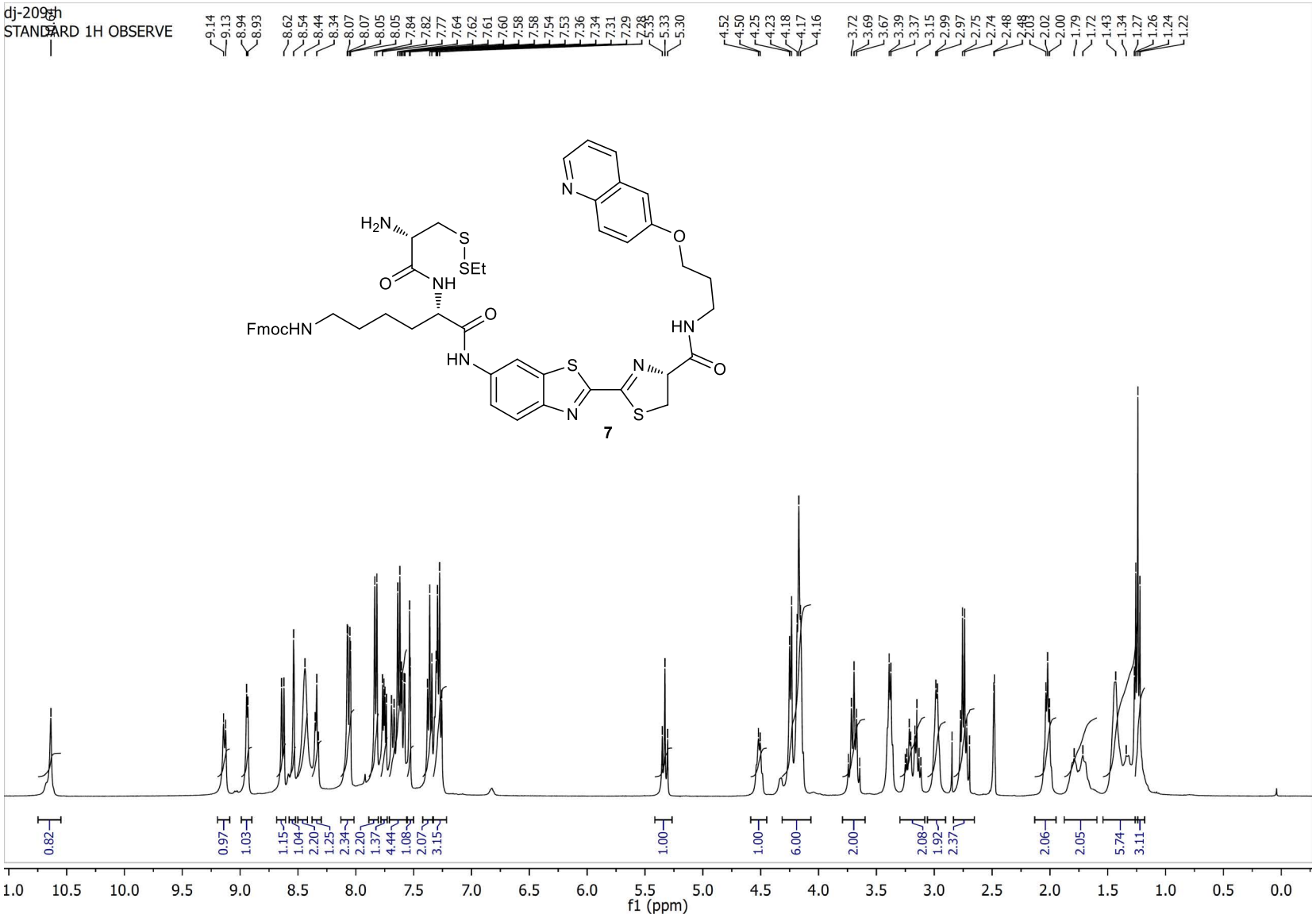
dj-209-h
STANDARD 1H OBSERVE
9.14
9.13
8.94
8.93
8.62
8.54
8.44
8.34
8.07
8.07
8.05
8.05
7.84
7.82
7.77
7.64
7.62
7.61
7.60
7.58
7.58
7.54
7.53
7.36
7.34
7.31
7.29
5.33
5.30
4.52
4.50
4.25
4.23
4.18
4.17
4.16
3.72
3.69
3.67
3.39
3.37
3.15
2.99
2.97
2.75
2.74
2.48
2.02
2.00
1.79
1.72
1.43
1.34
1.27
1.26
1.24
1.22
H2N
S
SEt
O
NH
FmocHN
O
HN
N
O
HN
S
N
N
S
O
7
0.82
0.97
1.03
1.15
1.04
2.20
1.25
2.34
2.20
1.37
4.44
1.08
2.07
3.15
1.00
1.00
6.00
2.00
2.08
1.92
2.37
2.06
2.05
5.74
3.11
1.0
10.5
10.0
9.5
9.0
8.5
8.0
7.5
7.0
6.5
6.0
5.5
5.0
4.5
4.0
3.5
3.0
2.5
2.0
1.5
1.0
0.5
0.0
f1 (ppm)

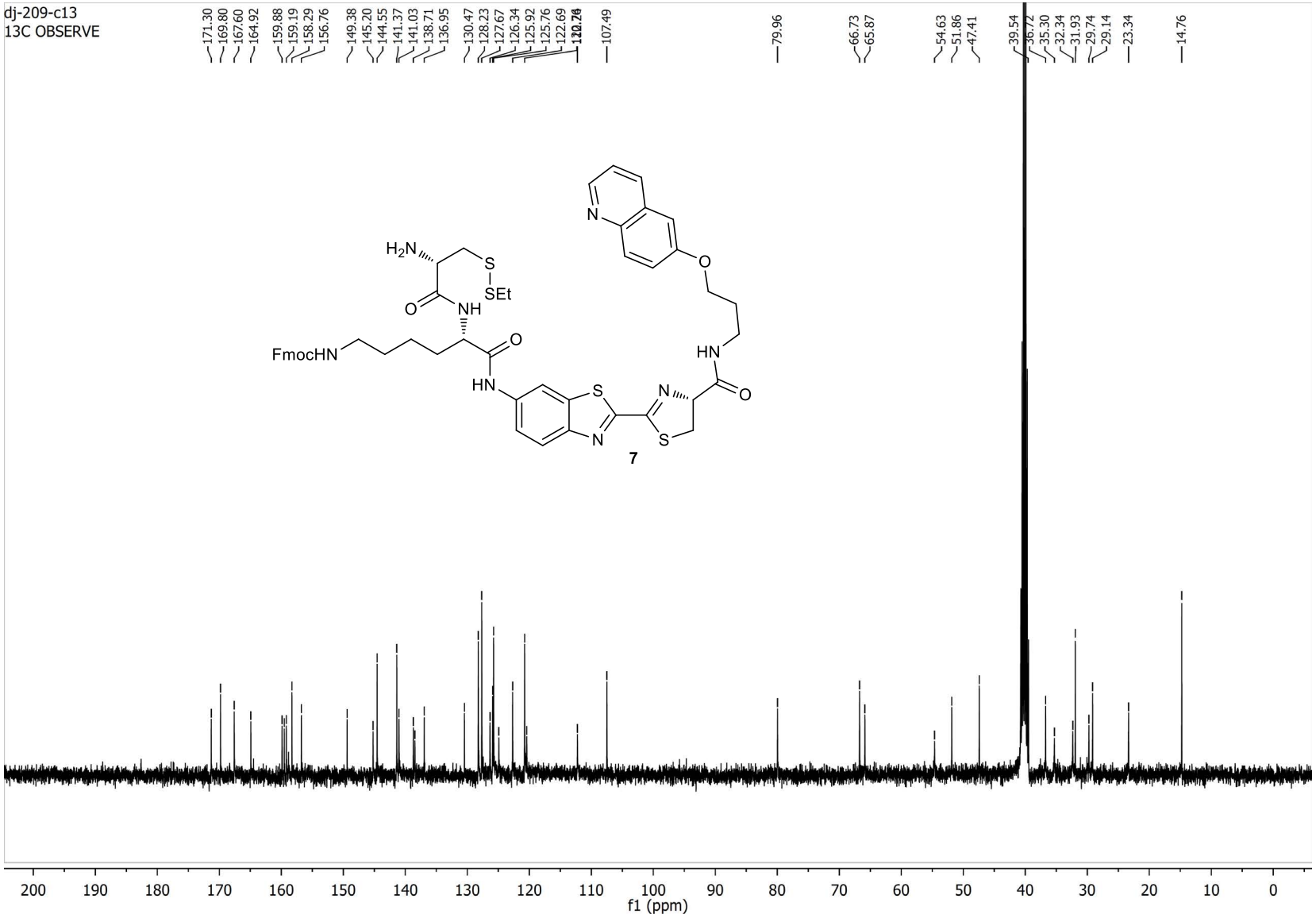
dj-209-c13
13C OBSERVE
171.30
169.80
167.60
164.92
159.88
159.19
158.29
156.76
149.38
145.20
144.55
141.37
141.03
138.71
136.95
130.47
128.23
127.67
126.34
125.92
125.76
122.69
107.49
79.96
66.73
65.87
54.63
51.86
47.41
39.54
36.72
35.30
32.34
31.93
29.74
29.14
23.34
14.76
H2N
S
SEt
O
NH
FmocHN
O
HN
S
N
N
O
HN
O
N
S
7
200
190
180
170
160
150
140
130
120
110
100
90
80
70
60
50
40
30
20
10
0
f1 (ppm)

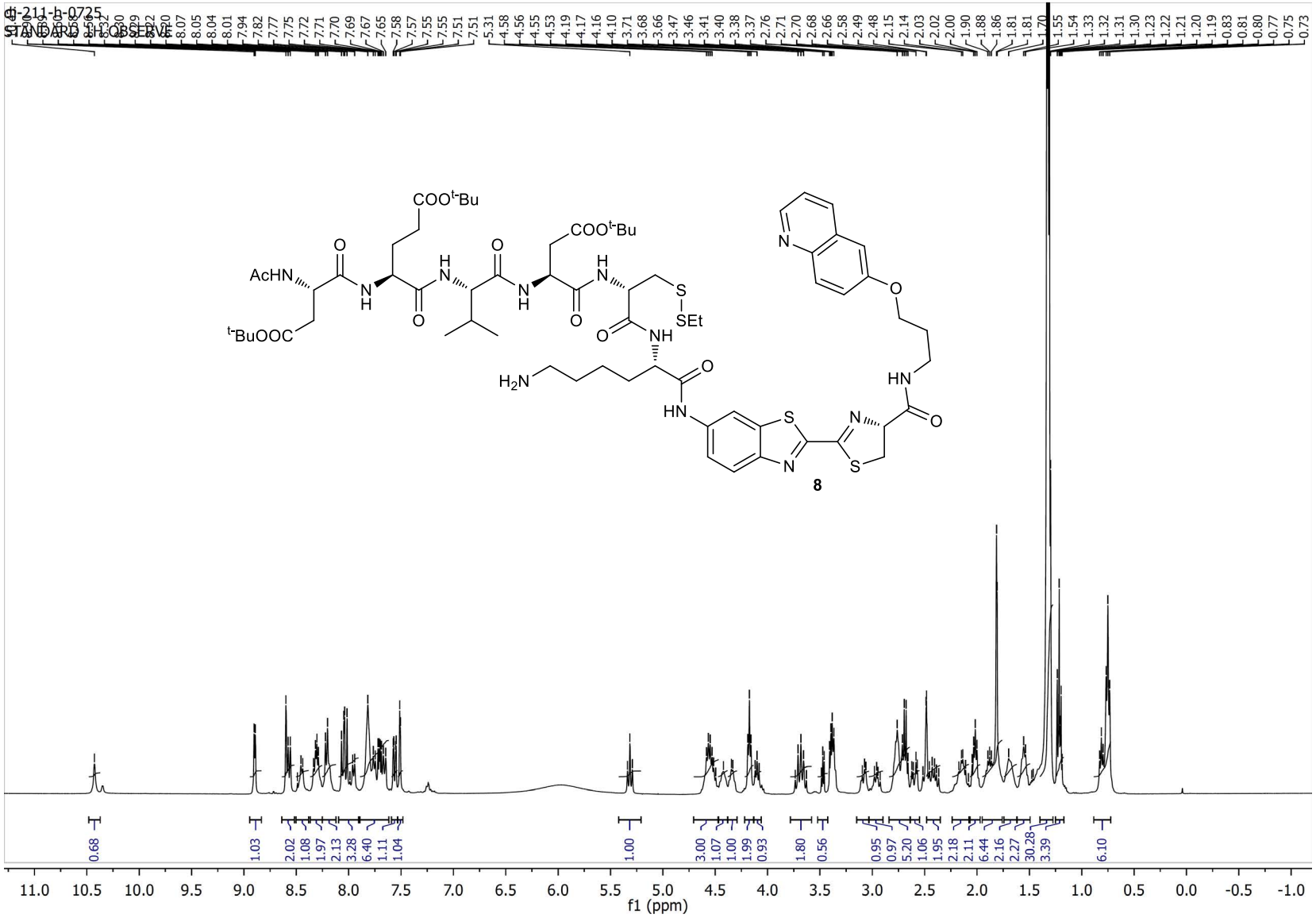
dj-211-h-0725
STANDARD 1H OBSERVE
AcHN
COO^{t}Bu
^{t}BuOOC
SEt
H_2N
HN
8
f1 (ppm)

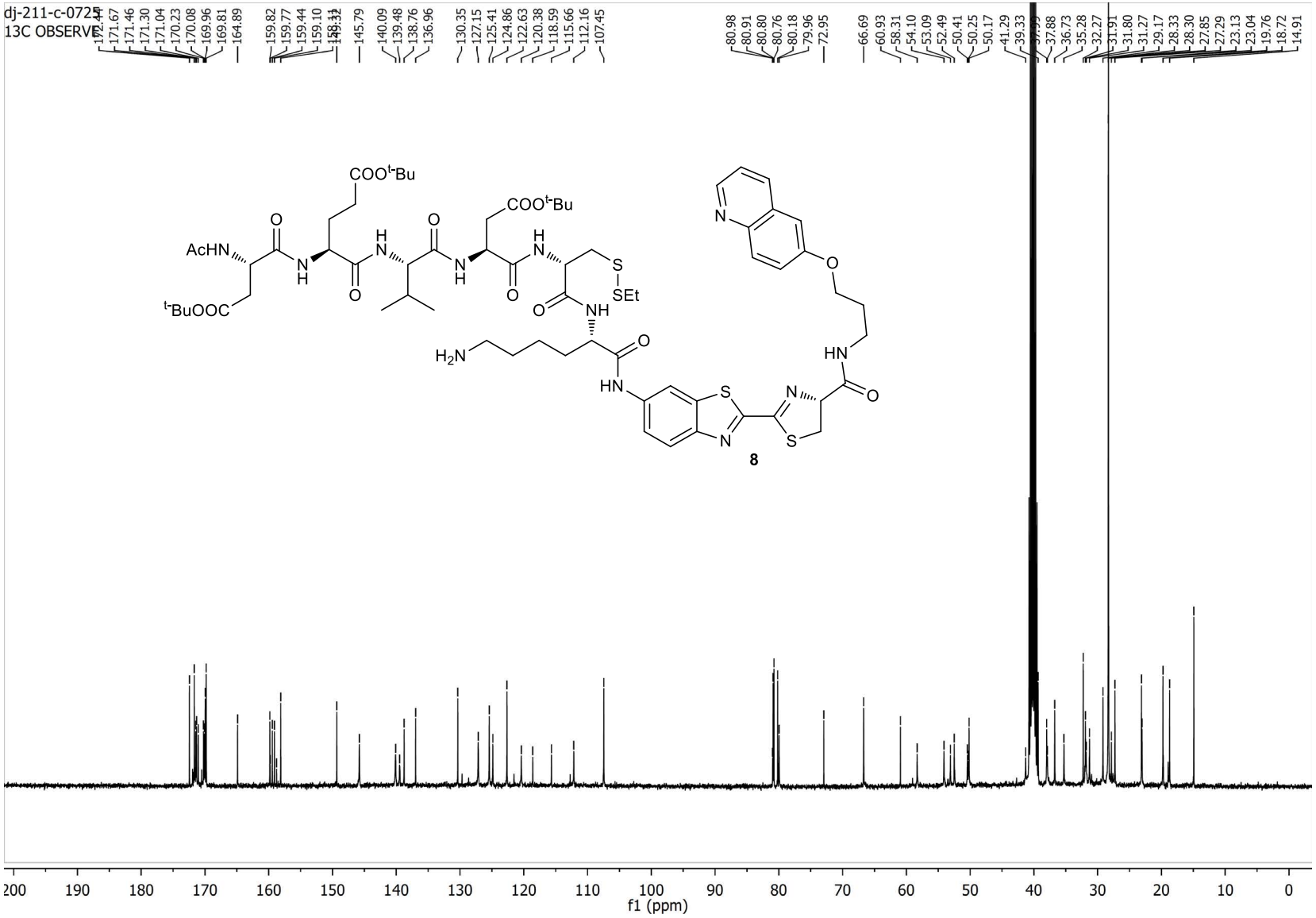
dj-211-c-0725
13C OBSERVE
f1 (ppm)
8

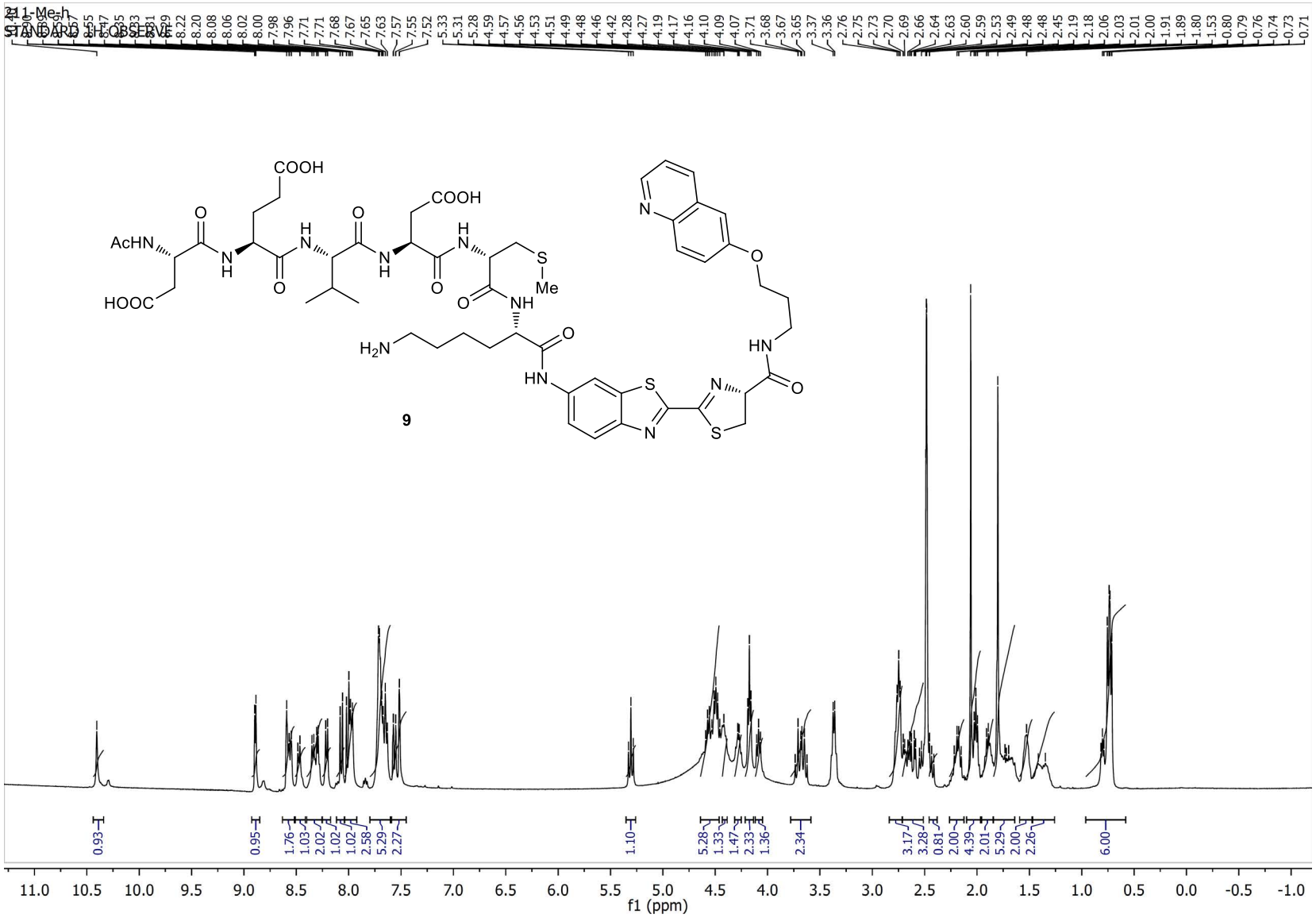
211-Me-h
STANDARD 1H OBSERVE
COOH
AcHN
HOOC
COOH
Me
NH
H_2N
HN
HN
9
f1 (ppm)

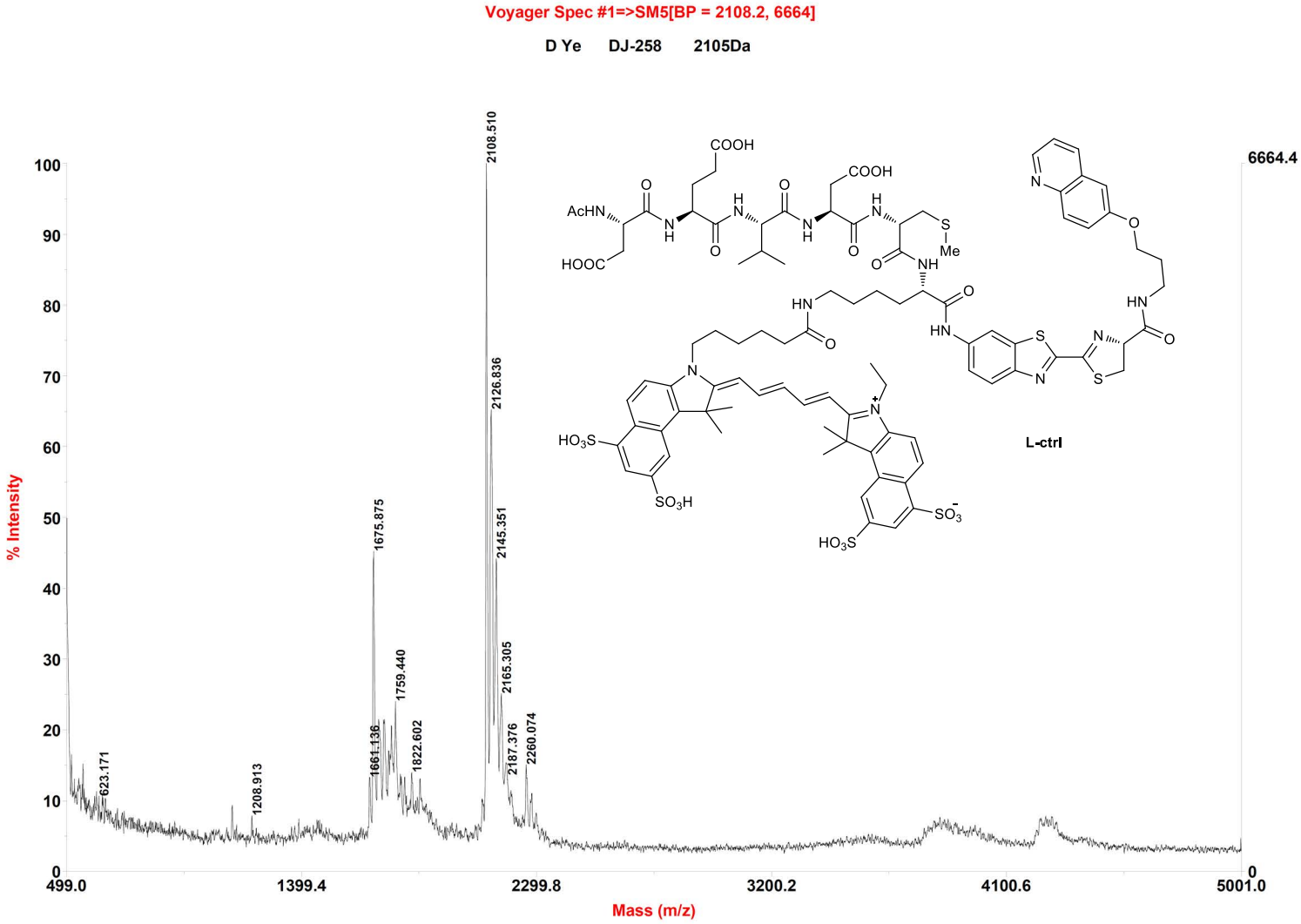
Voyager Spec #1=>SM5[BP = 2108.2, 6664]
D Ye DJ-258 2105Da
% Intensity
Mass (m/z)
2108.510
2126.836
1675.875
2145.351
1759.440
2165.305
1661.136
1822.602
2187.376
2260.074
623.171
1208.913
6664.4
L-ctrl
D Ye DJ-258 2105Da DHB/lin/pos
D:\...\DJ-258_0007.dat
Acquired: 15:10:00, October 22, 2012

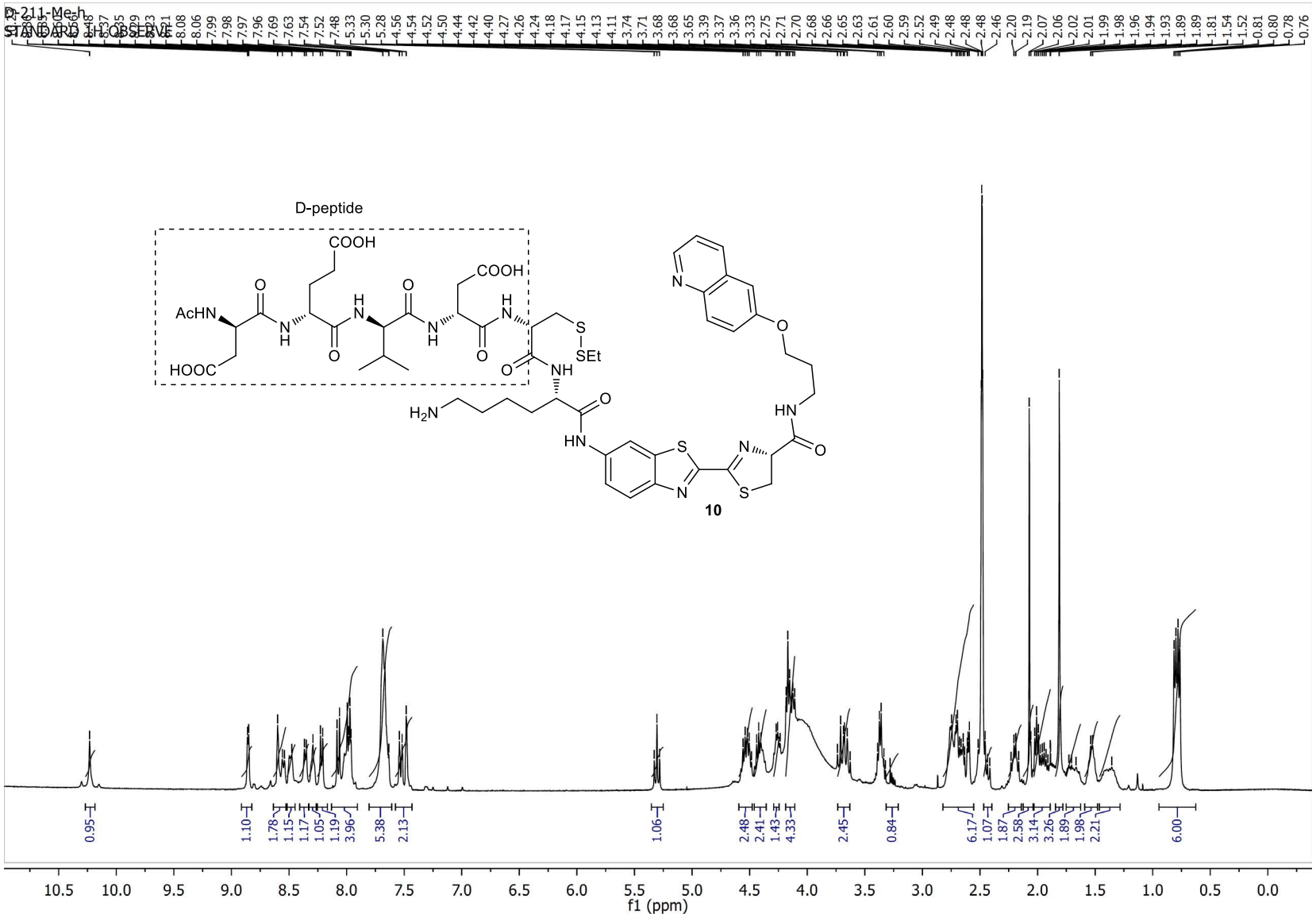
D-peptide
10
f1 (ppm)

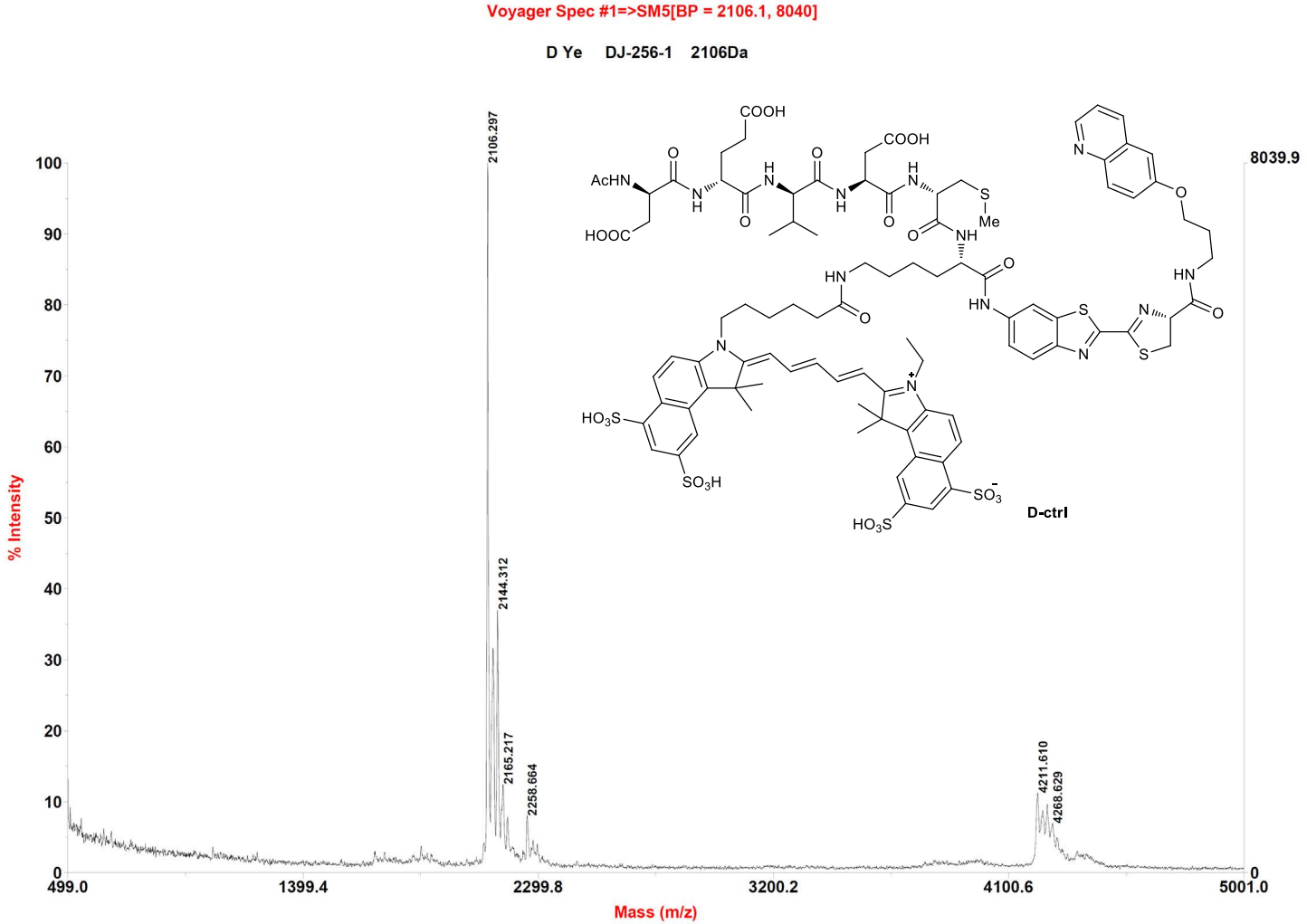
Voyager Spec #1=>SM5[BP = 2106.1, 8040]
D Ye DJ-256-1 2106Da
% Intensity
Mass (m/z)
2106.297
2144.312
2165.217
2258.664
4211.610
4268.629
8039.9
D-ctrl
D Ye DJ-256-1I 2106Da DHB/lin/pos
D:\...\DJ-256-1_0002.dat
Acquired: 18:31:00, January 08, 2013

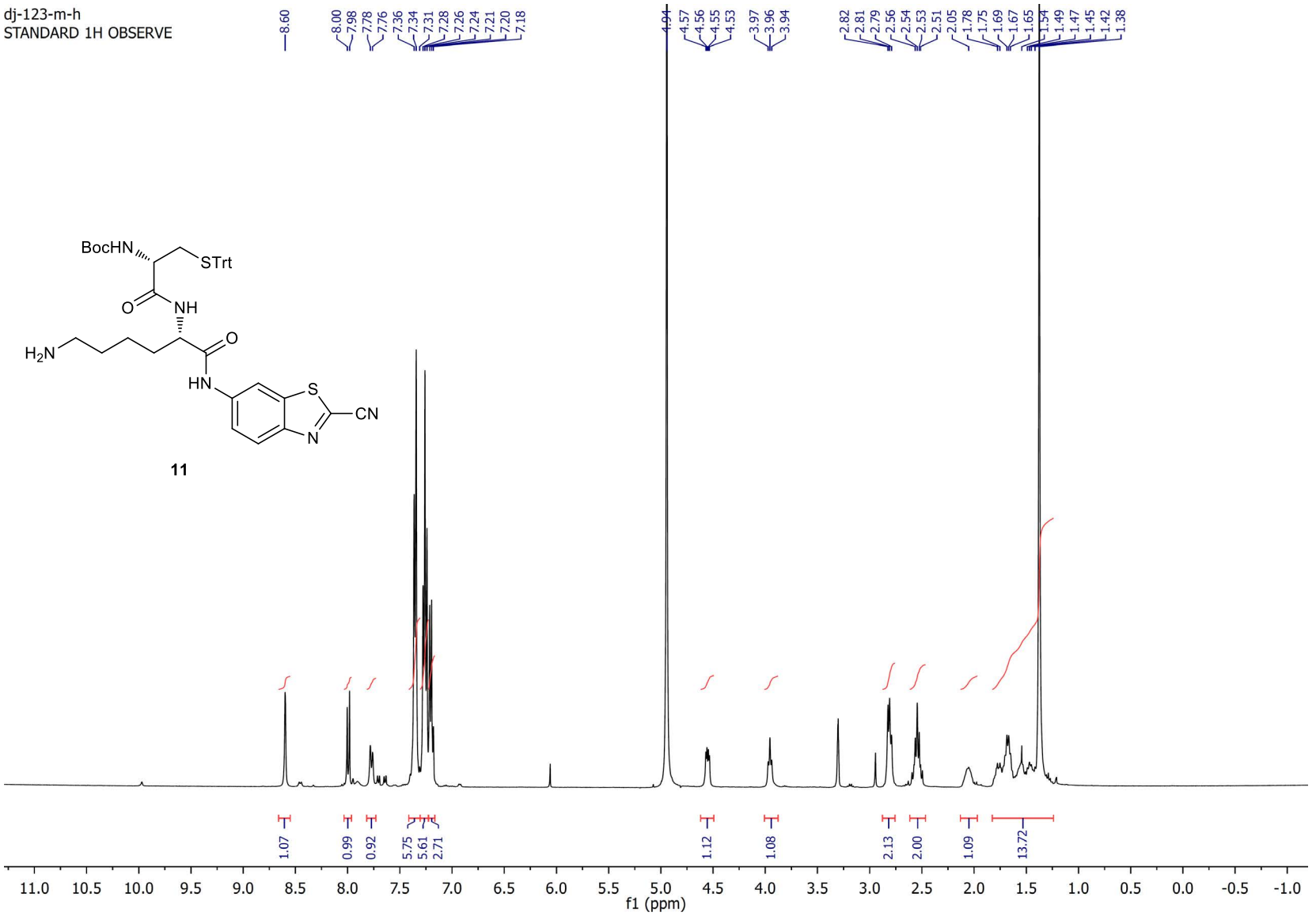
dj-123-m-h
STANDARD 1H OBSERVE
BocHN
STrt
O
NH
H2N
O
HN
S
CN
N
11
f1 (ppm)

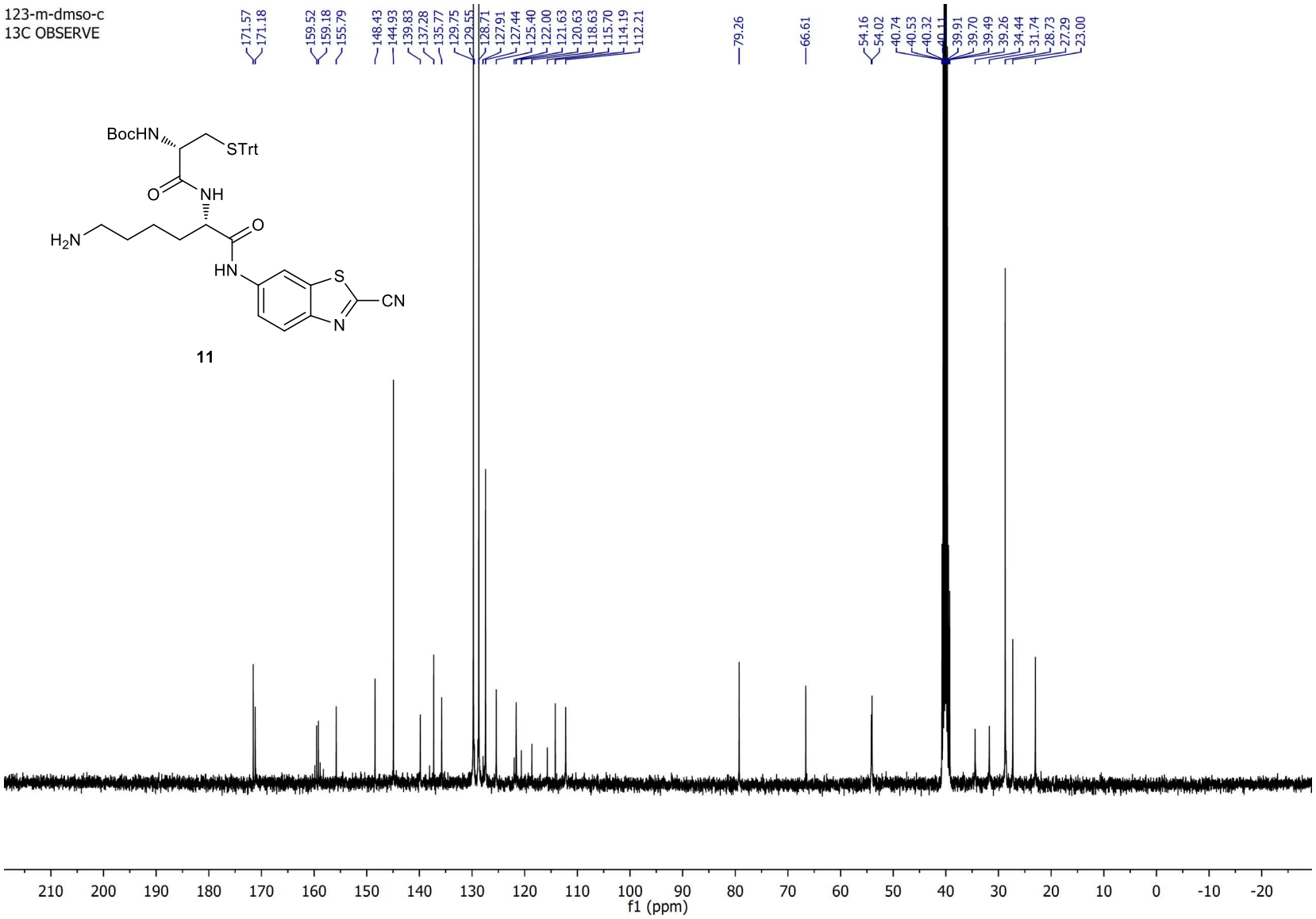
123-m-dmso-c
13C OBSERVE
171.57
171.18
159.52
159.18
155.79
148.43
144.93
139.83
137.28
135.77
129.75
129.55
128.71
127.91
127.44
125.40
122.00
121.63
120.63
118.63
115.70
114.19
112.21
79.26
66.61
54.16
54.02
40.74
40.53
40.32
40.11
39.91
39.70
39.49
39.26
34.44
31.74
28.73
27.29
23.00
BocHN
STrt
O
NH
O
H2N
HN
S
CN
N
11
210
200
190
180
170
160
150
140
130
120
110
100
90
80
70
60
50
40
30
20
10
0
-10
-20
f1 (ppm)

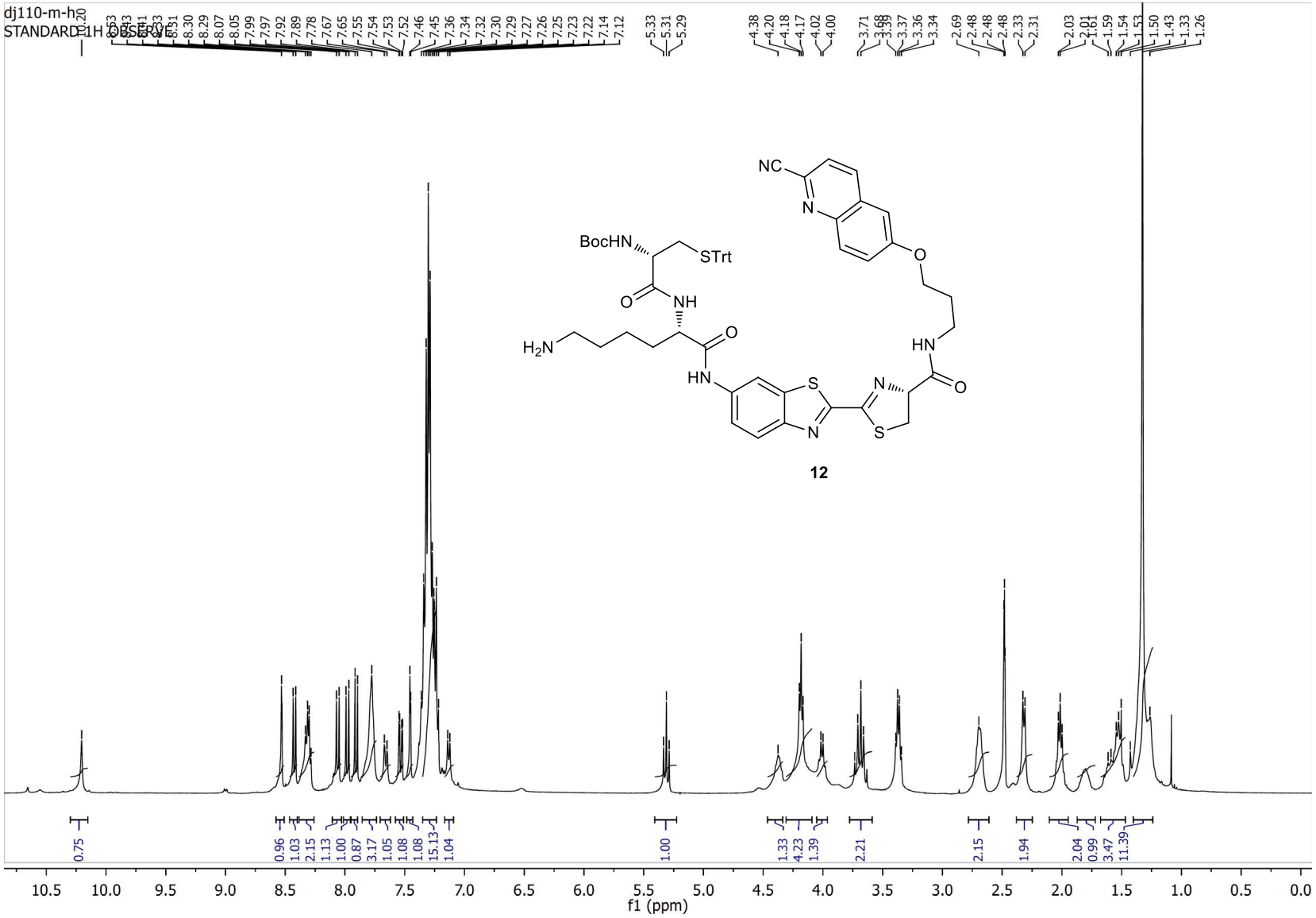
dj110-m-h
STANDARD 1H OBSERVE
NC
N
O
HN
O
BocHN
STrt
O
NH
H2N
O
HN
S
N
N
S
O
12
f1 (ppm)

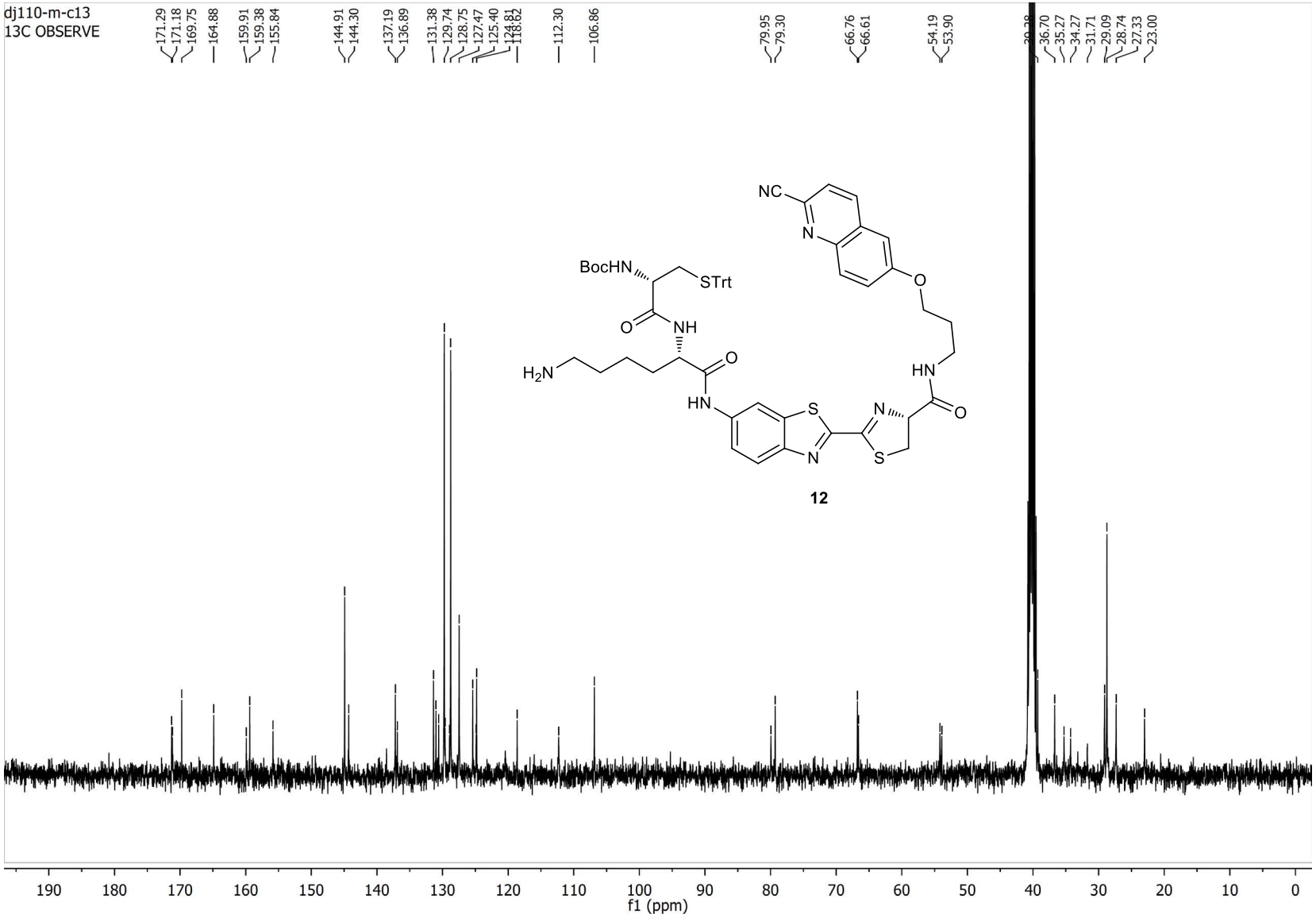
dj110-m-c13
13C OBSERVE
171.29
171.18
169.75
164.88
159.91
159.38
155.84
144.91
144.30
137.19
136.89
131.38
129.74
128.75
127.47
125.40
124.81
118.62
112.30
106.86
79.95
79.30
66.76
66.61
54.19
53.90
36.70
35.27
34.27
31.71
29.09
28.74
27.33
23.00
NC
N
O
BocHN
STrt
O
NH
H2N
O
HN
HN
S
N
O
N
S
190
180
170
160
150
140
130
120
110
100
90
80
70
60
50
40
30
20
10
0
f1 (ppm)

12

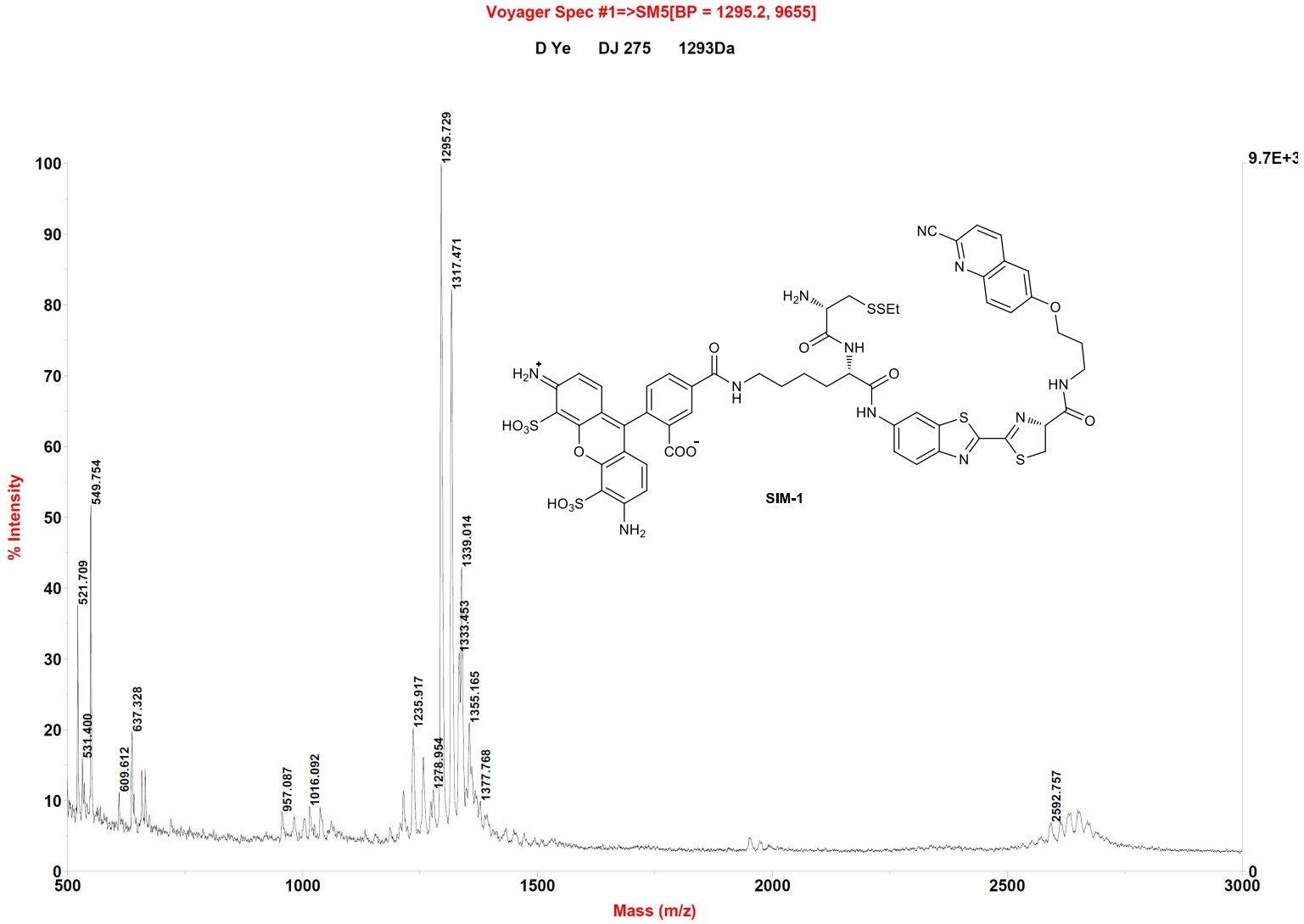
Voyager Spec #1=>SM5[BP = 1295.2, 9655]
D Ye DJ 275 1293Da
% Intensity
Mass (m/z)
9.7E+3
1295.729
1317.471
549.754
521.709
1339.014
1333.453
637.328
1235.917
1355.165
531.400
609.612
1278.954
1377.768
957.087
1016.092
2592.757
SIM-1
D Ye DJ 275 1293Da DHB/lin/pos
D:\...\DJ 275_0004.dat
Acquired: 16:57:00, December 10, 2012

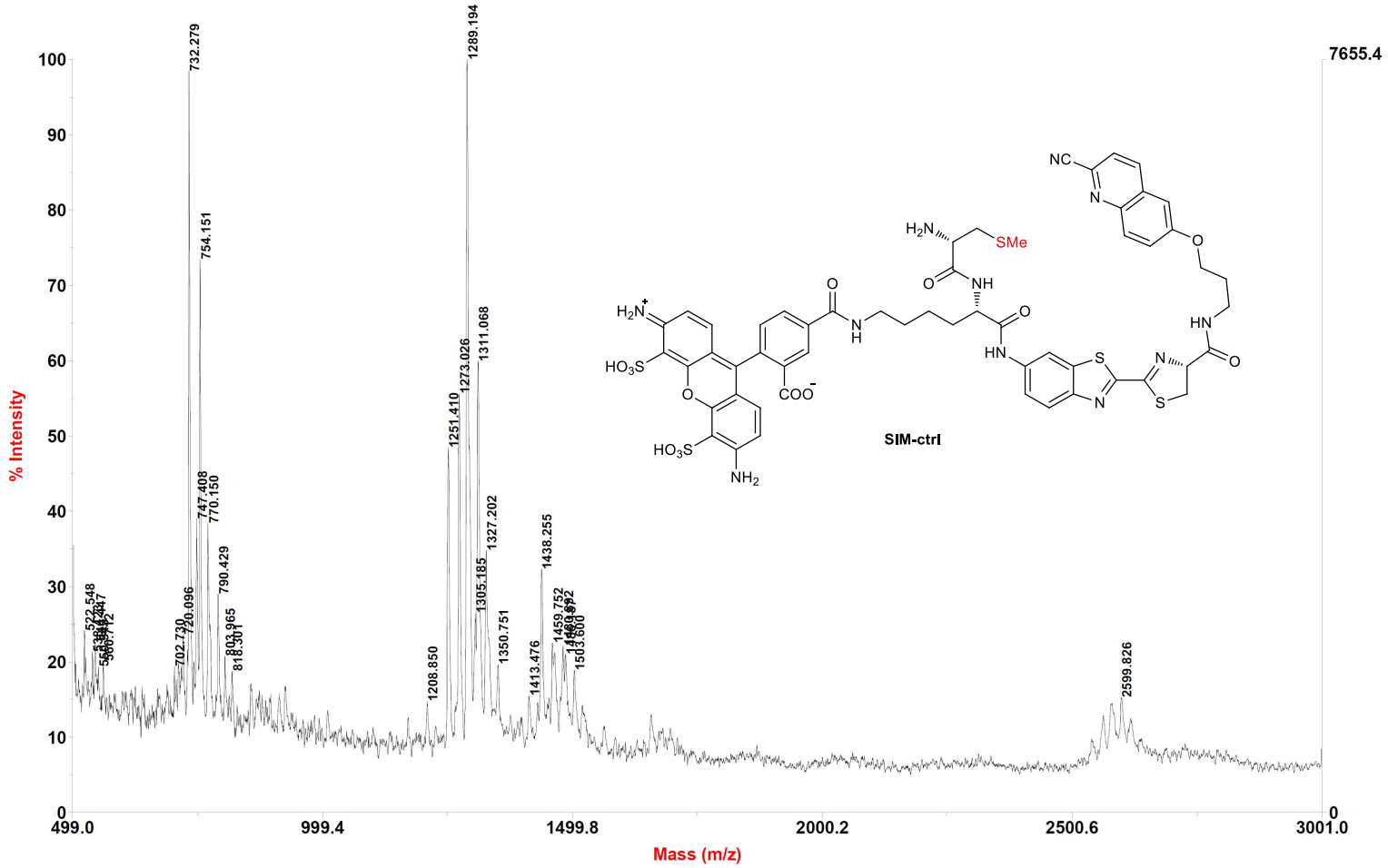
Voyager Spec #1=>SM5[BP = 1289.1, 7655]
D Ye dj 275-Me 1247Da
% Intensity
Mass (m/z)
7655.4
732.279
1289.194
754.151
1311.068
1273.026
1251.410
747.408
770.150
1327.202
790.429
1438.255
1305.185
1350.751
1208.850
1413.476
2599.826
SIM-ctrl
D Ye dj 275-Me 1247Da DHB/LIN/POS
D:\...\dj 275-Me_0003.dat
Acquired: 18:20:00, January 15, 2013

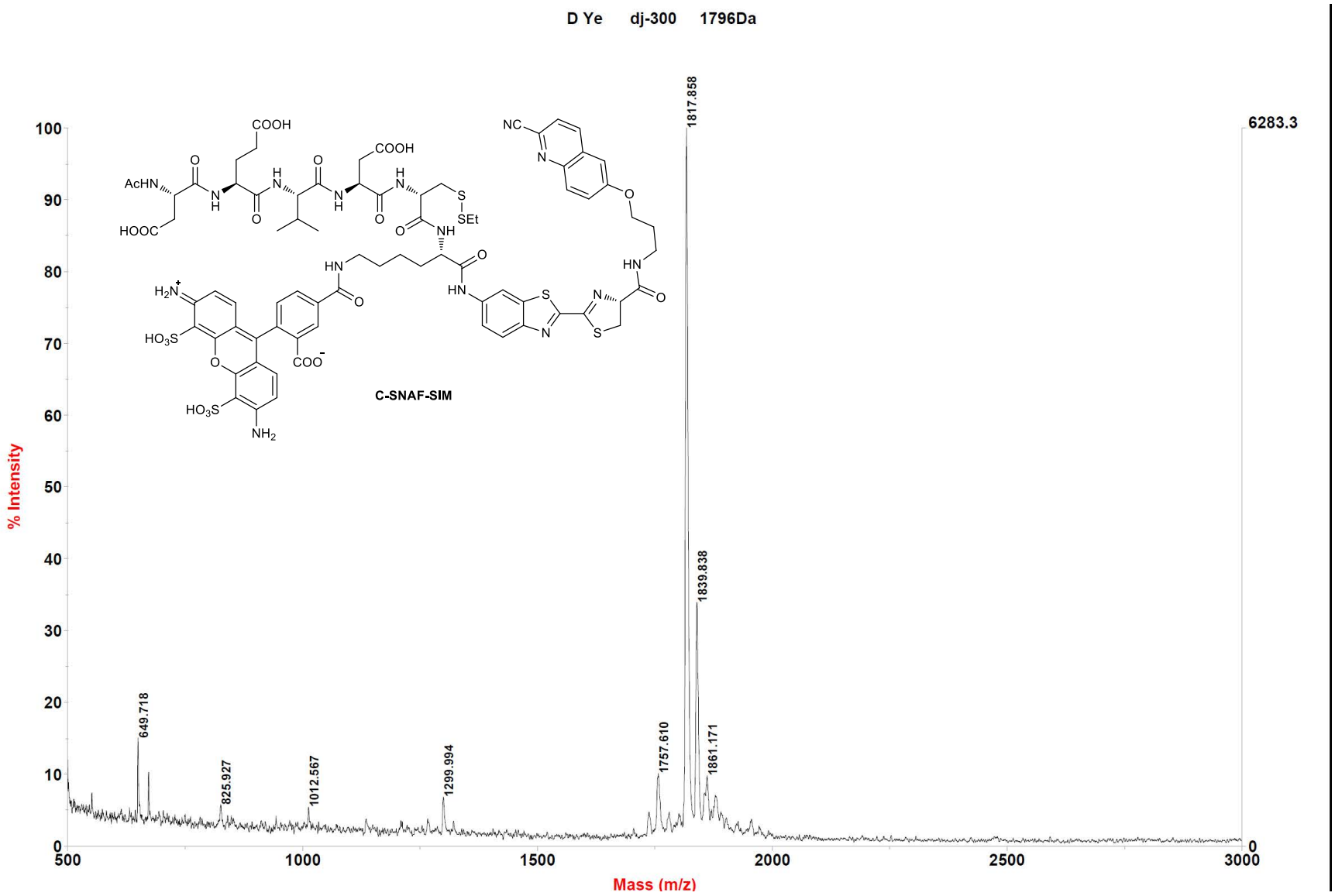
D Ye dj-300 1796Da
C-SNAF-SIM
% Intensity
Mass (m/z)
6283.3
1817.858
1839.838
649.718
825.927
1012.567
1299.994
1757.610
1861.171

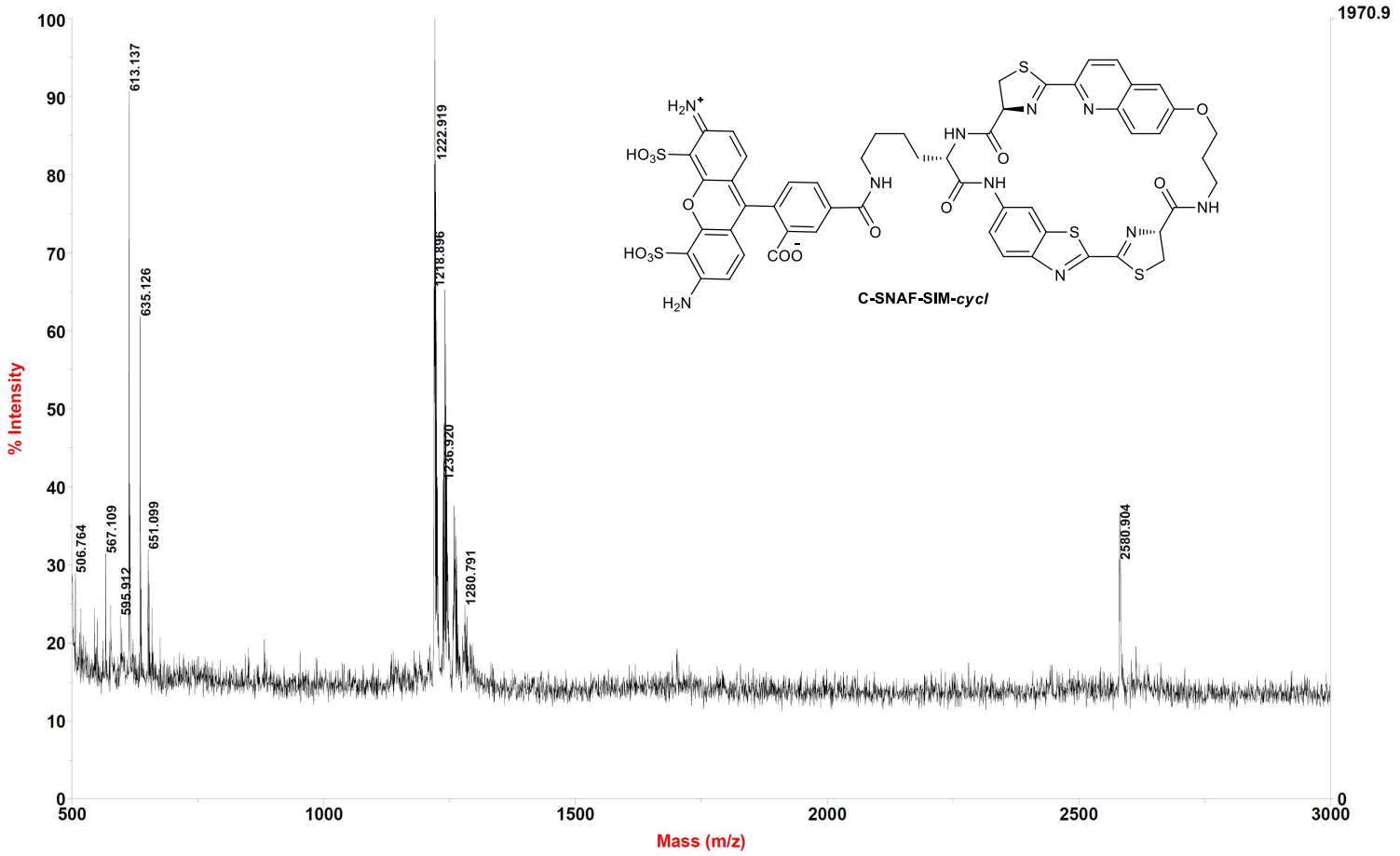
Voyager Spec #1[BP = 1220.8, 1971]
Deju Ye 300-C-1
1970.9
100
90
80
70
60
50
40
30
20
10
0
% Intensity
613.137
1222.919
635.126
1218.896
1236.920
506.764
567.109
651.099
595.912
1280.791
2580.904
500
1000
1500
2000
2500
3000
0
Mass (m/z)
C-SNAF-SIM-cycl
Deju Ye 300-C-1 1220.33 Da DHB/lin/pos
D:\...\300-C-1_0003.dat
Acquired: 17:04:00, August 28, 2013

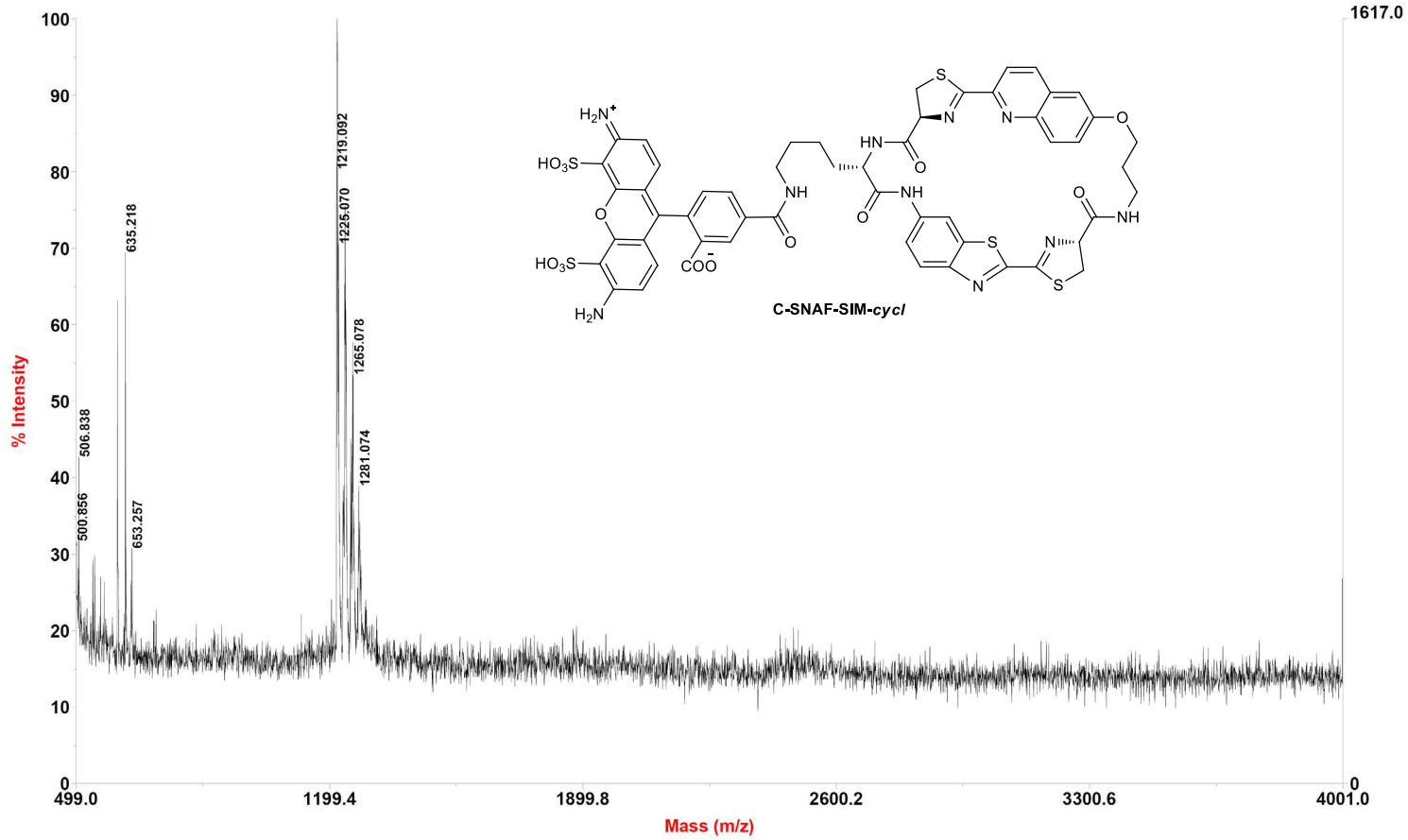
Voyager Spec #1[BP = 1221.1, 1617]
Deju Ye 300-C-2
1617.0
100
90
80
70
60
50
40
30
20
10
0
% Intensity
635.218
1219.092
1225.070
1265.078
506.838
1281.074
500.856
653.257
C-SNAF-SIM-cycl
499.0
1199.4
1899.8
2600.2
3300.6
4001.0
Mass (m/z)
Deju Ye 300-C-2 1220.33 Da DHB/lin/pos
D:\...\300-C-2_0003.dat
Acquired: 17:10:00, August 28, 2013

Voyager Spec #1[BP = 1727.6, 6200]

Deju Ye DJ-315

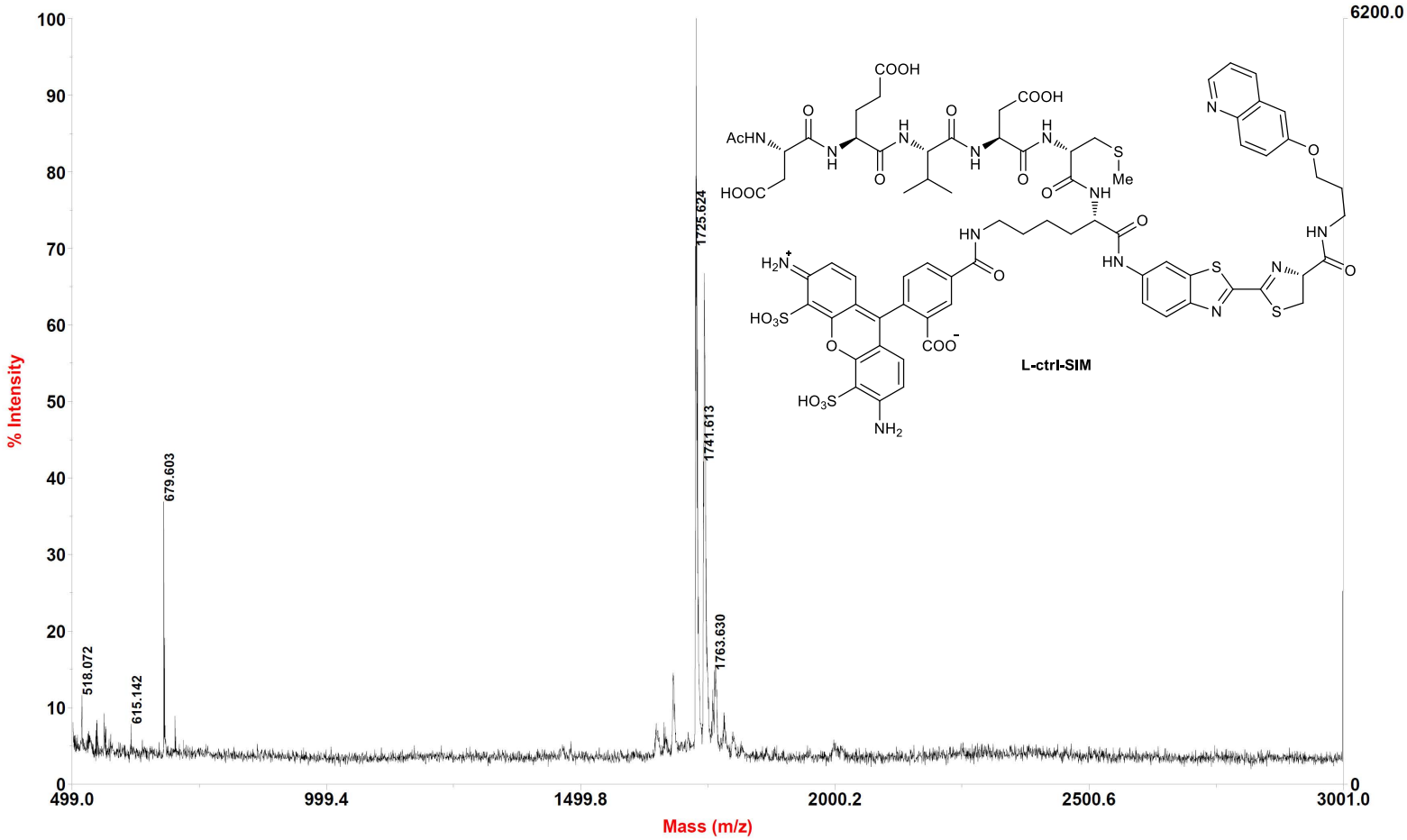

Deju Ye DJ-315 1726.83 Da DHB/ref/pos
D:\...\DJ-315_0005.dat
Acquired: 13:51:00, August 15, 2013

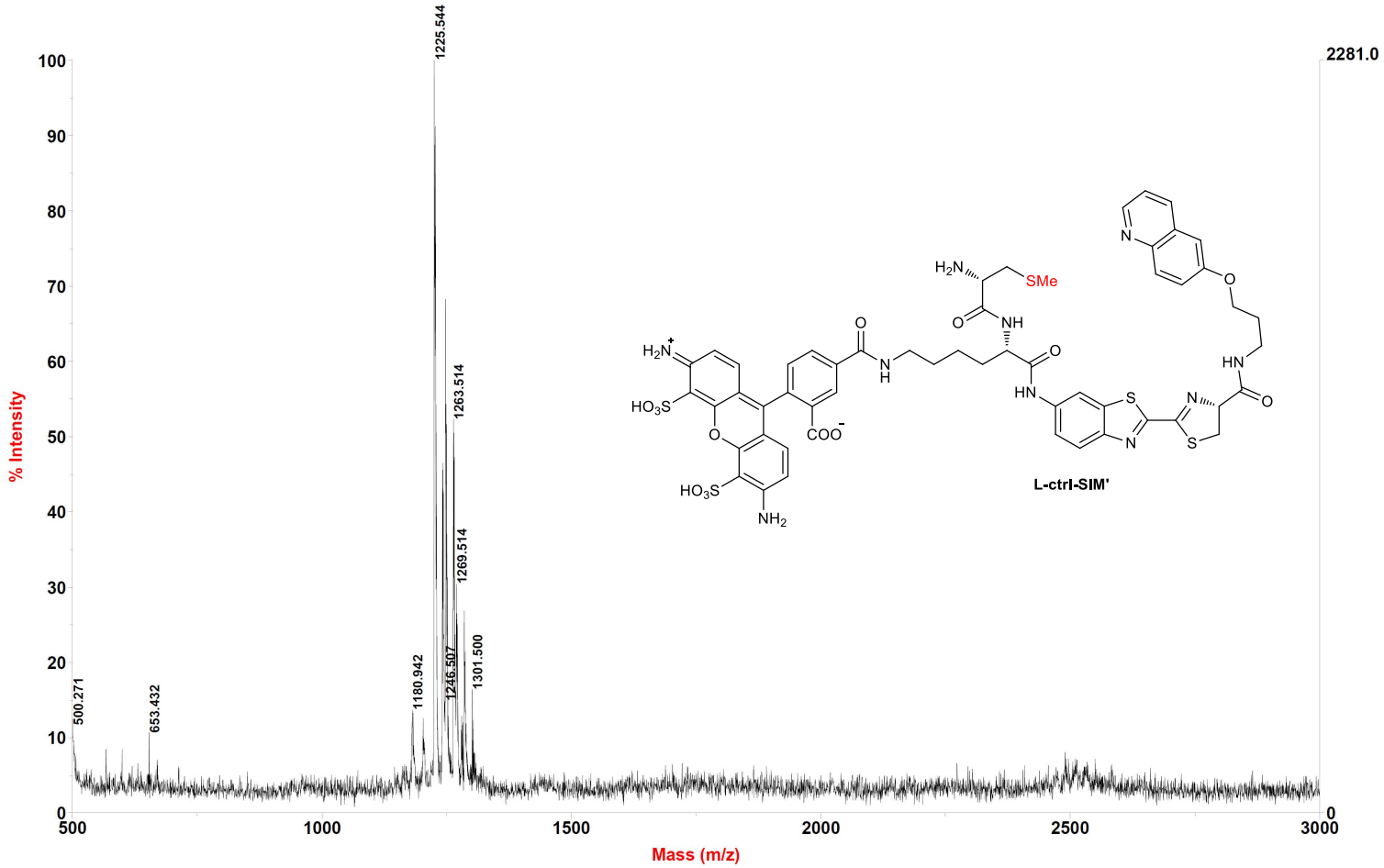
Voyager Spec #1[BP = 1225.6, 2281]
Deju Ye 315-C-2
1225.544
2281.0
100
90
80
70
60
50
40
30
20
10
0
% Intensity
500.271
653.432
1180.942
1246.507
1263.514
1269.514
1301.500
500
1000
1500
2000
2500
3000
Mass (m/z)
L-ctrl-SIM'
Deju Ye 315-C-2 1226.38 Da DHB/lin/pos
D:\...\315-C-2_0001.dat
Acquired: 17:18:00, August 28, 2013

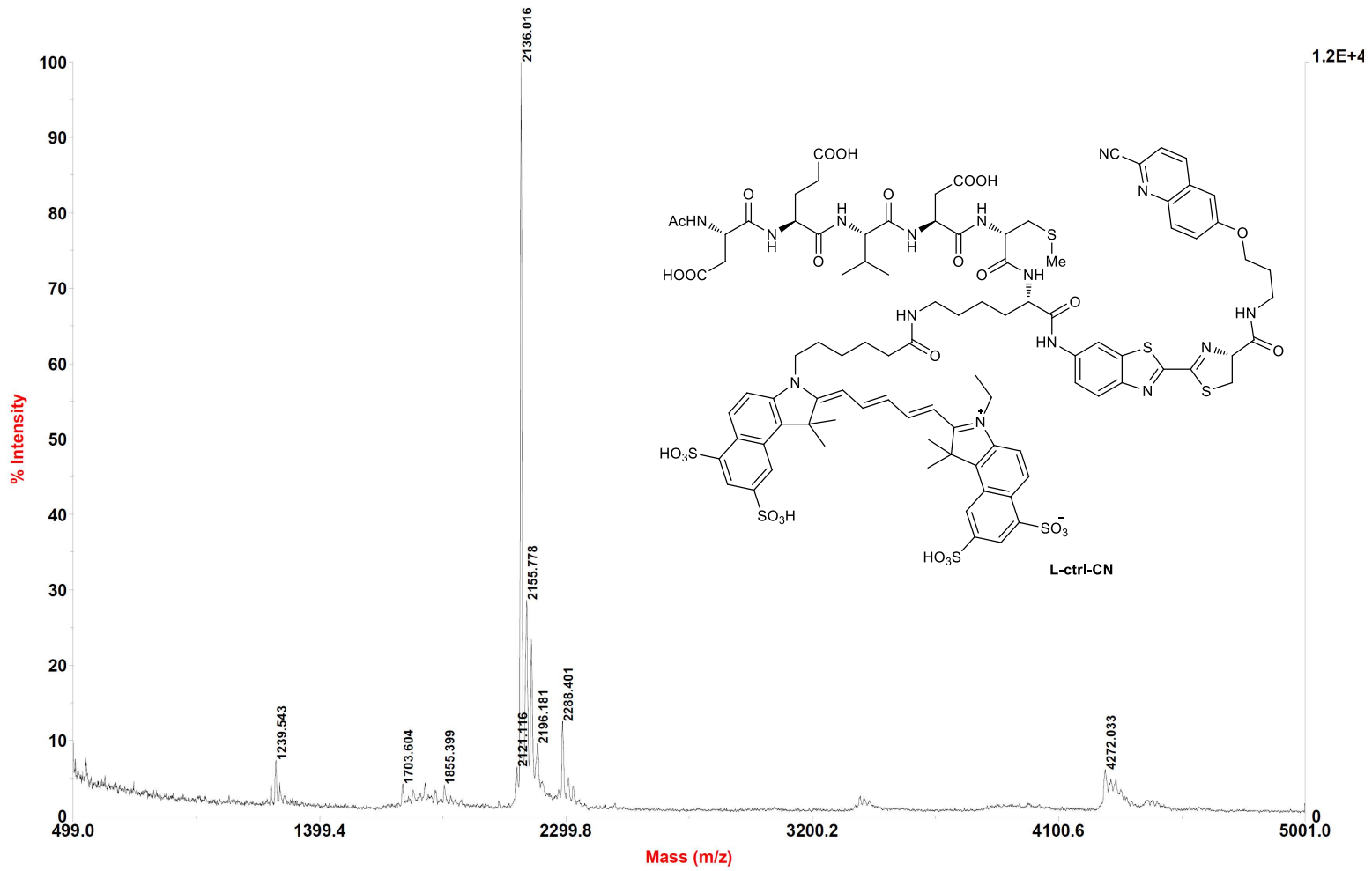

Deju Ye DJ308 2131.56 Da DHB/lin/pos
D:\...\DJ308_0001.dat
Acquired: 17:08:00, July 23, 2013

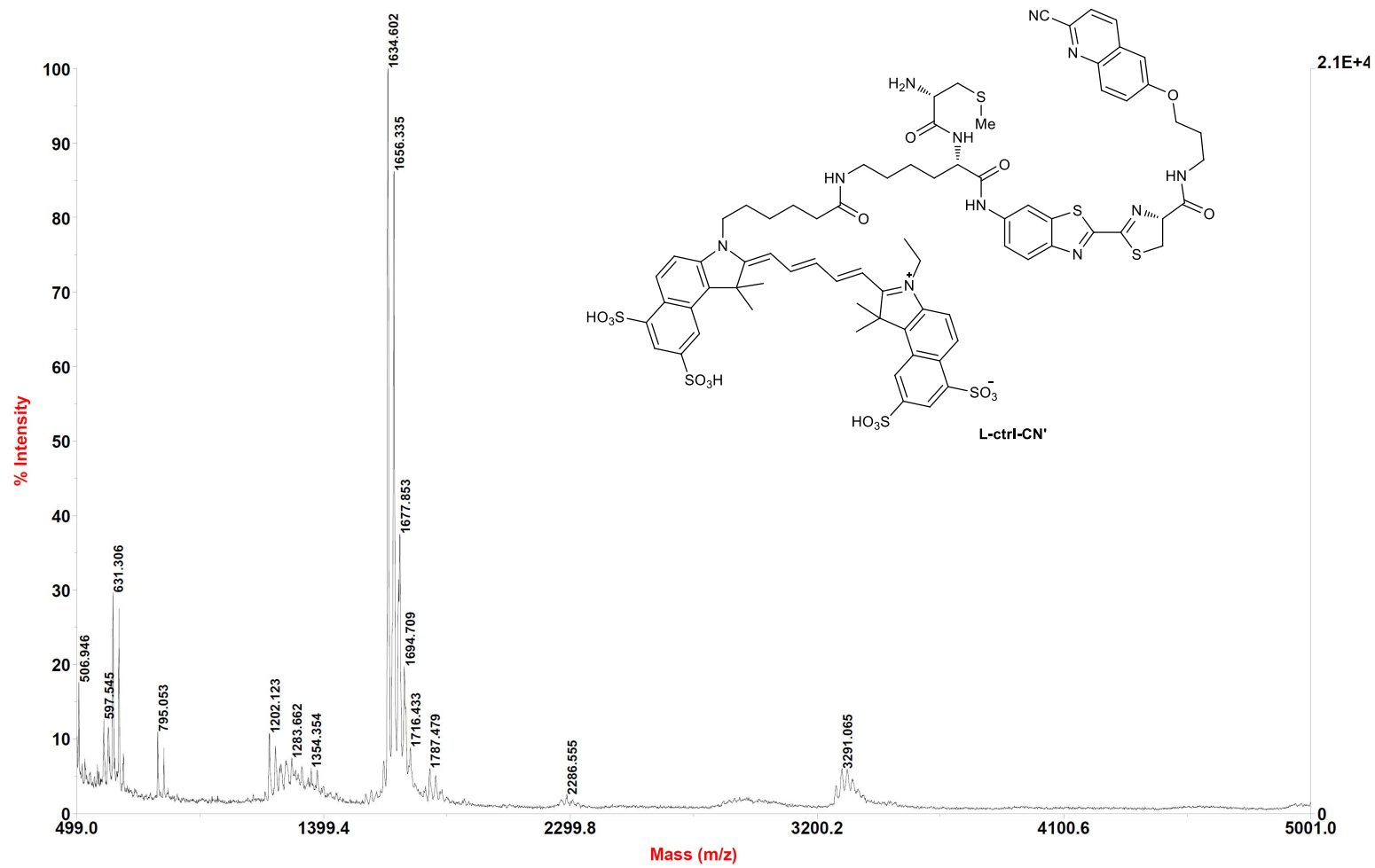
Voyager Spec #1=>SM5[BP = 1634.4, 20670]
Deju Ye 308-T 1633.9715 Da
% Intensity
Mass (m/z)
2.1E+4
0
100
90
80
70
60
50
40
30
20
10
0
499.0
1399.4
2299.8
3200.2
4100.6
5001.0
1634.602
1656.335
1677.853
631.306
506.946
597.545
795.053
1202.123
1283.662
1354.354
1694.709
1716.433
1787.479
2286.555
3291.065
L-ctrl-CN'
Deju Ye 308-T 1633.9715 Da DHB/lin/pos
D:\...\308-T_0003.dat
Acquired: 16:24:00, July 31, 2013

Voyager Spec #1=>SM5[BP = 2079.7, 28180]

D YE DJ313

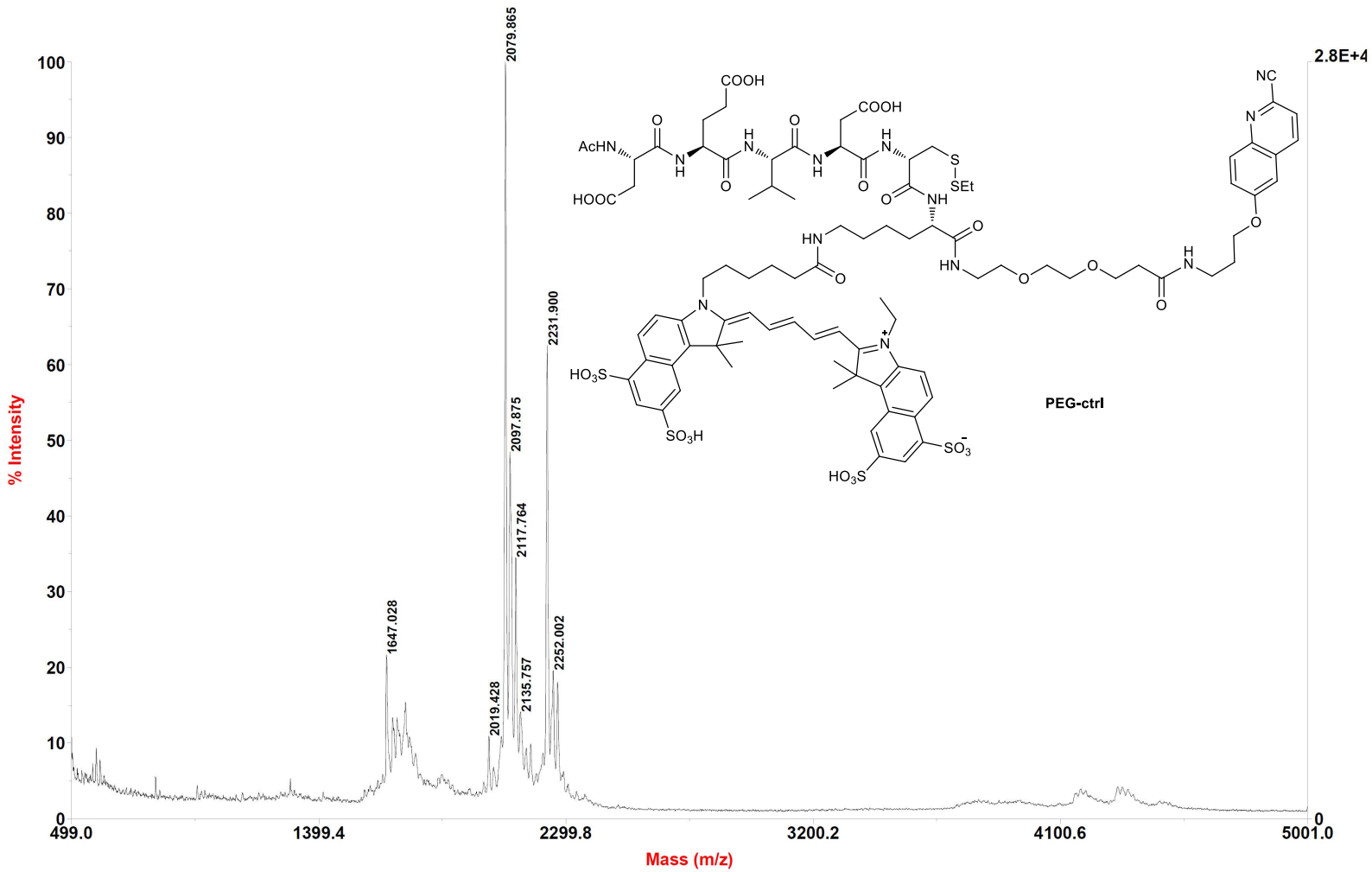

D YE DJ313 2078DA DHB/LIN/POS
D:\...\DJ313_0005.dat
Acquired: 17:24:00, August 06, 2013

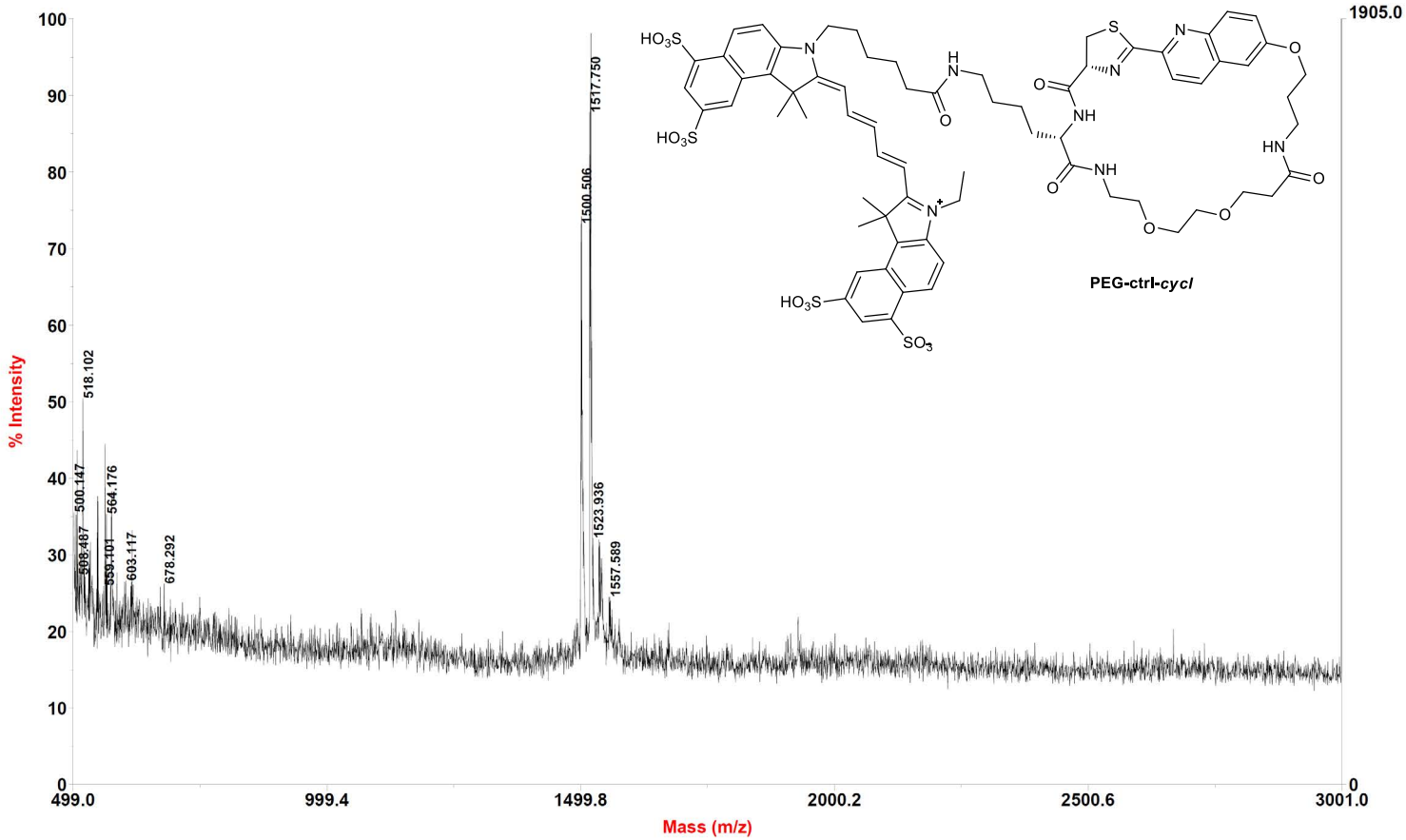
Voyager Spec #1[BP = 3000.0, 1905]
Deju Ye DJ-313-C
100
90
80
70
60
50
40
30
20
10
0
% Intensity
518.102
500.147
564.176
508.487
559.101
603.117
678.292
1517.750
1500.506
1523.936
1557.589
1905.0
499.0
999.4
1499.8
2000.2
2500.6
3001.0
Mass (m/z)
PEG-ctrl-cycl
Deju Ye DJ-313-C 1500.77 Da DHB/ref/pos
D:\...\DJ-313-C_0004.dat
Acquired: 12:01:00, August 15, 2013